

# **PKC $\gamma$ -mediated phosphorylation of CRMP2 regulates dendritic outgrowth in cerebellar Purkinje cells**

**Inauguraldissertation**

zur

Erlangung der Würde eines Doktors der Philosophie  
vorgelegt der  
Philosophisch-Naturwissenschaftlichen Fakultät  
der Universität Basel

von

Sabine Celine Winkler

aus Deutschland

Basel, 2021

Genehmigt von der Philosophisch-Naturwissenschaftlichen Fakultät  
auf Antrag von

Prof. Dr. Markus Rüegg

Prof. Dr. Josef Kapfhammer

Prof. Dr. Josef Bischofberger

Basel, den 13.10.2020

Prof. Dr. Martin Spiess

Dekan der Philosophisch-Naturwissenschaftlichen Fakultät

“Sometimes science is more art than science...

A lot of people don't get that.”

- **Rick Sanchez**

---

# Acknowledgements

---

I guess it takes a small village to complete a PhD. At least for me, the completion of my thesis would not have been possible without all the people that have greatly supported me along the way.

First, I want to begin by thanking Prof. Dr. Josef Kapfhammer for giving me the opportunity to work on my project and freely pursue my ideas. I feel very grateful and lucky to have had such a knowledgeable supervisor who approaches problems with a calm and practical attitude and always (quite literally) keeps an open door for questions.

I furthermore want to thank the members of my dissertation committee, Prof. Dr. Markus Rüegg and Prof. Dr. Josef Bischofberger and for their constructive input and enthusiasm for my project. I greatly valued the open discussions in my committee meetings and the support with which they enabled the smooth progression of my project.

Of course, I also want to thank the members of my group:

An especially big THANK YOU to Etsuko Shimobayashi, who was always open to help me and answer any of my questions. It was of great help to me to have someone so knowledgeable to discuss my project with and support me through many instances of troubleshooting. I also want to thank my fellow PhD student, Qinwei Wu, for his kind and helpful spirit and the positive attitude he brings to the lab. Many thanks also to Markus Saxer, who kept our lab running behind the scenes during most of my PhD and Aleksandar Kovacevic for taking over from him.

Prof. Dr. Nicole Schaeren-Wiemers I want to thank for offering encouragement and advice to me both in- and outside of our lab meeting and for the support that she provides to the PhD Club.

And while I am at it: Thanks also to my PhD Club colleagues! I had a lot of fun working with you and hope the next generation will carry on our legacy the same way.

Now onto the chunky part:

Friends, friends, friends, where to begin....?

Special thanks to Theresa, Nicole, Sophia, Natalia and Maria who surely provided the lion's share of emotional support and wine in times of crisis (or any other time). I hope to keep you around for much longer (Retirement-WG one day?), even if we don't live in the same city anymore.

My in-house Natalia (a.k.a. Efthalia) I want to thank here for the lunch breaks, horoscopes, nanodrop-chatter and for luring me into the organization team for the Pint of Science. It was a lot of fun to have a fellow-neuro-enthusiast to visit conferences and fan-girl about tissue-clearing with.

A big thank you I also want to give to my friend Matheus for lots of happy memories in a too short period of time. We would still love for you to move to Switzerland someday!

Of course, there were many, many more, who have all made my time in Basel very special. Thank you for sharing with me all the Rhine-swims, BBQs, retreats, happy days, happy hours, dinners, yoga sessions, vacations, frustrations, moves, pandemics and whatever I'm forgetting right now. All these memories are very dear to me and I can't believe how many experiences you can cram into only 5 short (hahaha...) years.

You all make my heart overflow with love and happiness and I am very grateful to have met you!

Und natürlich zum Schluss das größte Dankeschön an meine Familie: Eure Unterstützung, eure Geduld, die kleinere und größere Aufmunterungen während dem PhD und euer Interesse an meiner Arbeit bedeuten mir unfassbar viel. Ohne euch wäre nichts von all dem möglich gewesen!

---

## Summary

---

Spinocerebellar Ataxia (SCA) is a group of diseases characterized by cerebellar degeneration along with progressive motor dysfunction. SCA subtype 14 (SCA14) is caused by mutations in the protein kinase C  $\gamma$  gene (PRKCG) of which many lead to an over-activation of the kinase in vitro [1]. We have shown that increased PKC $\gamma$  activity is associated with impaired dendritic development in cerebellar Purkinje cells. Mice expressing the S361G mutation (PKC(S361G)-mice) develop mild cerebellar ataxia. Purkinje cell dendritic development in PKC(S361G)-cerebellar slice cultures is impaired similarly as after pharmacological activation of PKC [2]. The mechanisms behind this dendritic growth inhibition, however, remain largely obscure.

In this study we used cerebellar lysates from PKC(S361G)-mice for the immunoprecipitation of PKC $\gamma$  followed by mass spectrometry analysis. We thereby identified collapsin response mediator protein 2 (CRMP2) as a potential interactor and confirmed our finding with the Duolink™ proximity ligation assay. Using organotypic cerebellar slice cultures, we found that the levels of CRMP2 phosphorylated at threonine 555, a known PKC target site, are strongly increased in Purkinje cells of PKC(S361G)-mice. miRNA mediated knockdown of CRMP2 led to decreased dendritic outgrowth of Purkinje cells in dissociated cerebellar cultures. Furthermore, transfection of CRMP2 mutants either lacking (T555A) or mimicking (T555D) Thr555 phosphorylation impaired Purkinje cell dendritic development.

We generated a knock-in mouse expressing the T555A-mutant to further characterize the role of unphosphorylated CRMP2. While cerebella from these mice appear morphologically sound, Purkinje cells in dissociated cerebellar cultures show reduced dendritic development. This reduction was rescued by transfecting Wt-CRMP2 or by introducing the T555D-mutant.

Taken together, our findings demonstrate that CRMP2 is an important modulator of dendritic development in cerebellar Purkinje cells and that coordinated phosphorylation via PKC $\gamma$  is required to allow for its correct function.

---

# Table of Contents

---

<b>Acknowledgements</b>	<b>I</b>
<b>Summary</b>	<b>III</b>
<b>Table of Contents</b>	<b>IV</b>
<b>List of Tables and Figures</b>	<b>VI</b>
<b>Abbreviations</b>	<b>VIII</b>
<b>1. Introduction</b>	<b>1</b>
1.1 The cerebellum	1
1.2 Protein kinase C (PKC)	7
1.3 Spinocerebellar ataxia	12
1.4 The collapsin response mediator proteins (CRMPs)	16
<b>Aims of the thesis</b>	<b>23</b>
<b>2. Results</b>	<b>25</b>
PKC $\gamma$ -mediated phosphorylation of CRMP2 regulates dendritic outgrowth in cerebellar Purkinje cells	25
2.1 Abstract	25
2.2 Introduction	26
2.3 Materials & Methods	27
2.4 Results	35
2.5 Discussion	47
<b>3. Additional Data</b>	<b>57</b>
3.1 Phosphorylation of CRMP2 in PKC $\gamma$ (S361G)-mice is unchanged at GSK3 $\beta$ and Cdk5 target sites	57
3.2 Inhibition of CaMKII does not decrease Thr555 phosphorylation in PKC $\gamma$ (S361G)-mice	60
3.3 Impaired dendritic development of Purkinje cells from PKC $\gamma$ (S361G)-mice cannot be rescued through the transfection of CRMP2	61
3.4 Tubulin stabilization is impaired in PKC $\gamma$ (S361G)-mice	63
3.5 Climbing- and parallel fiber inputs appear normal in CRMP2 <sup>ki/ki</sup> -mice	65
3.6 CRMP2 <sup>ki/ki</sup> -mice are not protected from the effects of PMA-mediated reduction of dendritic growth	66

<b>4. General Discussion</b>	<b>68</b>
4.1 The role of CRMPs in Purkinje cells	68
4.2 Mechanisms of disrupted CRMP2 signaling in cerebellar Purkinje cells	69
4.3 Differential phosphorylation of CRMP2	70
4.4 CRMP2 and microtubule dynamics	72
<b>5. Conclusion and Outlook</b>	<b>73</b>
<b>6. Materials &amp; Methods</b>	<b>76</b>
<b>7. References</b>	<b>80</b>
<b>8. Curriculum Vitae</b>	<b>100</b>

---



---

# List of Tables and Figures

---

## Figures

---

Figure I	Architecture of the cerebellum	2
Figure II	Cerebellar celltypes and their connectivity	4
Figure III	Postnatal development of cerebellar Purkinje cells	6
Figure IV	Domain structure of different PKC isoforms	8
Figure V	Life cycle of PKC	10
Figure VII	PRKCG mutations associated with SCA14	16
Figure VIII	CRMP2 domain structure	20
Figure 1	Interaction of CRMP2 and PKC $\gamma$	36
Figure 2	Phosphorylation of CRMP2 is increased in PKC $\gamma$ (S361G)-mice	39
Figure 3	CRMP2 regulates dendritic development of cerebellar Purkinje cells	40
Figure 4	Dendritic development in Purkinje cells is modulated by CRMP2 phosphorylation	42
Figure 5	Generation of CRMP2 <sup>ki/ki</sup> -mice	42
Figure 6	CRMP2 phosphorylation at Thr555 is abolished in CRMP2 <sup>ki/ki</sup> -mice	45
Figure 7	Dendritic development in CRMP2 <sup>ki/ki</sup> -mice is impaired in dissociated cerebellar cultures and can be rescued by transfection of Wt- or T555D-CRMP2	47
Figure 8	Model for the regulation of Purkinje cell dendritic development via PKC $\gamma$ activity and CRMP2 phosphorylation	50
Suppl. Figure 1	miRNA-mediated knockdown of CRMP2	52
Suppl. Figure 2	CRMP2 phosphorylation in PKC $\gamma$ (S361G)-mice	53
Suppl. Figure 3	Examples of transfected cells for the overexpression of CRMP2 or its phospho- mimetic and phospho-defective mutants	54
Suppl. Figure 4	Examples of transfected cells for the knockdown of CRMP2	55
Suppl. Figure 5	Examples of transfected CRMP2 <sup>ki/ki</sup> cultures transfected with wildtype CRMP2 or the T555D-mutant	56

---

Figure IX	Phosphorylation of different CRMP2 target sites	58
Figure X	Treatment of organotypic slice cultures with inhibitors of CRMP2 phosphorylation	60
Figure XI	Inhibition of CaMKII does not decrease Thr555 phosphorylation in PKC $\gamma$ (S361G)-mice	61
Figure VIII	Reconstitution of CRMP2 phosphorylation does not rescue dendritic development in PKC $\gamma$ (S361G)-dissociated cultures	62
Figure IX	Tubulin acetylation is decreased in PKC $\gamma$ (S361G)-mice	64
Figure X	Tubulin acetylation in cerebellar lysates	65
Figure XI	Parallel and climbing fiber innervation is normal in CRMP2 <sup>ki/ki</sup> -mice	66
Figure XII	Purkinje cells from CRMP2 <sup>ki/ki</sup> -mice are not protected from the effects of PMA-stimulation	67

## Tables

Table I	CRMP nomenclature	17
Table II	CRMP2 post-translational modifications	22
Table 1	Mass spectrometry analysis of cerebellar lysates from PKC $\gamma$ (S361G)- and PKC $\gamma$ <sup>-/-</sup> -mice	35
Suppl. Table 1	Report of results LC-MS/MS	56
Table III	Stock solutions of naringenin and N7O	76

---

## Abbreviations

---

aa	– Amino acid	LKE	– Lanthionine ketimine ester
ADCA	– Autosomal dominant cerebellar ataxia	LPA	– Lysophosphatidic acid
Ca	– Calcium	LTD	– Long-term depression
CaMKII	– Calcium/calmodulin-dependent protein kinase II	LTP	– Long-term potentiation
Cav2.2	– (N-type) voltage-gated calcium channel	MEM	– Minimal essential medium
Cdk5	– Cyclin-dependent kinase 5	mGluR1	– Metabotropic glutamate receptor 1
CNS	– Central nervous system	MICAL-L1	– MICAL-like protein 1
cPKC	– Classical protein kinase C	Nav1.7	– Voltage gated sodium channel $\alpha$ -subunit 1.7
CRMP	– Collapsin response mediator protein	NCX3	– Sodium-calcium exchanger 3
DAG	– Diacylglycerol	NGF	– Nerve growth factor
DGKy	– Diacylglycerol kinase $\gamma$	NGS	– Normal goat serum
DMEM	– Dulbecco's modified eagle's medium	NT-3	– Neurotrophin 3
DPYSL	– Dihydropyrimidase-like protein	OTSC	– Organotypic slice culture
DRP	– Dihydropyrimidase-related protein	p	– Postnatal day
EHD1	– Eps 15 homology domain protein 1	PAM	– Protospacer adjacent motif
FACS	– Fluorescence-activated cell sorting	PB	– Phosphate buffer
FBS	– Fetal bovine serum	PDK1	– Pyruvate dehydrogenase kinase 1
FDR	– False discovery rate	PHLPP	– PH domain and leucine rich repeat protein phosphatases
GSK3 $\beta$	– Glycogen synthase kinase 3 $\beta$	PKC $\gamma$	– Protein kinase C $\gamma$
HBSS	– Hank's balanced salt solution	PLC	– Phospholipase C
HSP70	– Heat-shock protein 70	PMA	– Phorbol 12-myristate 13-acetate
IP3	– Inositol 1,4,5-trisphosphate	PRKCG	– Protein kinase C $\gamma$ gene
iPSCs	– Induced pluripotent stem cells	PS-domain	– Pseudosubstrate domain
		ROCK2	– Rho-associated protein kinase 2
		SCA	– Spinocerebellar ataxia
		SCI	– Spinal cord injury

## Abbreviations

---

Shh	–	Sonic hedgehog	Ulip	–	Uncoordinated 33-like protein
CBD3	–	Ca <sup>2+</sup> channel-binding domain 3	vGlut1	–	Vesicular glutamate transporter 1
TOAD	–	Turned on after division, 64 kDA protein	WAVE1	–	WASP-family verprolin homologous protein 1
TTBK1	–	Tau-tubulin kinase 1			
TTX	–	Tetrodotoxin			
TUC	–	Toad64/Ulip/CRMP			

---

# 1. Introduction

---

## 1.1 The cerebellum

### 1.1.1 Overview

Although the cerebellum, literally translating to “little brain”, makes up the small hind portion of the brain, comprising about 10% of the whole brain in weight, it contains around 60% of all excitatory neurons (Erö et al., 2018). As trauma and degeneration of the cerebellum generally lead to pathologies of motor functions, the main function of the cerebellum has long been considered to be the coordination of motoric input from sensory-motor areas. However, it is becoming more and more clear that the cerebellum is also involved in learning, attention and emotional behavior. The expansion of the cerebellum during evolution, especially in areas not associated with motor function, has suggested that it developed crucial functions in the augmentation of cognition in humans (Weaver, 2005). Over the years, data collected in anatomical tracing studies have shown that the cerebellum is connected to virtually all areas of the cerebrocortex (Kelly and Strick, 2003; Suzuki et al., 2012; Aoki et al., 2019). It has been proposed, that the computational modules of the cerebellum, which are largely homogenous in their setup, function similarly in different circuits (D’Angelo and Casali, 2013). The role of the cerebellum is therefore a lot more diverse than initially thought and has gathered a new wave of attention.

### 1.1.2 General anatomy of the cerebellum

The cerebellum is connected to the brain stem via three pairs of peduncles. Anatomically, the cerebellum can be divided into the central cerebellar vermis and the two hemispheres (see Figure I). Extensive transverse folding of the cerebellar cortex substantially expands the total cortical surface thereby compacting a large number of neurons into its relatively small volume. In the sagittal plane, the cerebellar foliae divide the vermis into 10 lobules which are relatively conserved between species.

Functionally, the cerebellum is often divided into three distinct sections: the vestibulocerebellum, the spinocerebellum and the cerebrocerebellum. The vestibulocerebellum, made up of the flocculonodular lobe, receives input from and projects back to the vestibular nuclei of the brain stem. It is largely instrumental in the coordination of balance and eye movements. The spinocerebellum consists of the vermis and the adjacent paravermal parts of the hemispheres. It receives mostly proprioceptive signals from spinal

cord tracts, as well as somatosensory input from the cuneocerebellar tracts and brainstem nuclei and regulates posture and locomotion. The cerebrocerebellum comprises the areas of the cerebellar hemispheres lateral of the spinocerebellum and receives input from the contralateral cerebral cortex. Its function is the coordination of the distal limbs and learning of motor tasks. Damage to any of the aforementioned areas results in motor impairments of the ipsilateral side of the body.

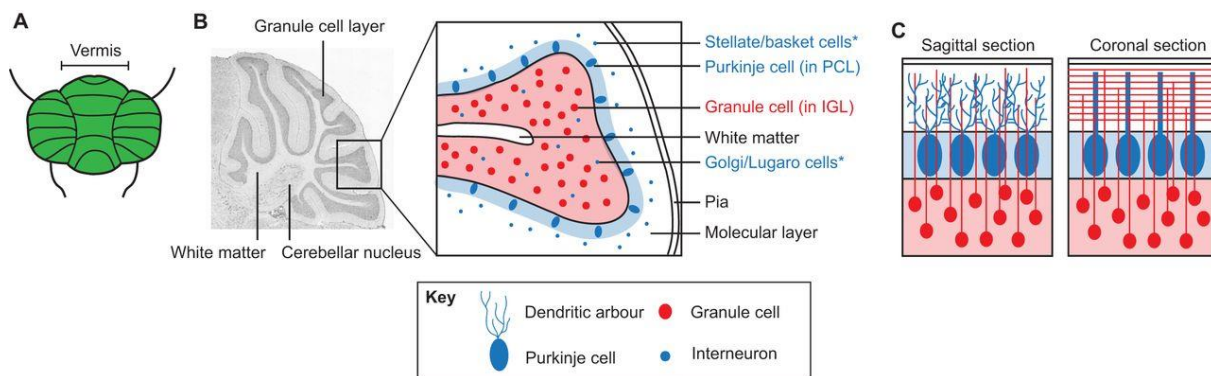


**Figure 1 Architecture of the cerebellum**

A) The superficial structure of the mammalian cerebellum shows its division into the central vermis and the two lateral hemispheres. The cerebellar cortex is folded into transverse foliae. B) Sagittal section showing the different cerebellar layers. The white matter lies internal to the granule cell layer and contains the deep cerebellar nuclei. The box insert shows the different layers more closely with the molecular layer bordering the pia mater (uncolored), the Purkinje cell layer (shown in blue) and the granule cell layer (shown in red). C) The layers are largely comprised of their namesake cell types, while the molecular layer contains mostly granule cell axons and Purkinje cell dendrites. (Butts, Green and Wingate, 2014).

The cerebellar cortex is made up of three distinct layers: the molecular layer underneath of the pia-mater, the Purkinje cell layer and the granule cell layer. The granule cell layer, which is the innermost layer adjacent to the white matter of the cerebellum, contains mostly granule cells, as well as unipolar brush cells, Golgi cells and Lugaro cells. Granule cells receive input from mossy fibers coming from nuclei of the brain stem and the spinal cord. Unipolar brush cells are excitatory interneurons and facilitate the mossy fiber input onto granule cells, while Golgi cells provide inhibitory input. Lugaro cells are also inhibitory interneurons, but synapse onto Golgi cells, as well as basket and stellate cells in the molecular layer. Here, stellate and basket cells deliver inhibitory input onto Purkinje cells. The molecular layer is otherwise mostly occupied by axons and especially dendrites of Purkinje cells, which have their somata in the Purkinje cell layer. Purkinje cells receive excitatory input from parallel fibers of granule cells and climbing fibers from cells in the inferior olive. Purkinje cells themselves project to the deep cerebellar nuclei which project

out of the cerebellum to the thalamus and brain stem. Furthermore, they also project back to the inferior olive, thereby completing the loop of cerebellar signal processing (see Figure II).

Contained in the cerebellar white matter are the deep cerebellar nuclei, which contain the main output neurons of the cerebellum. Cerebellar afferents from different brain areas or from the pontine nuclei and the cerebellar efferents from the deep cerebellar nuclei together form the cerebellar peduncles. The approximately 250 million mossy fibers from the pontine nuclei transmit the signals to around 50 billion cerebellar granule cells, which in turn innervate roughly 15 million Purkinje cells. The Purkinje cells in turn synapse onto around 1 million cells in the dentate gyrus, which project out of the cerebellum. This divergence and convergence of incoming signals has been proposed to provide an efficient system to enable pattern separation (Marr, 1969; Albus, 1971; Cayco-Gajic and Silver, 2019; Sanger et al., 2020).

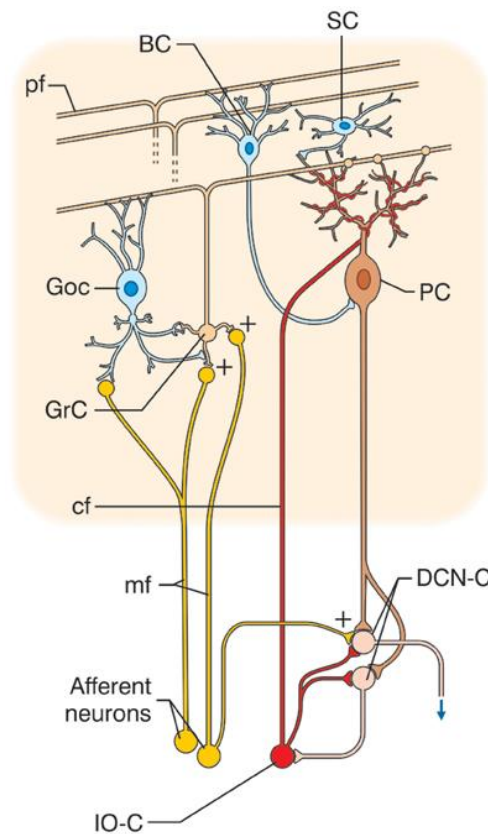


**Figure II Cerebellar cell types and their connectivity**

Schematic representation of the cerebellar cyto-architecture. The orange background shows the cortical portion of the cerebellar network. The input signals are coming from afferent neurons in the brain stem and the cerebellum as mossy fibers (mf) and from the inferior olive (IO-C) as climbing fibers (cf). The deep cerebellar nuclei (DCN-C), which also emit the cerebellar output, receives collaterals from the mossy and from the climbing fibers. The main cell types present in the cerebellar cortex are granule cells (GrC), Golgi cells (GoC), Purkinje cells (PC), stellate and basket cells (SC, BC), Lugaro cells, and unipolar brush cells (not shown). Mossy fibers (mf) innervate granule cells and Golgi cells (GrC and GoC) and the deep cerebellar nuclei. Granule cells receive inhibitory input from Golgi cells and project axons horizontally through the molecular layer (parallel fibers, pf) where they form excitatory synapses onto Purkinje cells and inhibitory interneurons (SC, and BC). Climbing fibers (cf) originating from cells in the inferior olive deliver a second excitatory input to Purkinje cells in a one-to-one fashion. The Purkinje cells in turn form inhibitory synapses with cells of the deep cerebellar nuclei and thereby complete the complex cerebellar signaling loop (Figure from D'Angelo and Casali, 2012).

### 1.1.3 Cerebellar development in the mouse

As opposed to other parts of the brain, development of the cerebellum is not yet finalized at the time of birth. First, the dorsal aspect of the anterior hindbrain, called rhombomere 1, defines the cerebellar anlage. The rhombic lip starts forming at E9.5 posterior of the cerebellar anlage and is the origin of glutamatergic neurons, such as granule cells and cells



of the deep cerebellar nuclei (Alder et al., 1996; Wang et al., 2005). The earliest populations originating from the rhombic lip are born at E9.5-12.5 and migrate to gather in two clusters to both sides of the midline called the nuclear transitory zones. The second important stem cell niche, the ventricular zone, gives rise to the progenitors of interneurons, astrocytes, Purkinje cells and Bergmann glia around E13.5 (Goldowitz and Hamre, 1998; Hoshino et al., 2005). Bergmann glia act as an important component of cerebellar organization, as they provide a lattice for dendrites in the molecular layer and are crucial for cerebellar foliation by interacting with the basement membrane (Qu and Smith, 2005).

At E10-13 Purkinje cells begin to emerge. As they express sonic hedgehog (Shh), Purkinje cells also are crucial for the development and proliferation of most other cell types in the cerebellum (Dahmane and Ruiz, 1999). Deletion of Shh in Purkinje cells reduces the number of interneurons and astroglia, while application of Shh to cerebellar slice cultures increases interneuron generation (Fleming et al., 2013; De Luca et al., 2015).

Cells emerging after E13.5 generally become granule cell precursors that proliferate in the external granule layer. The growing external granule layer and the cerebellar anlage then push the nuclear transitory zones to the interior-posterior, where they divide into two groups of the three nuclei: the fastigial nuclei, the dentate nuclei and the interpositus (which in human are two nuclei, the emboliform nuclei and the globose nuclei). At E18.5 the isthmus links the cerebellum to the tectum, a process mediated by Fgf8 and WNT1 expression (McMahon and Bradley, 1990; Thomas and Capecchi, 1990; Chi et al., 2003). Generally, Fgf8 mediates midbrain development through its interaction with the transcription factor OTX2, while interaction with GBX2 regulates hindbrain development (Joyner et al., 2000).

At E18.5, foliation of the cerebellum becomes apparent in the vermis and is complete at around 2 weeks after birth (Sotelo, 2004; Sudarov and Joyner, 2007). At the same time, granule cell precursors start to migrate along Bergmann glia processes into the internal granule cell layer, where they differentiate into mature granule cells.

#### 1.1.4 Purkinje cell development

Purkinje cells are born in waves and settle in the anterior-posterior axis under the surface of the cerebellar cortex in a multi-layer plate called Purkinje cell plate. By E18.5 Purkinje cells organize into the Purkinje cell layer that only becomes a monolayer at around p5. Migrating Purkinje cells already possess an apical neurite and an axon, which trails behind them during migration. At birth, Purkinje cells have a stellate morphology with multiple dendrites, a state in which they remain until about p6. At p8, Purkinje cells enter a stage of rapid dendritic growth and their conformation changes to a bipolar morphology with an

elaborate dendritic tree that flattens out in the sagittal plane (see Figure III). The dendritic tree then reaches its final size around 4 weeks after birth (Kapfhammer, 2004; Sotelo and Dusart, 2009).

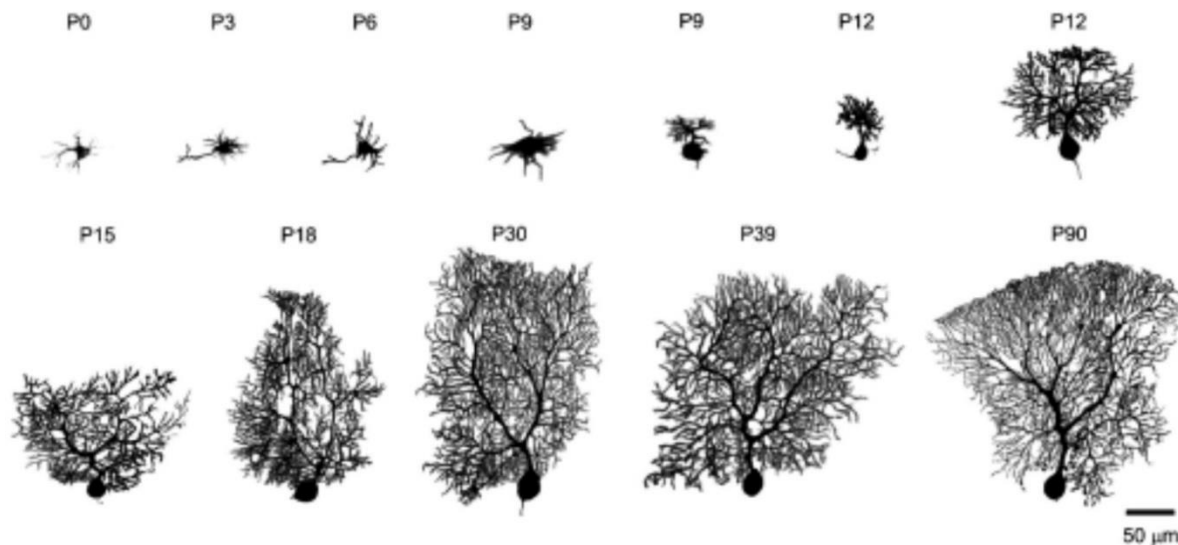


**Figure III Postnatal development of cerebellar Purkinje cells**

Purkinje cells form a primary dendrite at around postnatal day 8 and then go through a stage of rapid dendritic expansion (Adapted from McKay and Turner, 2005).

Innervation of Purkinje cells occurs early on and climbing fibers originating from the inferior olive have been described to form synapses with Purkinje cells as early as E16.5 (Rossi and Strata, 1995; Kita et al., 2015). Initially, multiple climbing fibers synapse onto each Purkinje cell. However, during the second and third postnatal week, they undergo a process of elimination, resulting in only one CF innervating each Purkinje cell through thousands of synapses. The second excitatory input onto Purkinje cells is provided by parallel fibers from granule cells. Activation of climbing fibers along with parallel fibers results in LTD at parallel fiber-Purkinje cell synapses and is thought to be crucial for motor learning (Marr, 1969; Albus, 1971; Ito, 2006).

Purkinje cells first organize into hundreds of parasagittal stripes, distinguished by the expression or lack of zebrin II (Brochu et al., 1990) and are characterized by their connectivity and the expression of specific genes (Hallem et al., 1999; Armstrong et al., 2000; Sarna et al., 2006; Chung et al., 2008; Ebner et al., 2012). It is believed that the distinct stripes act as functional compartments because a disruption of stripe patterning leads to severe motor deficits (Sarna and Hawkes, 2003; Strømme et al., 2011; White et al., 2014).

Purkinje cell development is guided and influenced by several different factors such as several hormones and growth factors, afferent input and overall Purkinje cell activity.

Hypothyroidism was shown to cause defects in the arborization and synaptogenesis of Purkinje cells (Nicholson and Altman, 1972; Brown et al., 1976; Wang et al., 2014) while treatment with thyroid hormone induces Purkinje cell dendritic outgrowth (Lindholm et al., 1993). Triiodothyronine affects the production of different growth factors such as insulin-like growth factor 1, neurotrophin 3 (NT-3), NGF and BDNF and dendritic arbor size of Purkinje cells in hypothyroid rats could also be rescued by the expression of NT-3 (Neveu and Arenas, 1996; Elder et al., 2000).

Apart from thyroid hormones, Purkinje cell development is also stimulated by the steroid hormones progesterone and estrogen, which can both be produced in Purkinje cells themselves (Tsutsui et al., 2000; Sakamoto et al., 2003; Ardesiri et al., 2006). Estrogen has furthermore been shown to facilitate Purkinje cell-parallel fiber transmission (Hedges et al., 2018).

The activity of afferent inputs onto Purkinje cells, as well as their own activity is another important factor influencing the development of Purkinje cells. With a lack of excitatory input via granule cell parallel fibers as induced by either X-ray radiation or in transgenic mouse models such as the weaver mouse or Atoh1 deletion, Purkinje cells develop with abnormal dendritic arborization and defects in the planarization of the dendritic tree (Schmidt, 1964; Rakic and Sidman, 1973; van der Heijden et al., 2020). Pharmacological activation of climbing fiber innervation caused dendritic irregularities and decreased the dendritic restriction in one plane (Kaneko et al., 2011). Furthermore, when Purkinje cell activity was suppressed with tetrodotoxin (TTX) or glutamate receptors were blocked, dendritic tree development was strongly impaired in dissociated cerebellar cultures (Schilling et al., 1991; Tanaka et al., 2006). However, in cerebellar slice cultures, the inhibition of either AMPAR, NMDAR or mGluR1 was not sufficient to decrease Purkinje cell dendritic outgrowth and a combination of blocking all glutamate receptors was necessary to induce a small reduction of Purkinje cell dendritic tree size (Adcock et al., 2004).

## **1.2 Protein kinase C (PKC)**

The protein kinase C family of serine/threonine kinases comprises several subtypes, such as conventional (classical), novel and atypical PKCs. The three subtypes are classified by their mode of activation. Classical PKCs (cPKCs), including PKC  $\alpha$ ,  $\beta$  and  $\gamma$  are activated by binding to calcium and diacylglycerol (DAG) and phosphatidylserine. Novel PKCs (PKC  $\delta$ ,  $\epsilon$ ,  $\eta$ , and  $\theta$ ), while being independent of  $\text{Ca}^{2+}$ , require binding of DAG and PS. Their setup of

domains is also slightly different, lacking the C2 module in the regulatory domain. Atypical PKCs ( $\zeta$  and  $\lambda$ ) require neither  $\text{Ca}^{2+}$  nor DAG to be activated (Nishizuka, 1992).

### 1.2.1 PKC domain structure

All PKC family members are made up of an N-terminal, regulatory domain and a C-terminal catalytic domain, linked by a flexible hinge region. The pseudosubstrate domain (PS-domain) at the N-terminal end normally occupies the substrate binding pocket, keeping the enzyme in a deactivated conformation. The structure of the pseudosubstrate unit resembles a substrate motif, in which the phospho-acceptor site is an alanine and therefore, cannot be phosphorylated. In the truncated PKM $\zeta$  isoform of PKC $\zeta$ , the pseudosubstrate domain is missing and leads to constitutive activation of the kinase (Sacktor et al., 1993). The hinge region is susceptible to cleavage by caspase-3, which renders the kinase unable to self-inhibit. It then remains in an activated state in which it is more vulnerable to degradation (Smith et al., 2000).

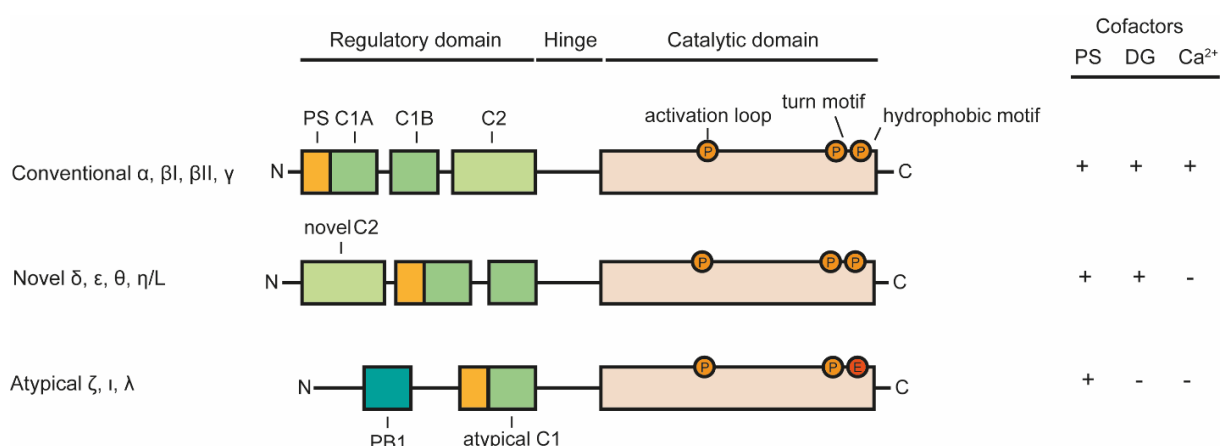


**Figure IV Domain structure of different PKC isoforms**

Proteins of the PKC superfamily contain a regulatory domain comprised of the C1 (C1A and C1B) and C2 domains, a flexible hinge region and a catalytic domain containing the three phosphorylation sites necessary for the activation of PKC. Novel PKCs differ in their arrangement of the regulatory domains. Atypical PKCs possess a PB1 domain in place of a C2 domain and also contain an atypical C1 region. At the phosphorylation site in the hydrophobic motif, atypical PKCs have a glutamate, which mimics phosphorylation. While classical PKCs can be activated in the presence of  $\text{Ca}^{2+}$ , diacylglycerol or phosphatidylserines,  $\text{Ca}^{2+}$  is not necessary for the activation of novel and atypical PKCs. Furthermore, atypical PKCs are activated independent of diacylglycerol as well (Adapted from Newton, 2018).

Before becoming fully activated, PKCs must undergo several steps of phosphorylation and interact with specific binding-partners to acquire its mature, fully functional state. In conventional PKCs, three subsequent phosphorylation events, one in the activation loop, one in the turn motif and one in the hydrophobic motif, are necessary to enable the consecutive

interactions with its binding partners. Newly generated PKC is membrane-associated with its PS-domain still unbound, which allows for the binding of HSP90, enabling phosphorylation of the activation loop by phosphoinositide-dependent kinase-1 (PDK1). This first phosphorylation allows for a repositioning of the PKC domains to gain full accessibility and opens up the phospho-acceptor site. Autophosphorylation of two more sites at the C-terminus then induces the conformational change in which the PS-domain can bind to the substrate binding pocket. In atypical PKCs, there is no autophosphorylation of the hydrophobic motif, however, these isoforms possess a glutamic acid residue mimicking phosphorylation. In fact, this phosphorylation step seems to be protective for PKC, as dephosphorylation is normally followed by degradation (Parker et al., 1995; Wang et al., 2016). This mature PKC now remains in the cytosol and can readily be activated by binding partners. In its closed, inactive conformation, PKC is protected from proteolysis (Dutil and Newton, 2000) and the C1 domain is masked, preventing erroneous activity (Antal et al., 2014).

Mature cPKCs are activated by calcium and locate back to the membrane upon it binding to the C2 domain. Here, the C1B domain can interact with DAG or phosphatidylserines which then triggers the release of the PS-domain. Novel PKCs lack a functional C2 domain, however, their C1B domain has a much higher affinity to DAG and they are therefore most commonly located in DAG rich membranes such as those of the Golgi apparatus (Dries et al., 2007). Due to the higher presence of DAG, novel PKCs commonly remain active for a longer timespan than classical PKCs, whose activity and membrane residence time correlates with dynamic calcium spikes (Gallegos et al., 2006). The activation of atypical PKCs is entirely independent of  $\text{Ca}^{2+}$  or DAG and activation is achieved by the binding of its PB domain to other proteins such as Par6 and lipid components like phosphatidylinositol and ceramide (Lin et al., 2000; Wang et al., 2009). The binding of different cofactors thereby modulates the membrane retention time and turnover speed of PKC subspecies differentially.

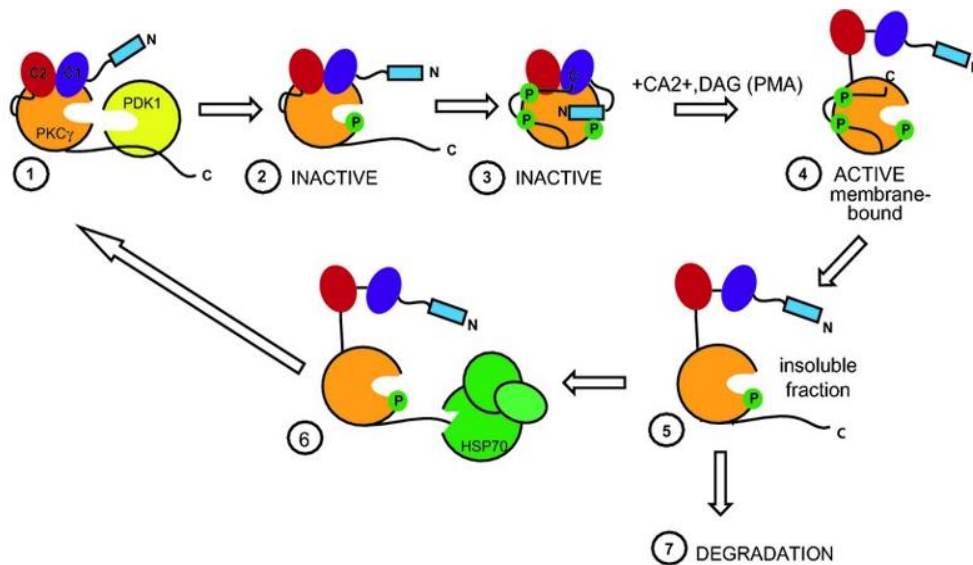


**Figure V Life cycle of PKC**

Model of the life cycle of classical PKCs. Inactive PKC binds to and is phosphorylated by PDK1 at Thr514. (1). This is followed by two autophosphorylations at Thr655 and Thr674 (2), which leads to its final mature, closed conformation with the pseudosubstrate domain occupying the substrate binding pocket (3). In following activation through  $\text{Ca}^{2+}$  and DAG or pharmacological application of PMA, PKC translocates to the plasma membrane. PKC is now in its active conformation (4). Upon dephosphorylation, PKC is targeted to the insoluble fraction (5). Dephosphorylated PKC can bind HSP70, which allows PKC recycling (6) or is degraded (7) (Jezierska et al., 2014).

Independently of their regular binding partners, PKCs can also be activated by other factors such as reactive oxygen species (Lin and Takemoto, 2005) oxidizing a cysteine residue in the C1B domain. Novel PKC family members are furthermore phosphorylated by Src kinases which causes a relocalization to the nucleus and is followed by calpain-mediated cleavage of the hinge domain resulting in constitutive activation without translocation to the membrane (Konishi et al., 1997, 2001; Humphries et al., 2008).

When PKCs have reached their activated state, they become susceptible to dephosphorylation and degradation. PH domain Leucine-rich repeat Protein Phosphatase (PHLPP) first dephosphorylates the hydrophobic motif (Gao et al., 2008) of PKC. This first dephosphorylation induces a conformational change making the activation loop and the turn motif accessible for dephosphorylation via PP2A phosphatases. Dephosphorylated PKC is then ubiquitinated and degraded (Lee et al., 1996). Dephosphorylated PKC can be bound by heat-shock protein 70 (HSP70), which leads to stabilization and prevents degradation, making PKC available to re-enter the activation cycle.

## 1.2.2 PKC $\gamma$

### *Overview*

PKC $\gamma$  is one of the members of the classical PKCs and involved in a multitude of downstream processes. It is predominantly present in neurons of the central nervous system (CNS), where it is most highly expressed in hippocampal pyramidal cells and Purkinje cells of the cerebellum, where it is located in the soma, dendrites and axons (Kikkawa et al., 1988). In the cerebellar cortex, all cPKC isoforms are expressed, with granule cells expressing PKC $\alpha$  and PKC $\beta$ I/II, while Purkinje cells express the isoforms PKC $\alpha$  and PKC $\gamma$  (Takahashi et al., 2017).

### *PKC $\gamma$ Signaling*

In Purkinje cells, PKC $\gamma$  can be activated downstream of metabotropic glutamate receptor 1 (mGluR1). Upon glutamate binding, mGluR1 is activated which then leads to the release of DAG and IP $_3$  via PLC. IP $_3$  then causes a release of calcium from the ER into the cytosol. The increase in Ca $^{2+}$  and the increased availability of DAG then in turn activates PKC $\gamma$ .

Many interesting findings could be derived from PKC $\gamma$  knockout mice, revealing its role in the modulation of receptors, long-term depression (LTD), long-term potentiation (LTP) and climbing fiber elimination in the cerebellum. One early observation was made by Abeliovich *et al.* (1993), who first created a PKC $\gamma$  knockout mouse and showed, that LTP in this mouse was strongly impaired, while LTD remained unaltered. The impairment of LTP was however, not uniform and dependent of the stimulation protocol. When the induction of LTP was preceded by a low frequency stimulation, hippocampal slices were still able to produce normal LTP. PKC $\gamma$  might therefore play an important part in the successful generation of LTP, however, is not solely responsible for it.

Previously it had been shown, that inhibition of PKC resulted in decreased LTD, while the administration of PKC was able to elicit LTD in cultured Purkinje cells (Linden and Connor, 1991). A blockage of LTD was furthermore found in a transgenic mouse model expressing a PKC inhibitor in Purkinje cells (De Zeeuw et al., 1998). Further studies showed also that PKCs were able to phosphorylate the GluR2 subunit of AMPA, a subunit expressed at parallel-fiber synapses onto Purkinje cells, causing a desensitization to glutamate (Matsuda et al., 1999). However, it was later on found that this phosphorylation was mediated by PKC $\alpha$  (Leitges et al., 2004) and studies using several knockout models could show that LTD was

independent of PKC $\gamma$  (Colgan et al., 2018). Nevertheless, in mice carrying the S119P mutation in the PRKCG gene, a mutation associated with SCA14, LTD was disrupted (Shuvaev et al., 2011). The authors furthermore report a reduction of membrane residence time of PKC $\alpha$  and hypothesize that an overactivation of PKC $\gamma$  in the cytoplasm could lead to increased Diacylglycerol kinase  $\gamma$  (DGK $\gamma$ ) phosphorylation, a kinase involved in the DAG homeostasis in the membrane. Dysregulation of DAG presence would then in turn lead to a decrease in membrane association of PKC $\alpha$  and PKC $\gamma$ . Interestingly, a recent study using DGK $\gamma$  knockout mice also observed impaired LTD in their mouse model (Tsumagari et al., 2020). In this mouse model, the activity of PKC $\gamma$  was upregulated and inhibition of PKC $\gamma$  led to restored LTD. PKC $\gamma$ , as the predominant isoform in Purkinje cells, may therefore exert a modulatory effect on LTD. However, this effect is likely to be indirect and mediated via other signaling molecules.

One of the most significant findings in PKC $\gamma$  knockout mice was that about 40% of cerebellar Purkinje cells remained enervated by multiple climbing fibers (Kano et al., 1995). In fact, it was later found that also in knockout mice of mGluR1 (Kano et al., 1997) and PLC $\beta$ 4 (Kano et al., 1998) climbing fiber elimination is disrupted, outlining the importance of the mGluR1-PLC-PKC $\gamma$  signaling cascade in this process.

### *PKC $\gamma$ and dendritic development*

In cerebellar Purkinje cells, PKC $\gamma$  furthermore seems to be a major regulator of dendritic development. Our laboratory had shown previously that stimulation of cerebellar organotypic slice cultures with the PKC activator PMA induces a reduction in dendritic outgrowth of cerebellar Purkinje cells (Metzger and Kapfhammer, 2000). On the other hand, in organotypic slice cultures from PKC $\gamma$  knockout mice or from cultures in which PKC activity was inhibited pharmacologically, expansion of the Purkinje cell dendritic tree is increased (Metzger and Kapfhammer, 2000; Schrenk et al., 2002). Since the pathways involved in PKC $\gamma$ -mediated inhibition of dendritic development have not been fully established, additional knowledge of these mechanisms will be required for a better understanding and eventually for the development of treatments for PKC $\gamma$ -related disorders.

## **1.3 Spinocerebellar ataxia**

The term ataxia has been used to describe a patient's loss of control over different motor functions, aptly fitting the original meaning of the word in Greek - "loss of order". Similarly, neurodegenerative diseases with concurring loss of motor function



have been termed ataxia as well, with spinocerebellar ataxia (SCA) describing disorders affecting the cerebellum and its related pathways. SCAs are a very heterogeneous group of diseases, with most SCAs being of the hereditary, autosomal-dominant type (ADCA), however, also recessive types, X-linked and non-genetic types have been described. The age of onset depends strongly on the subtype, which could be as early as childhood or as late as in old age. In general, most patients start showing symptoms in mid-adulthood. Patients commonly develop difficulties of the coordination of fine movements such as talking, grasping and oculomotion as well as in walking. Additionally, especially in late stages of the disease, also psychological symptoms like depression and sleep-deprivation can occur. Amongst ADCAs, the genetic cause are often polyglutamine repeats, which can be located in different genes, for SCAs often in the group of the *ataxin* genes. The second type of ADCAs are SCAs caused by point mutations or small deletions in a variety of different genes, which further expands the group of possibly affected loci. Up to date, around 48 different autosomal-dominant cerebellar ataxias have been identified (Bird, 2019). Globally, the prevalence of SCAs has been assumed to be around 3 in 100.000 (Ruano et al., 2014). However, the heterogeneous nature of the disease makes testing challenging and could result in many cases not correctly identified.

### 1.3.1 SCA14

Spinocerebellar ataxia type 14 is caused by mutations in the *PRKCG* gene. The variety of mutations in the *PRKCG* include point mutations, missense mutations and deletions in virtually all of the protein's domains. Up to now, more than 40 different mutations have been found in patients presenting with SCA14 (Wong et al., 2018; Shirafuji et al., 2019). Typically, the age of onset of this subtype is between early and late 30s and patients generally seem to not have a decreased life-expectancy.

Patients generally experience cerebellar ataxia, especially affecting their gait, coordination and balance. Commonly, also more precise movements such as speech and eye movement are affected. In some cases, patients also develop vertigo or psychological symptoms such as depression, psychosis or a decline in their cognitive abilities. MRI scans of SCA14 patients show cerebellar atrophy in the hemispheres and especially the vermis (Brkanac et al., 2002; Klebe et al., 2007; Chelban et al., 2018). Post-mortem histological analyses showed mild to severe Purkinje cell atrophy in the cerebellar cortex (Brkanac et al., 2002; Wong et al., 2018).

Several studies have addressed the mechanisms as to how PKC $\gamma$  mutations may lead to the occurring pathogenicity. Since SCA14 is inherited in an autosomal-dominant way, it is unlikely that PKC $\gamma$  mutations lead to a loss of function. Furthermore, as stated earlier, PKC $\gamma$  inhibition increases dendritic outgrowth in cerebellar Purkinje cells and PKC $\gamma$  knockout mice show no signs of ataxia or cerebellar atrophy (Chen et al., 1995; Kano et al., 1995). Therefore, instead of a loss-of function of PKC $\gamma$ , a negative effect of increased kinase activity or a toxic gain-of function seem to be the underlying cause for the pathology of SCA14.

### *Changes in the activity of PKC $\gamma$*

In fact, several in-vitro studies have shown an increase in kinase activity for more than 20 spontaneous PKC $\gamma$  mutations (Verbeek et al., 2005; Adachi et al., 2008). Until now there have been few mouse models of SCA14. Zhang *et al.* (2009) developed a transgenic mouse expressing the H101Y mutant PKC $\gamma$  under a universal promotor and report that the mice develop ataxia as well as alterations in Purkinje cell dendritic development.

Our group as well has created a transgenic mouse expressing the human S361G mutation under the control of the L7-promotor, ensuring Purkinje cell specific expression (Ji et al., 2014). These mice develop mild cerebellar ataxia, as well as Purkinje cell atrophy especially in lobule VII of the cerebellum (Ji et al., 2014). Interestingly, the morphology of Purkinje cells in organotypic slice cultures prepared from these mice show a similar morphology to cells after stimulation with PMA, a PKC activator (Metzger and Kapfhammer, 2000; Gugger et al., 2012).

In further studies using dissociated cerebellar cultures we showed that transfection of several mutant PKC $\gamma$  constructs led to increased kinase activity in two out of three kinase-domain mutations (Shimobayashi and Kapfhammer, 2017). However, none of the regulatory-domain mutations tested seemed to increase the activity of PKC $\gamma$  which outlines that depending on the location, PRKCG-mutations could affect PKC $\gamma$  function in different ways.

### *Changes in Protein Structure*

PKC $\gamma$  mutations have also been shown to impair the protein structure and lead to aggregation (Seki et al., 2005; Doran et al., 2008; Shuvaev et al., 2011; Wong et al., 2018) that can in turn alter protein degradation and result in defective membrane translocation or target phosphorylation (Yamamoto et al., 2010; Wong et al., 2018). However, in primary cultures of cerebellar Purkinje cells, SCA14 associated mutant PKC $\gamma$  led to decreased dendritic development independent from protein aggregation (Seki et al., 2009). Additionally,

wildtype PKC $\gamma$  has been shown to be able to form amyloid-like fibrils (Takahashi et al., 2015). Aggregation may therefore not cause SCA pathology per se, but likely contribute to it.

### *Impaired downstream signaling*

Apart from aggregation, PKC $\gamma$  mutations in the C1B domain have been shown to also lead to a change in the conformation of PKC $\gamma$ , resulting in higher accessibility of the C-terminus and decreased downstream MAPK signaling (Verbeek et al., 2008; Jezierska et al., 2014), which would argue that at least in some cases PKC $\gamma$  mutations could ultimately lead to decreased biological activity. In vitro, it has been found that several PKC $\gamma$  mutations lead to a lack of inhibition of the transmembrane cation channel TRPC3, resulting in an increase of intracellular calcium (Adachi et al., 2008). In fact, dysregulation of intracellular calcium is a common theme amongst several hereditary SCAs which are caused by mutations in some crucial modulators of Ca<sup>2+</sup><sub>i</sub>, such as CACNA1A (SCA6) and CACNA1G (SCA42). Interestingly, some of the mutations leading to SCA are found in molecules which share common pathways with PKC $\gamma$  such as TRPC3 (SCA41), IP3R1 (SCA15/16/29) and GluD2 (SCAR18). It is therefore possible, that also in SCA14 a dysregulation of intracellular calcium homeostasis contributes to the pathology.

### *Generation of in vitro iPSC models*

Most of the studies mentioned above have been performed in vitro. A recent study furthermore explored the use of patient-derived induced pluripotent stem cells (iPSCs) as a tool to model the pathology observed in human brains (Wong et al., 2018). While in this study the iPSCs were not differentiated further, another study has used iPSCs derived from SCA6-patients to generate Purkinje cells which developed the characteristic morphology of Purkinje cells in vivo (Ishida et al., 2016). In the future these models will hopefully provide new approaches to get a better understanding of the disease burden on cerebellar Purkinje cells and aid in the discovery of potential medications.

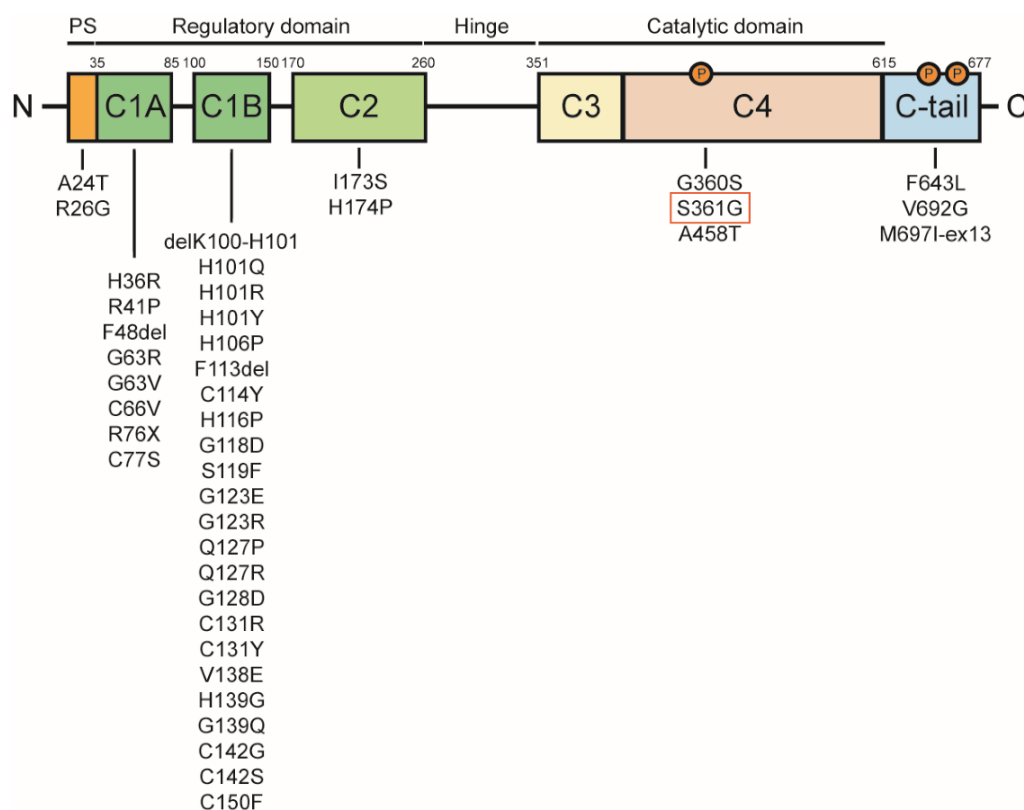


**Figure VI PRKCG mutations associated with SCA14**

Localization of different mutations in PKC $\gamma$  associated with SCA14. Most known mutations are found in the C1 (C1A and C1B) and C2 domains. The S361G-mutation investigated in our studies is highlighted in a red box and located in the C4 catalytic domain. The three PKC $\gamma$  phosphorylation sites (Thr514, Thr655 and Thr674) are marked in orange. PS = pseudosubstrate domain (the figure was adapted from Wong *et al.* (2018); included Shirafuji *et al.* (2019) and Riso *et al.* (2020)).

## 1.4 The collapsin response mediator proteins (CRMPs)

Collapsin response mediator proteins (CRMPs) are a group of cytosolic proteins associated with many neurodevelopmental processes such as neurite outgrowth and differentiation, dendritic spine organization and axonal transport. CRMP2 was found to be involved in the Semaphorin-3A (Sema3A, also known as collapsin) pathway giving the group of proteins their now most established name. CRMP genes were discovered in different species and published around the same time resulting in a complex nomenclature including the terms CRMP (Goshima *et al.*, 1995), turned on after division, 64 kDA protein (TOAD) (Minturn *et al.*, 1995), unc 33-like protein (Ulip) (Byk *et al.*, 1996), and dihydropyrimidase-related protein (DRP) (Hamajima *et al.*, 1996). The term Toad64/Ulip/CRMP (TUC) was introduced to simplify the discussion of this protein family but has not been adopted by the community (Quinn *et al.*, 1999). Due to its structural similarity to liver enzyme

dihydropyrimidase, the name dihydropyrimidase-like protein (DPYSL) is widely used to label the respective CRMP genes.

**Table I CRMP nomenclature**

(adapted from Tan, Thiele and Li, 2014).

<b>CRMP1</b>	<b>CRMP2</b>	<b>CRMP3</b>	<b>CRMP4</b>	<b>CRMP5</b>
DPYSL1	DPYSL2	DPYSL4	DPYSL3	DPYSL5
Ulip3	Ulip2	Ulip4	Ulip1	Ulip6
DRP1	DRP2	DRP4	DRP3	DRP5
TUC-1	TUC-2	TUC-3	TUC-4	
C22	TOAD-64		hUlip	CRAM

Initially, CRMP1-4 were identified as members of the same family as they share about 70% homology (Byk et al., 1998). CRMP5 was identified later and it was first proposed to comprise its own subfamily, since it only shares about 50% homology with the other family members (Fukada et al., 2000). CRMP1, 2 and 4 possess alternatively spliced isoforms that appear to be involved in distinct processes (Quinn et al., 2003).

Crystal structures have shown that the CRMPs are largely similar to the liver enzyme dihydropyrimidase (Hamajima et al., 1996). However, CRMPs lack the necessary His residues in their catalytic site that usually enable enzymatic activity (Hamajima et al., 1996; Wang and Strittmatter, 1997; Deo et al., 2004). Commonly, CRMPs oligomerize and can form homo- as well as heterotetramers, wherein certain family members preferentially interact, while others do not (Wang and Strittmatter, 1996, 1997; Fukada et al., 2000). It is speculated that tetramer combination provides a first level of modulating CRMP function in several pathways (Zhang et al., 2008; Ponnusamy and Lohkamp, 2013). CRMP proteins are involved in a multitude of processes such as neuronal differentiation, neurite outgrowth, intracellular protein transport and synaptic transmission (Inagaki et al., 2001; Quach et al., 2004; Kawano et al., 2005; Kimura et al., 2005). It has been found that CRMP functions are largely regulated via post-translational modifications such as phosphorylation, SUMOylation, O-GlcNAcylation or oxidation (Arimura et al., 2000; Khidekel et al., 2007; Dustrude et al., 2013; Marques et al., 2013) and that altered CRMP phosphorylation is correlated with neurodegeneration and disease (Crews et al., 2011; Petratos et al., 2012; Mokhtar et al., 2018).

CRMPs are expressed most highly in the central nervous system, the spinal cord and peripheral nerves. Generally CRMPs are highly expressed during early development and

decrease in expression during adulthood (Byk et al., 1996, 1998; Wang and Strittmatter, 1996; Fukada et al., 2000; Inatome et al., 2000). Several CRMP isoforms have also been detected in other tissues such as the placenta (CRMP1) (Qiao et al., 2015), heart and lung tissue (CRMP2) (Hamajima et al., 1996) and the testis (CRMP1/4/5) (Taketo et al., 1997; Kato et al., 1998; Ricard et al., 2001). CRMP2 mRNA was furthermore detected in human monocytes and hypothesized to potentially act as a mediator of differentiation (Rouzaut et al., 2000). While CRMPs are generally cytosolic proteins, several studies have reported their localization in membrane-rafts (Rosslénbroich et al., 2003; Mileusnic and Rose, 2011) where they could interact with several membrane-proteins.

Almost all CRMP family members (CRMP1, 2, 4 and 5) have been found to be differentially regulated in various types of cancer (Shih et al., 2001; Yu et al., 2001; Wu et al., 2008; Gao et al., 2010; Pan et al., 2011), in which their expression has been associated with tumor migration, invasion and differentiation. Furthermore, anti-CRMP5 antibodies have been detected in patients presenting with small-cell lung cancer and paraneoplastic cerebellar ataxia (Honnorat et al., 1996; Yu et al., 2001).

### 1.4.1 CRMP2

#### *Overview*

CRMP2 is the best studied CRMP family member as it was identified early on for its role in Semaphorin 3A signaling (Goshima et al., 1995). It is expressed most highly in neurons of the CNS, however, it has also been detected in oligodendrocytes and, in low levels, in microglia (Ricard et al., 2001; Zhang et al., 2014). CRMP2 expression is highest during development and especially early after birth. However, unlike other CRMPs, it also remains expressed at lower levels in the adult brain (Wang and Strittmatter, 1996; Bretin et al., 2005). In neural stem cells, overexpression of DPYSL2 induces their differentiation into neurons (Xiong et al., 2020), which could be linked to its interaction with numb (Nishimura et al., 2003), a protein shown to be critical in neurogenesis (Zhong et al., 2000). Due to its involvement in Semaphorin 3A signaling, especially the effect of CRMP2 on axonal outgrowth has been extensively researched. Overexpression of CRMP2 was shown to increase axonal growth and lead to the formation of multiple axons in hippocampal neurons, while on the other hand, knockdown of CRMP2 decreased axonal outgrowth (Inagaki et al., 2001; Yoshimura et al., 2005).

In recent years, three CRMP2 knockout mouse models were established: one brain-specific knockout (Zhang et al., 2016), one general knockout (Makihara et al., 2016) and one neuronal knockout model (Moutal et al., 2019a). While the latter has not been thoroughly

characterized yet, the other two models revealed disrupted dendritic spine formation as well as altered dendritic and axonal patterning. Interestingly, the effects observed appeared to be more prominent in the brain specific knockout, which could be attributable to other CRMP family members compensating the lack of CRMP2 in the general knockout. Zhang *et al.* (2016) furthermore observed defective synapse formation and reduced LTP. It has been known that CRMP2 can regulate the membrane localization of several ion-channels, such as voltage gated sodium-channels (Nav1.7) (Dustrude *et al.*, 2013), voltage gated calcium channels (Cav2.2), sodium-calcium exchanger 3 (NCX3) and NMDA receptors (Brustovetsky *et al.*, 2014), which could provide the means to alter synaptic plasticity.

CRMP2 can regulate protein localization or mediate protein trafficking either by direct binding, or through interactions with components of the cytoskeleton and its associated proteins dynein and kinesin (Kawano *et al.*, 2005; Kimura *et al.*, 2005; Arimura *et al.*, 2009). In hippocampal neurons, CRMP2 and 4 have been proposed to link microtubules and actin thereby supporting coordinated cytoskeletal movement (Tan *et al.*, 2015). Through interactions with the light chain of kinesin-1, CRMP2 is furthermore involved in the transport of the actin-regulating WASP-family verprolin homologous protein 1 (WAVE1) protein complex and tubulin dimers to the distal portion of the extending axon (Kawano *et al.*, 2005; Kimura *et al.*, 2005). Apart from anterograde transport mechanisms, CRMP2 also controls retrograde protein transport by negatively regulating cytosolic dynein through direct binding (Arimura *et al.*, 2009). This interaction has been shown to enforce the organized retrograde transport of vesicles via MICAL-like protein 1 (MICAL-L1) and Eps 15 homology domain protein 1 (EHD1) (Rahajeng *et al.*, 2010). Outside of the CNS, CRMP2 was furthermore shown to interact with another cytoskeletal protein, vimentin, and thereby regulate lymphocyte migration (Vincent *et al.*, 2005).

One of the most extensively researched functions of CRMP2 is its role in microtubule stabilization (Inagaki *et al.*, 2001; Quach *et al.*, 2004; Kawano *et al.*, 2005; Kimura *et al.*, 2005). CRMP2 can interact with both, soluble  $\alpha/\beta$ -tubulin dimers (Fukata *et al.*, 2002) and stabilized microtubules. These interactions are likely to be conferred by different binding domains in the CRMP2 protein. A central domain of CRMP2 (aa323-381) was shown to enable tubulin binding, however, these sites are probably not easily accessible on tetramerized CRMP2 and therefore require its disassociation before binding (Fukata *et al.*, 2002; Niwa *et al.*, 2017). The direct binding and stabilization of microtubules was shown to be dependent of residues in the C-terminus of CRMP2 (Lin *et al.*, 2011), which contain the phosphorylation target sites of cyclin-dependent kinase 5 (Cdk5), glycogen synthase kinase 3 $\beta$  (GSK3 $\beta$ ), Rho-associated protein kinase 2 (ROCK2) and PKC. Phosphorylation of these

residues has been proposed to add additional negative charges to the domain thereby enabling for precise control of interactions (Sumi et al., 2018). In fact, various posttranslational modifications provide regulation of most CRMP2 functions.

### *CRMP2 post-translational modifications*

Several targets of phosphorylation, SUMOylation, O-GlcNAcylation, oxidation and carbonylation have been identified in CRMP2 (Arimura et al., 2000; Khidekel et al., 2007; Ju et al., 2013; Marques et al., 2013; Toyoshima et al., 2019). Most of these modification sites cluster in the C-terminus, where also several binding domains for cytoskeletal and motor proteins have been identified (Kawano et al., 2005; Kimura et al., 2005; Arimura et al., 2009; Rahajeng et al., 2010; Lin et al., 2011).

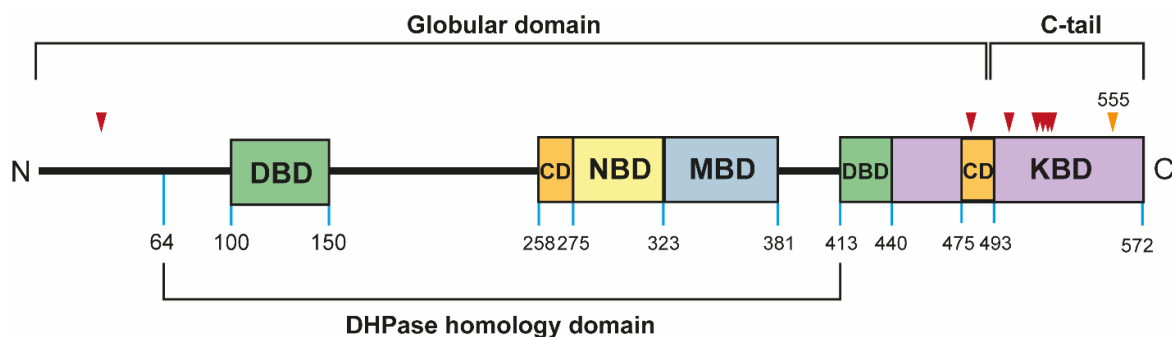


**Figure VII CRMP2 domain structure**

The CRMP2 protein consists of a large globular domain and a c-terminal tail domain. A central domain is largely homologous to liver DHPase. The active sites are, however, missing. Several domains have been identified to mediate binding to molecules such as dynein heavy chain (DBD), calmodulin (CD), Numb protein (NBD) and kinesin light chain (KBD). Two domains have been identified to take part in binding to free tubulin or polymerized microtubules (MBD), one in the globular domain and one located in an unspecified segment of the c-terminal tail. CRMP2 can be phosphorylated at various target sites (red arrowheads) with most known sites located in the c-terminus. The location of the Thr555 phosphorylation site is indicated with a yellow arrowhead (adapted from Rahajeng et al., 2010).

Recently, dysregulation of CRMP2 modifications have been associated with disease such as Alzheimer's disease, multiple sclerosis and Huntington's disease (Cole et al., 2007; Petratos et al., 2012; Lim et al., 2014; Mokhtar et al., 2018). Furthermore, CRMP2 SUMOylation is involved in the mediation of pain by modulating Nav1.7 (Dustrude et al., 2013; Moutal et al., 2018). After spinal cord injury (SCI), phosphorylated CRMP2 is upregulated (Gögel et al., 2010) and blocking CRMP2 phosphorylation in a knock-in mouse model improved recovery after SCI (Nagai et al., 2016). In psychological disorders such as schizophrenia and bipolar disorder, CRMP2 was identified as one of the target molecules in



lithium treatments and increased post-translational modification has been reported in both diseases (Tobe et al., 2017; Garza et al., 2018; Toyoshima et al., 2019).

CRMP2 O-GlcNAcylation and oxidation are some of the lesser understood CRMP2 PTMs and are potentially regulating CRMP2 phosphorylation (Cole and Hart, 2001; Morinaka et al., 2011; Gellert et al., 2013; Leney et al., 2017; Muha et al., 2019).

Phosphorylation of CRMP2 has been shown to be the most powerful modulator of its functions. Amongst the kinases targeting CRMP2 are Fyn, Yes, GSK3 $\beta$ , Cdk5, ROCK2 and CaMKII, most of which lead to a reduction of neurite outgrowth (Arimura et al., 2000, 2005; Uchida et al., 2005, 2009; Yoshimura et al., 2005; Hou et al., 2009; Varrin-Doyer et al., 2009). Phosphorylation at Ser522 by Cdk5 enables subsequent phosphorylation through GSK3 $\beta$  at Thr509, Thr514 and Ser518 and provides an additional level of modulation (Brown et al., 2004; Uchida et al., 2005; Yoshimura et al., 2005; Cole et al., 2006). Also ROCK2 mediated phosphorylation at Thr555 has been proposed to be involved in the Thr555-Ser522-Thr514 phosphorylation cascade (Ikezu et al., 2020). To elucidate the role of the mentioned PTMs, several knock-in mice models have been established, focussing on the Ser522 site (Yamashita et al., 2012; Niisato et al., 2013; Moutal et al., 2019c). In these studies, the Ser522 site was mutated to an alanine to disable phosphorylation. Layer V cortical neurons from these mice showed a larger number of primary dendrites, an effect that was even increased when combined with the knockout of CRMP1 (Yamashita et al., 2012). In another study, the hippocampal CA1 pyramidal neurons from knock-in mice did not show any overt changes, however, when CRMP4 was knocked out in addition, the neurons showed an increased amount of proximal bifurcation (Niisato et al., 2013). Furthermore, in combined CRMP2 knock-in/CRMP4 knockout mice, addition of Sema3A could not induce dendritic outgrowth as it does in wildtype. These studies highlight the role of CRMP2 in dendritic outgrowth and also, how several CRMPs are involved and can compensate defects in shared pathways.

Recently it was demonstrated that migration and positioning of Purkinje cells were impaired in mice, in which the S522A knock-in was combined with the knockout of CRMP1 and 4 (Yamazaki et al., 2020) which proposes a novel role for CRMP2 in the cerebellum. In the cerebellum, CRMP2 is expressed in oligodendrocytes, granule cells and Purkinje cells, where it is localized throughout the cell (Bretin et al., 2005).

Marques *et al.* (2013) have shown that PKC-mediated phosphorylation of CRMP2 at threonine 555 leads to a delay in maturation and neurite outgrowth of dorsal root ganglion neurons. They furthermore argue that PKC can phosphorylate GSK3 $\beta$ , leading to its inhibition and subsequently resulting in a downregulation of Thr514-phosphorylated CRMP2,

which had a neurite promoting effect. PKC therefore can regulate CRMP2 related neurite outgrowth in a bidirectional manner.

As PKC $\gamma$  is an important signaling molecule in dendritic development of cerebellar Purkinje cells, the investigation of a potential relationship of the two proteins could provide valuable new insights in a signaling cascade which has not yet been looked at in detail.

**Table II CRMP2 post-translational modifications**

(adapted from Moutal, White, *et al.*, 2019)

Residue(s) (Modification)	Enzyme	Function	Targeting peptides and compounds
Y32 (phosphorylation)	Fyn, Fes/Fps	Inhibition of neurite outgrowth, Decreased CRMP2 SUMOylation and NaV1.7 membrane localization	Unknown
Y479 (phosphorylation)	Yes, Fer, Fyn, Fes/Fps	Cytoskeletal reorganization in T cell migration, loss of affinity for microtubules, disruption of CRMP2 tetramers	Unknown
Y499 (phosphorylation)	Fer	Loss of affinity for microtubules, disruption of CRMP2 tetramers	Unknown
T509/T514/S518 (phosphorylation)	GSK3 $\beta$	Loss of affinity for tubulin, cellular proliferation, disruption of CRMP2 tetramers	Naringenin, (S)- lacosamide, lanthionine ketimine ester, edonergic maleate
S522 (phosphorylation)	Cdk5	Loss of affinity for tubulin, cancer cell proliferation, promotes CaV2.2 and NaV1.7 membrane localization, disruption of CRMP2 tetramers	(S)-lacosamide, lanthionine ketimine ester, edonergic maleate
T555 (phosphorylation)	ROCK2, CaMKII PKC	Decreased affinity for tubulin, decreased neurite outgrowth	Unknown
K374 (SUMOylation)	Ubc9	NaV1.7 trafficking	CRMP2 SUMOylation motif peptide
S517 (O-GlcNAcylation)	Unknown	Unknown	Unknown
C504 (oxidation)	Unknown	CRMP2 dimerization, microtubule regulation, growth cone collapse	Unknown

---

# Aims of the thesis

---

## **I. Identify PKC $\gamma$ -mediated effector molecules involved in dendritic development**

The primary aim of this thesis was to identify downstream targets of PKC $\gamma$  which have the potential to influence dendritic development of cerebellar Purkinje cells. To achieve this, we used the transgenic PKC $\gamma$ (S361G)-mouse model, expressing a mutant variant of PKC $\gamma$  which is also found in patients suffering from spinocerebellar ataxia 14. In these mice, mutant PKC $\gamma$  is expressed exclusively in Purkinje cells and causes a reduction of dendritic outgrowth especially in lobule VII. We used cerebellar lysates prepared from these mice to immunoprecipitate PKC $\gamma$  and identify associated proteins using mass spectrometry analysis.

The analysis revealed collapsin response mediator protein 2 (CRMP2) as one of the proteins specifically precipitated with PKC $\gamma$ . These results were also corroborated by Western blot detection of the immunoprecipitates that showed both proteins being pulled down with one another. An additional confirmation of the interaction was provided by the Duolink proximity ligation method, which produces a fluorescent signal only if two labelled proteins are in close enough proximity to each other.

As CRMP2 was shown to be a potent mediator of both, axonal and dendritic development, we chose to investigate its role in Purkinje cell dendritic development in more detail, a field that so far had not been looked at in detail.

## **II. Investigate the role of CRMP2 as a mediator of impaired dendritic development in PKC $\gamma$ (S361G)-animals**

Since we had shown that CRMP2 can interact with PKC $\gamma$  in the cerebellum, we now wanted to understand, how this interaction could confer a negative impact on the dendritic development of cerebellar Purkinje cells. CRMP2 is a microtubule-associated molecule largely regulated by post-translational modifications. While we did not observe any differences in gene- or protein expression of CRMP2 between wildtype and PKC $\gamma$ (S361G)-mice, we found that phosphorylation of CRMP2 at the known PKC target site threonine 555 was strongly upregulated in PKC $\gamma$ (S361G)-mice. Intriguingly, this pCRMP2 upregulation was restricted specifically to Purkinje cells, which supports the notion that it is dependent of PKC $\gamma$  activity.

We then explored the effect of CRMP2 phosphorylation in dissociated cerebellar cultures which we transfected with either wildtype, phospho-defective (T555A) or phospho-mimetic (T555D) versions of CRMP2. While expression of wildtype CRMP2 did not impact Purkinje

cell dendritic development, both, the phospho-mimetic and the phospho-defective CRMP2 mutants were able to decrease dendritic outgrowth, with the T555D-mutant being more effective in doing so.

These results suggested that dysregulation of CRMP2 phosphorylation rather than CRMP2 expression can hinder dendritic development. As phosphorylation of CRMP2 is commonly thought to lead to its inactivation and to negatively regulate neurite outgrowth, we hypothesized that transfection of T555D-CRMP2 could model the effects of CRMP2 hyperphosphorylation in PKC $\gamma$ (S361G)-mice, which then ultimately leads to impaired dendritic outgrowth.

### **III. Characterization of dendritic development in a CRMP2<sup>ki/ki</sup>-mouse model**

While in transfection experiments, it is possible to test the effect of increased phosphorylation by overexpressing the phospho-mimetic form, this is more complicated for the non-phosphorylatable form, because the endogenous wildtype form is still present. We therefore wanted to eliminate the background effects of the wildtype CRMP isoform which could have quenched the effect of the T555A-mutant in Purkinje cells in dissociated cultures. We generated a CRMP2 knock-in mouse model using the CRISPR/Cas9-system, introducing the T555A point-mutation. These mice show normal cerebellar development and Purkinje cells also develop normally in organotypic cerebellar slice cultures. Purkinje cells in dissociated cerebellar cultures, however, showed strongly decreased dendritic development. Interestingly, this dendritic outgrowth inhibition could be partially rescued by transfecting the T555D-CRMP2 mutant and was fully recovered after the transfection of wildtype CRMP2.

These results suggest that CRMP2 is required in both, its phosphorylated and unphosphorylated state to ensure correct dendritic development. Moreover, the ability to dynamically switch its phosphorylation state appears to be a crucial aspect of CRMP2 function for Purkinje cell dendritic outgrowth.

---

## 2. Results

---

### 2.1 PKC $\gamma$ -mediated phosphorylation of CRMP2 regulates dendritic outgrowth in cerebellar Purkinje cells

Sabine C. Winkler<sup>1</sup>, Etsuko Shimobayashi<sup>1</sup>, Josef P. Kapfhammer<sup>1</sup>

1) Anatomical Institute, Department of Biomedicine, University of Basel, Switzerland

### 2.2 Abstract

The signaling protein PKC $\gamma$  is a major regulator of Purkinje cell development and synaptic function. We have shown previously that increased PKC $\gamma$  activity impairs dendritic development of cerebellar Purkinje cells. Mutations in the protein kinase  $\gamma$  gene (PRKCG) cause spinocerebellar ataxia type 14 (SCA14). In a transgenic mouse model of SCA14 expressing the human S361G mutation, Purkinje cell dendritic development is impaired in cerebellar slice cultures similar to pharmacological activation of PKC. The mechanisms of PKC $\gamma$ -driven inhibition of dendritic growth are still unclear.

Using immunoprecipitation-coupled mass spectrometry analysis we have identified collapsin response mediator protein 2 (CRMP2) as a protein interacting with constitutive active PKC $\gamma$ (S361G) and confirmed the interaction with the Duolink™ proximity ligation assay. We show that in cerebellar slice cultures from PKC $\gamma$ (S361G)-mice, phosphorylation of CRMP2 at the known PKC target site Thr555 is increased in Purkinje cells confirming phosphorylation of CRMP2 by PKC $\gamma$ . miRNA-mediated CRMP2 knockdown decreased Purkinje cell dendritic outgrowth in dissociated cerebellar cultures as did the transfection of CRMP2 mutants with a modified Thr555 site. In contrast, dendritic development was normal after wildtype CRMP2 overexpression. In a novel knock-in mouse expressing only the phospho-defective T555A-mutant CRMP2, Purkinje cell dendritic development was reduced in dissociated cultures. This reduction could be rescued by transfecting wildtype CRMP2 but only partially by the phospho-mimetic T555D-mutant.

Our findings establish CRMP2 as an important target of PKC $\gamma$  phosphorylation in Purkinje cells mediating its control of dendritic development. Dynamic regulation of CRMP2 phosphorylation via PKC $\gamma$  is required for its correct function.

Key words:

Purkinje cell dendritic development, Protein kinase C gamma, spinocerebellar ataxia type 14, Collapsin response mediator protein 2.

## 2.3 Introduction

The Protein kinase C family comprises several isoforms of serine/threonine kinases expressed in a variety of tissues where they are involved in a multitude of signaling cascades. PKC $\gamma$  is one of the classical PKC isozymes, which are activated by binding diacylglycerol and calcium. It is expressed exclusively in neurons of the central nervous system and in the cerebellum where it is strongly and specifically expressed in Purkinje cells (Kikkawa et al., 1988). We have previously shown that activation of PKC via PMA causes a reduction in dendritic outgrowth of cerebellar Purkinje cells in organotypic slice cultures (Metzger and Kapfhammer, 2000). In contrast, inhibition of PKC in culture or knockout of PKC $\gamma$  lead to an increased dendritic tree expansion (Metzger and Kapfhammer, 2000; Schrenk et al., 2002) showing that PKC $\gamma$  is a powerful mediator of dendritic development in cerebellar Purkinje cells.

Interestingly, mutations in the PRKCG gene coding for PKC $\gamma$  are associated with Purkinje cells loss and impaired motor functions in spinocerebellar ataxia 14 (SCA14). Spinocerebellar ataxias (SCAs) are disorders defined by progressive motor dysfunction along with atrophy of the cerebellum. Up to now, more than 40 mutations in the PRKCG gene are known to cause SCA14 (Wong et al., 2018; Shirafuji et al., 2019). Most of these mutations were shown to have an increased kinase activity in vitro (Verbeek et al., 2005; Adachi et al., 2008). In a transgenic mouse model in which the human S361G point-mutation associated with SCA14 is expressed specifically in cerebellar Purkinje cells (PKC $\gamma$ (S361G)-mice) (Ji et al., 2014), the mice develop mild symptoms of cerebellar ataxia and show decreased dendritic development of Purkinje cells throughout the cerebellum (Trzesniewski et al., 2019), especially in lobule VII (Ji et al., 2014). In organotypic slice cultures prepared from these mice, Purkinje cell dendritic trees develop a stunted morphology with thickened branches (Ji et al., 2014), which is similar to that seen after pharmacological stimulation of PKC (Metzger and Kapfhammer, 2000; Gugger et al., 2012). These findings indicate that the S361G-mutation leads to increased activity of PKC $\gamma$  (Shimobayashi and Kapfhammer, 2017). However, little is known about the molecular mechanisms by which PKC $\gamma$  regulates dendritic growth in Purkinje cells.

In this study we used immunoprecipitation-coupled mass spectrometry analysis for identifying potential interactors of PKC $\gamma$  in the cerebellum and identified collapsin response mediator protein 2 (CRMP2) as a potential candidate. CRMP2 belongs to a family of five proteins (CRMP1-5), which share about 75% sequence homology, with the exception of CRMP5 only sharing ~50% homology with the others (Byk et al., 1998; Fukada et al., 2000).

CRMP family members are known to form homo- and heterotetramers, which may enact distinct functions depending on the composition (Wang and Strittmatter, 1996, 1997; Fukada et al., 2000). CRMP2 is predominantly expressed in the central nervous system where it reaches its peak early after birth, while it remains expressed during adulthood (Wang and Strittmatter, 1996). In the cerebellum, it is expressed in oligodendrocytes, granule cells and Purkinje cells, where it is localized throughout the cell (Bretin et al., 2005). Functions of CRMP2 include the regulation of cell polarization, neurite outgrowth and intracellular trafficking via the association to microtubules (Inagaki et al., 2001; Quach et al., 2004; Kawano et al., 2005; Kimura et al., 2005), which is largely modulated by posttranslational modifications such as SUMOylation, O-GlcNAcylation or phosphorylation (Arimura et al., 2000; Khidekel et al., 2007; Ju et al., 2013; Marques et al., 2013).

We found that phosphorylation of CRMP2 is increased in organotypic slice cultures from PKC $\gamma$ (S361G)-mice. When CRMP2 was knocked down or a phospho-mimetic or phospho-defective CRMP2 mutant was transfected into Purkinje cells, dendritic development of Purkinje cells in dissociated cerebellar cultures was impaired. The impairment of dendritic growth was also seen in Purkinje cells from a novel CRMP2 knock-in mouse with a phospho-defective T555A mutation of CRMP2 and could be rescued by transfection of normal CRMP2. Our results suggest that CRMP2 is an important modulator of dendritic development in cerebellar Purkinje cells and that its function depends critically upon the regulation of phosphorylation at Thr555.

## 2.4 Materials & Methods

### *Immunoprecipitation*

The whole cerebellum from PKC $\gamma$ -S361G transgenic mice was homogenized in ice-cold RIPA buffer with added protease- and phosphatase-inhibitors (Roche, Mannheim, Germany) (50 mM Tris-HCl, pH 7.4; 0.15 M NaCl, 0.25% Deoxycholic acid/sodium deoxycholate, 1% NP-40, 1 mM EDTA). Samples were homogenized using an ultrasound probe and then centrifuged at 14500 g for 15 minutes. Immunoprecipitations were performed using the Pierce® Crosslink Immunoprecipitation Kit (Thermo Fisher Scientific, Rockford, USA) according to standard protocols. Briefly, 5  $\mu$ g of primary rabbit anti-CRMP2 (Sigma-Aldrich, St. Louis, USA; C2993), rabbit anti-PKC $\gamma$  (Santa Cruz Biotechnology, Santa Cruz, USA; sc-211) or normal rabbit IgG (Santa Cruz, Santa Cruz, USA; sc-2027) were incubated with protein A/G-agarose beads for 1h at room temperature. The antibodies were crosslinked to the beads for 30 mins using disuccinimidyl suberate. Lysates were precleared with control

agarose resin for 1h at 4°C. 750 µg of protein in 400 µL immunoprecipitation buffer were incubated with each type of antibody-bead overnight at 4°C on a rotating platform. Beads were washed 6x with IP buffer and proteins were eluted under acidic conditions. The pH was neutralized with 1 M Tris buffer. Samples were mixed in 2x Laemmli buffer (Sigma-Aldrich, Buchs, Switzerland) and processed via SDS-PAGE and Western blotting.

### *LC-MS/MS identification and total protein quantification*

Immunoprecipitates were prepared as described above and used for shotgun LC-MS experiments. Eluted proteins were reduced with 5 mM TCEP for 10 min at 95°C, alkylated with 10 µM chloroacetamide for 30 min in the dark at room temperature. Sample were diluted with 0.1M ammoniumbicarbonate solution to a final concentration of 1% sodium deoxycholate before digestion with trypsin (Promega) at 37°C overnight (protein to trypsin ratio: 50:1). After digestion, the samples were supplemented with TFA to a final concentration of 0.5% and HCl to a final concentration of 50 mM. Precipitated sodium deoxycholate was removed by centrifugation (15 minutes at 4°C at 14,000 rpm). Then, peptides were desalted on C18 reversed phase spin columns according to the manufacturer's instructions (Macrospin, Harvard Apparatus), dried under vacuum and stored at -80°C until further processing. 1 µg of peptides of each sample were subjected to LC-MS analysis using a dual pressure LTQ-Orbitrap Elite mass spectrometer connected to an electrospray ion source (both Thermo Fisher Scientific) as described recently (Glatter et al., 2012) with a few modifications. In brief, peptide separation was carried out using an EASY nLC-1000 system (Thermo Fisher Scientific) equipped with a RP-HPLC column (75 µm × 30 cm) packed in-house with C18 resin (ReproSil-Pur C18-AQ, 1.9 µm resin; Dr. Maisch GmbH, Ammerbuch-Entringen, Germany) using a linear gradient from 95% solvent A (0.15% formic acid, 2% acetonitrile) and 5% solvent B (98% acetonitrile, 0.15% formic acid) to 28% solvent B over 90 min at a flow rate of 0.2 µl/min. The data acquisition mode was set to obtain one high resolution MS scan in the FT part of the mass spectrometer at a resolution of 120,000 full width at half-maximum (at m/z 400) followed by MS/MS scans in the linear ion trap of the 20 most intense ions using rapid scan speed. The charged state screening modus was enabled to exclude unassigned and singly charged ions and the dynamic exclusion duration was set to 30s. The ion accumulation time was set to 300 ms (MS) and 25 ms (MS/MS).

For label-free quantification, the generated raw files were imported into the Progenesis QI software (Nonlinear Dynamics (Waters), Version 2.0) and analyzed using the default parameter settings. MS/MS-data were exported directly from Progenesis QI in mgf format and searched against a decoy database the forward and reverse sequences of the predicted



proteome from *mus musculus* (UniProt, download date: 16/11/2015, total of 33,984 entries) using MASCOT (version 2.4.1). The search criteria were set as follows: full tryptic specificity was required (cleavage after lysine or arginine residues); 3 missed cleavages were allowed; carbamidomethylation (C) was set as fixed modification; oxidation (M) as variable modification. The mass tolerance was set to 10 ppm for precursor ions and 0.6 Da for fragment ions. Results from the database search were imported into Progenesis QI and the final peptide measurement list containing the peak areas of all identified peptides, respectively, was exported. This list was further processed and statically analyzed using our in-house developed SafeQuant R script (Glatter et al., 2012). The peptide and protein false discovery rate (FDR) was set to 1% using the number of reverse hits in the dataset.

### *Proximity ligation assay (Duolink)*

The Duolink Proximity ligation assay was used to determine the interaction between proteins following the manufacturers protocols. HELA cells were transfected with PKC $\gamma$  using Effectene (Qiagen, Hilden, Germany) and fixed after 24h with 4% PFA. Primary antibodies rabbit anti-CRMP2 (1:1000; Sigma-Aldrich; C2993), mouse anti-PKC $\gamma$  (PKC66; 1:500; Invitrogen; 13-3800) and mouse anti- $\alpha$ -tubulin (DM1A; 1:1000; Invitrogen; 14-4502-82) were used and labelled with the PLA probes anti-rabbit minus (Sigma-Aldrich, DUO92005), PLA probe anti-mouse plus (Sigma-Aldrich, 92001) and Duolink™ In Situ Detection Reagents Red (Sigma-Aldrich, DUO92008). The assay produces a signal when the distance between the PLA probes is less than 40 nm.

### *Reverse transcription PCR*

Total RNA was extracted from organotypic cerebellar slices harvested at DIV 5-7 and cDNA was synthesized with reverse transcription PCR using oligo(dT) primers (Applied Biosystems, Foster City, USA). For gene expression analysis, RT-qPCR reactions were conducted in a total volume of 20  $\mu$ l comprising 10  $\mu$ l of Mastermix with SYBR green (Applied Biosystems, Foster City, USA), 0.5  $\mu$ l of each primer (1.0  $\mu$ M), 0.3  $\mu$ l of sample cDNA, and 8.5  $\mu$ l ultrapure water. Real-time PCR reactions were run on a Real time PCR system (Applied Biosystems, Foster City, USA) under the following reaction conditions: 1 cycle of [95°C for 10 min], 40 cycles of [94°C for 15 s  $\rightarrow$  65°C for 60 s], and 1 cycle of [95°C for 15 s  $\rightarrow$  72°C for 30 s  $\rightarrow$  95°C for 15 s]. Oligonucleotide primers were designed using the Primer3 software (<http://bioinfo.ut.ee/primer3/>). Forward primer: 5'- ACG AGC GAT CGT CTT CTG AT -3'. Reverse primer: 5'- GAA GCG AGT ATG CAC GTC AA -3'. Reactions were quantified by relative standard curve system and the cycle threshold (Ct) method using the

SDS2.2 software (Applied Biosystems, Foster City, USA). A relative quantitation value (RQ) for each sample from the triplicates of that sample was calculated for each gene. The data were analyzed as RQ for the gene of PKC $\gamma$  transgenic mice/ RQ for control mice.

### *Organotypic cerebellar slice cultures*

Animal experiments were carried out in accordance with the EU Directive 2010/63/EU for animal experiments and were reviewed and permitted by Swiss authorities. Organotypic cerebellar slice cultures were prepared as previously described (Gugger et al., 2012). Briefly, postnatal day 8 mice were decapitated, the cerebellum removed and placed in ice-cold preparation medium (minimal essential medium (MEM) with Glutamax (Life Technologies, Zug, Switzerland), pH 7.3). The cerebellum was cleaned from choroid plexus and cerebral membranes, placed on a McIlwain tissue chopper and cut in sagittal slices of 350  $\mu$ m thickness. Millicell cell culture inserts (PICM03050, Millipore, Zug, Switzerland) were pre-wet with Neurobasal medium (Neurobasal A medium (Life Technologies, Zug, Switzerland) supplemented with B27 supplement (Life Technologies, Zug, Switzerland) and Glutamax, pH 7.3) and the slices carefully placed on the membrane. Cultures were maintained for seven days with medium changes every 2-3 days.

### *Western blot analysis*

Lysates were prepared by as described above. 2x Laemmli buffer was added and samples loaded onto polyacrylamide gels. Gels were run at 120 V for 75 minutes in running buffer (0.25 M Tris, 1.93 M glycine, 0.1% SDS). Proteins were transferred to nitrocellulose membranes (Bio-Rad Laboratories, Cressier, Switzerland) in transfer buffer (0.25 M Tris, 1.93 M glycine, 20% methanol) at 350 mA for 45 mins. Membranes were blocked in 5% BSA in TBS for 1h and incubated with primary antibodies including rabbit anti-CRMP2 (1:1000; Sigma-Aldrich; C2993), rabbit anti-PKC $\gamma$  (1:1000; Santa Cruz Biotechnology, Santa Cruz, USA; sc-211), rabbit anti-pCRMP2 (1:500; ECM Biosciences; CP2251) and mouse anti-actin (1:2000; Sigma-Aldrich; A5441) overnight at 4°C. Secondary antibodies IRDye® 800CW Donkey anti-mouse (Li-Cor, Bad-Homburg, Germany; 926-32212) and IRDye® 680LT Donkey anti-rabbit (Li-Cor; 926-68023) were added at a concentration of 1:5000 diluted in TBS-T. After washing signal was detected using a LI-COR Odyssey and software (LI-COR Biosciences, Bad Homburg, Germany). To determine the ratios pCRMP2/CRMP2 gels were run in parallel for total CRMP2 and pCRMP2. The immunoreactivity in each gel was normalized to the actin signal and the ratio evaluated by (pCRMP2/actin)/(CRMP2/actin) and then normalized to wildtype controls.

### *Nucleofection of dissociated cerebellar cultures*

Preparation of dissociated cultures was performed as previously described (Wagner et al., 2011; Shimobayashi et al., 2016). Briefly, mice were sacrificed by decapitation at postnatal day zero (p0). The cerebellum was removed from the skull, placed in ice-cold Hanks' balanced salt solution (HBSS, SigmaAldrich, Buchs, Switzerland) and cut into 1 mm<sup>2</sup> pieces. 300 µL of papain solution (HBSS containing 20 U/ml papain (Worthington, Lakewood, USA) were added and the mixture was incubated at 37°C for 20 minutes. Digestion was arrested by addition of 500 µL HBSS (including 5% FBS) and the solution was spun down at 700 rpm for 4 minutes. The pellet was then dispersed in 350 µL DNase1 solution (0.02% DNase1, 11.88 mM MgSO<sub>4</sub>, 1 mL HBSS) and passed through a 180 µm nylon net filter (Millipore, Zug, Switzerland). The cell solution was spun down, and the pellet was washed in 1 mL HBSS. After centrifugation, the pellet was dissociated in 85 µL transfection solution and 5 µL DNA (1 µg/µL) were added. The cell-DNA mixture was then transferred to Lonza cuvettes and transfected using the O-0003 program of the Nucleofector™ 2b. Immediately after transfection, 200 µL of dissociated culture medium (DMEM/F-12, 1x Glutamax, 1x N2-supplement (Life Technologies, Zug, Switzerland), 100 nM tri-iodothyronine (Merck, Darmstadt, Germany)) supplemented with 10% FBS were added to the cells and the suspension was transferred to 8-well chamber-slides. The cultures were maintained for 14-16 days and the medium changed every 4-5 days.

### *Plasmid construction*

Collapsin response mediator protein 2 (CRMP2) is encoded by the *DPYSL2* gene. For simplification we apply the most commonly used name, CRMP2, in this manuscript.

pCMV6-Dpysl2 (NM\_009955) Mouse Untagged Clone (Origene, Rockville, USA; MC205233) was used as a template and the CRMP2 coding sequence was amplified using the following primers: CRMP2-ORF-pL7-F: 5'-GTC CGG ACT CAG ATC TAT GTC TTA TCA GGG GAA GAA AAA T-3'; CRMP2-ORF-pL7-R: 5'-AGC AGG ATC CGT CGA CTT AGC CCA GGC TGG TGA TGT-3'. The pL7-GFP vector (Wagner et al., 2011) was linearized for 1h at 37°C in the appropriate buffer using BglII (New England BioLabs, Ipswich, USA; R0144S) and Sall-HF (New England BioLabs, Ipswich, USA; R3138S) restriction enzymes. The linearized vector and PCR product were then fused using the In-Fusion® HD Cloning kit (Clontech, Mountain View, USA; 638912).

### *Site-directed mutagenesis*

To insert the T555A and T555D mutation, the Muta GeneArt™ Site-Directed Mutagenesis system was used (Life Technologies, Carlsbad, USA) with the following primers and the pCMV6-Dpysl2 plasmid as template: T555A-F: 5'-ATT CCC CGC CGC ACC GCC CAG CGC ATC GTG GCA-3'; T555A-R: 5'-TGC CAC GAT GCG CTG GGC GGT GCG GCG GGG AAT-3'; T555D-F: 5'-ATT CCC CGC CGC ACC GAC CAG CGC ATC GTG GCA-3'; T555D-R: 5'-TGC CAC GAT GCG CTG GTC GGT GCG GCG GGG AAT-3'. In short, the pCMV6-Dpysl2 plasmid was methylated and amplified using the aforementioned primers. The original plasmid was then removed in an enzymatic reaction using McrBC endonuclease. The products were transformed into DH5 $\alpha$ ™-T1R E. Coli (included in kit). Colonies were picked and analyzed by Ecoli NightSeq (Microsynth, Balgach, Switzerland). The sequences including the respective mutations were then subcloned into the pL7-GFP vector as described above.

### *miRNA-mediated knockdown of CRMP2*

miRNA knockdown constructs were created using the BLOCK-iT™ Pol II miR RNAi Expression Vector Kit (Thermo Fisher Scientific, Rockford, USA). Pre-miRNAs were designed using the BLOCK-iT™ RNAi Designer and cloned into the BLOCK-iT™ Pol II miR RNAi expression vector according to the manufacturer's protocols. Briefly, Top- and bottom-strand oligos were annealed and the double stranded product was cloned into the linearized pcDNA™6.2-GW/miR vector. The ligation reaction was transformed into Stellar competent cells (Clontech, Mountainview, USA) and the bacteria plated onto agarose plates containing 50  $\mu$ g/mL spectinomycin. Colonies were analyzed using Ecoli NightSeq (Microsynth, Balgach, Switzerland). Vectors were then sequenced and tested for their efficacy by transfection into HEK293 cells using the Effectene transfection reagent (Qiagen, Hilden, Germany). The most effective sequence was subcloned into a pL7- vector containing a His-GST-fusion protein to validate miRNA expression after transfection. Transfections were performed as mentioned above.

### *Generation of CRMP2-T555A knock-in mice*

Animal experiments were carried out in accordance with the EU Directive 2010/63/EU for animal experiments and were reviewed and permitted by Swiss authorities. Knock-in mice with the single point mutation (c. 1663 A>G; p. Thr555Ala) in the *DPYSL2* gene

(Chromosome 14, 34.60 cM) were generated in an FVB background using the CRISPR/Cas9 engineering system at the Center of Transgenic Models, University of Basel, using the rapid oocyte injection method. Alt-R® CRISPR-Cas9 crRNA (5'-GGG TGC CAC GAT GCG CTG GGT GG-3'), Alt-R® CRISPR-Cas9 tracrRNA and Donor DNA (5'-CAC TCG TTT CTT GTC TCT TCT TTC TTC TCT AGG TGC TCA GAT TGA CGA CAA CAT TCC CCG CCG CAC AGC TCA GCG CAT CGT GGC ACC CCC TGG TGG CCG TGC CAA CAT CAC CAG CCT GGG CTA AAG CCC CTA GGC CTG CAG GCC ACT TGG GGA TGG GGG ATG GGA CAC CTG AGG ACA TTC TGA GAC TTC CTT TCT TCC AT-3') were obtained from Integrated DNA Technologies (USA). Crispr RNA, Cas9 and Donor DNA were injected into FVB zygotes at the pronuclear site and surviving embryos were transferred into pseudo-pregnant mice. To identify founders, genotyping with genomic DNA samples from biopsies was performed by PCR. The primers for genotyping were: Forward, 5'- AGG ATT GTT CCT GGG CAT AC - 3' and Reverse 5'- TCA TGA ACA CCA CAC CCA AG -3'. Then the point mutation at 1663 A>G *DPYSL2* gene was confirmed by DNA sequencing. The fragment for sequencing was obtained by PCR with genomic DNA samples and primers as mention above. The confirmed point mutation knock-in founders were crossed with FVB mice (Jackson Laboratory, Sacramento, USA) to generate heterozygous CRMP2-Thr555Ala mice. These were crossed with other heterozygous CRMP2-Thr555Ala mice to obtain wild type, heterozygous and homozygous CRMP2-Thr555Ala knock-in mice.

### *Immunohistochemistry of cerebellar slice cultures*

Cultures were fixed in 4% PFA and then washed three times with phosphate buffer (PB). Primary antibodies (mouse anti-Calbindin, 1:500, Swant, Marly, Switzerland; No. 300; rabbit anti-CRMP2, 1:1000; Sigma-Aldrich, St. Louis, USA, No. C2993 and rabbit anti-pCRMP2, 1:200; ECM Biosciences; No. CP2251) were diluted in PB with 0.03% Triton-X and 3% normal goat serum. Slices were then incubated overnight at 4°C under gentle agitation. Plates were washed three times with PB and secondary antibodies Alexa Fluor-568 goat anti-rabbit (Molecular Probes, Eugene, USA; A11011) and Alexa Fluor-488 goat anti-mouse (Molecular Probes, Eugene, USA; A11001) were added at a concentration of 1:500 in PB with 0.01% Triton-X. Plates were washed again three times for 5 minutes, detached from the membranes and then mounted in Mowiol. Confocal microscopy was performed on an upright laser scanning microscope (Zeiss LSM700) equipped with solid-state lasers. Images were acquired using a Plan-Apochromat 40x/1.3 Oil DIC M27 objective (Zeiss) and standard PMT detectors. Images were adjusted for contrast and brightness.

### *Immunohistochemistry of dissociated cultures*

Slides were fixed in 4% PFA and then washed 3x with phosphate buffer (PB). Primary antibodies including mouse anti-Calbindin (1:500; Swant, Marly, Switzerland; 300), rabbit anti-Calbindin (1:1000; Swant, Marly, Switzerland; CB38), rabbit anti-GFP (1:500; Abcam, Cambridge, UK; ab6556) and mouse anti-His (1:200; Life Technologies, Carlsbad, USA; 710286), were diluted in PB with 0.03% Triton-X and 3% normal goat serum and slides were incubated for 1 hour at RT. Slides were washed three times with PB and secondary antibodies Alexa Fluor-568 goat anti-rabbit (Molecular Probes, Eugene, USA; A11011), Alexa Fluor-488 goat anti-mouse (Molecular Probes, Eugene, USA; A11001), Alexa Fluor-568 goat anti-mouse (Molecular Probes, Eugene, USA; A11004), Alexa Fluor-488 goat anti-rabbit (Molecular Probes, Eugene, USA; A11008) were added at a concentration of 1:500 in PB with 0.01% Triton-X. Slides were washed three times, the wells were detached from the glass and the slide mounted in Mowiol. Cultures were viewed on an Olympus AX-70 microscope equipped with a Spot digital camera. Images were adjusted for contrast and brightness.

### *Statistical analysis*

The quantification of Purkinje cell dendritic tree size from organotypic slice cultures or dissociated Purkinje cell cultures was done as previously described (Gugger et al., 2012). Only Purkinje cells not overlapping with other cells were chosen for the analysis. Dendritic area was measured by outlining each cell in ImageJ. A minimum number of 40 cells per group from at least three independent experiments were included in the analysis. In case of transfection of CRMP2<sup>ki/ki</sup> dissociated cultures, two independent experiments were analyzed. GraphPad Prism was used for statistical analyses using the non-parametric Mann-Whitney's test. Statistical significance was assumed when  $p < 0.05$ .

## 2.5 Results

### *CRMP2 interacts with PKC $\gamma$ in the cerebellum*

Cerebella from p12 PKC $\gamma$ (S361G)-mice or PKC $\gamma$ <sup>-/-</sup>-mice were lysed and PKC $\gamma$  was immunoprecipitated using protein A/G coated agarose beads. Proteins pulled down along with PKC $\gamma$  were identified using a shotgun mass spectrometry approach. Beads prepared with anti-vGlut1 antibody, a glutamate transporter expressed in axon terminals of cerebellar granule cells, were included in the experiment as a negative control. To exclude falsely identified, non-specifically bound proteins, the same experiment was performed using cerebellar lysates prepared from PKC $\gamma$ <sup>-/-</sup>-mice. Amongst the proteins co-purified from PKC $\gamma$ (S361G)-lysates we identified CRMP2. Total identified spectra for CRMP2 were normalized to the total amount of spectra identified in each sample. The number of normalized total spectra counts for CRMP2 was strongly decreased in the PKC $\gamma$ <sup>-/-</sup>-pulldowns, confirming the specific binding of CRMP2 to PKC $\gamma$  (Table 1).

**Table 1 Mass spectrometry analysis of cerebellar lysates from PKC $\gamma$ (S361G)- and PKC $\gamma$ <sup>-/-</sup>-mice**

Numbers indicate normalized total spectra of two sample duplicates identified for the proteins indicated above (See Supplementary Table 1 for a detailed report).

Bait	PKC $\gamma$ (sp P63318 )		CRMP2 (sp O08553 )	
	PKC $\gamma$ (S361G)	PKC $\gamma$ <sup>-/-</sup>	PKC $\gamma$ (S361G)	PKC $\gamma$ <sup>-/-</sup>
<b>vGlut1</b>	1   1	0   0	5   5	4   1
<b>PKC<math>\gamma</math></b>	33   34	0   0	28   35	8   4
<b>CRMP2</b>	1   0	0   0	32   31	27   30
<b>Fold change (PKC<math>\gamma</math>(S361G)/PKC<math>\gamma</math><sup>-/-</sup>)</b>	0.0		0.2	
<b>p-value (students t-test)</b>	< 0.00010		0.027	

In PKC $\gamma$ -immunoprecipitations, CRMP2 was detected along with PKC $\gamma$  in immunoblots, which was not the case when control rabbit IgG was used in the precipitation. The same was true in precipitations of CRMP2, where PKC $\gamma$  and CRMP2 were both identified (Figure 1a).

In order to confirm the interaction, we used the Duolink™ proximity ligation assay in HeLa cells (Figure 1b). As a positive control of a known CRMP2 interaction, we performed the assay using primary antibodies against CRMP2 and alpha-tubulin, both natively expressed in HeLa cells. After the addition of the Duolink plus and minus probes, this reaction produced a positive signal. When primary antibodies were omitted, the PLA signal could be abolished. HeLa cells transfected with wildtype PKC $\gamma$  and labelled with antibodies against CRMP2 and PKC $\gamma$  also displayed the PLA signal, verifying the close association of the two proteins.

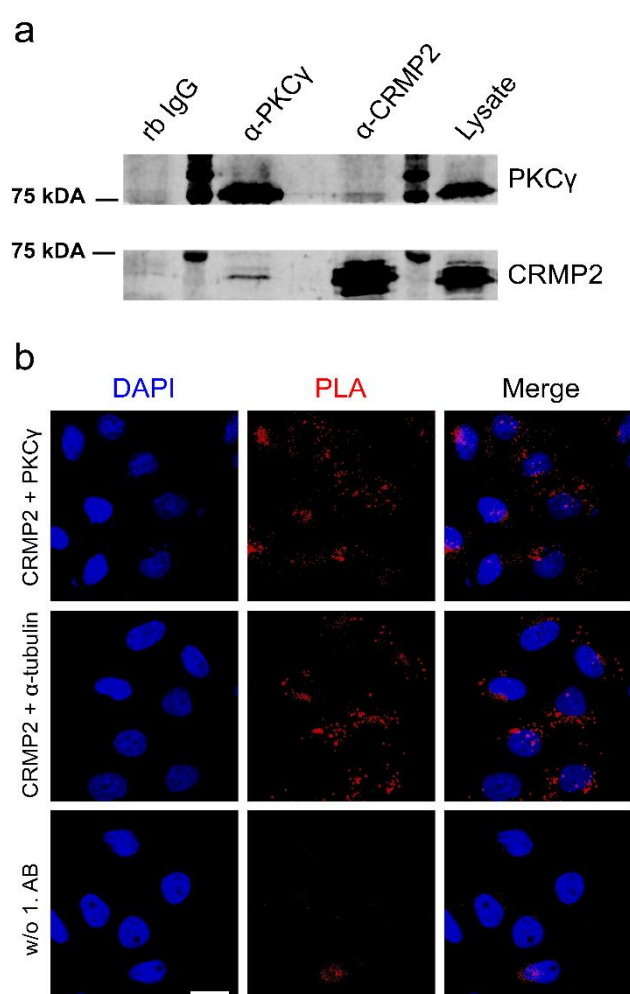


**Figure 1 Interaction of CRMP2 and PKC $\gamma$**

a) Immunoblot showing the co-immunoprecipitation of CRMP2 and PKC $\gamma$  from cerebellar lysates. Proteins were detected with the indicated antibodies. Normal rabbit IgG was used as a negative control. b) HELA cells were probed with  $\alpha$ -PKC $\gamma$  and  $\alpha$ -CRMP2 antibody and the interaction detected via Duolink proximity ligation assay (top row);  $\alpha$ -CRMP2 and  $\alpha$ -alpha-tubulin antibodies were used as a positive control (middle row) and primary antibodies were omitted as a negative control (bottom row). Blue = nuclei stained with DAPI; red = PLA signal. Scale bar = 20  $\mu$ m.



*Phosphorylation of CRMP2 is increased in PKC $\gamma$ (S361G)-mice*

In order to characterize the relation of CRMP2 to PKC $\gamma$ , we used organotypic slice cultures (OTSCs) prepared from wildtype and PKC $\gamma$ (S361G)-mice. Immunostainings confirmed that CRMP2 is expressed in various cell types of the cerebellum and that there was no apparent difference in localization or expression of the protein between wildtype and PKC $\gamma$ (S361G)-mice (Figure 2a). We further assessed the gene and protein expression of CRMP2 in PKC $\gamma$ (S361G)-mice. When we analyzed data from a gene chip microarray (Shimobayashi et al., 2016), we found no significant differences in CRMP2 mRNA expression between wildtype- and PKC $\gamma$ (S361G)-mice (Figure 2b). RT-qPCR confirmed that mRNA expression levels were unaltered (Figure 2c). We then used lysates of OTSCs prepared from PKC $\gamma$ (S361G)-mice for Western blotting and detected no differences in CRMP2 expression in PKC $\gamma$ (S361G)-mice (Figure 2d).

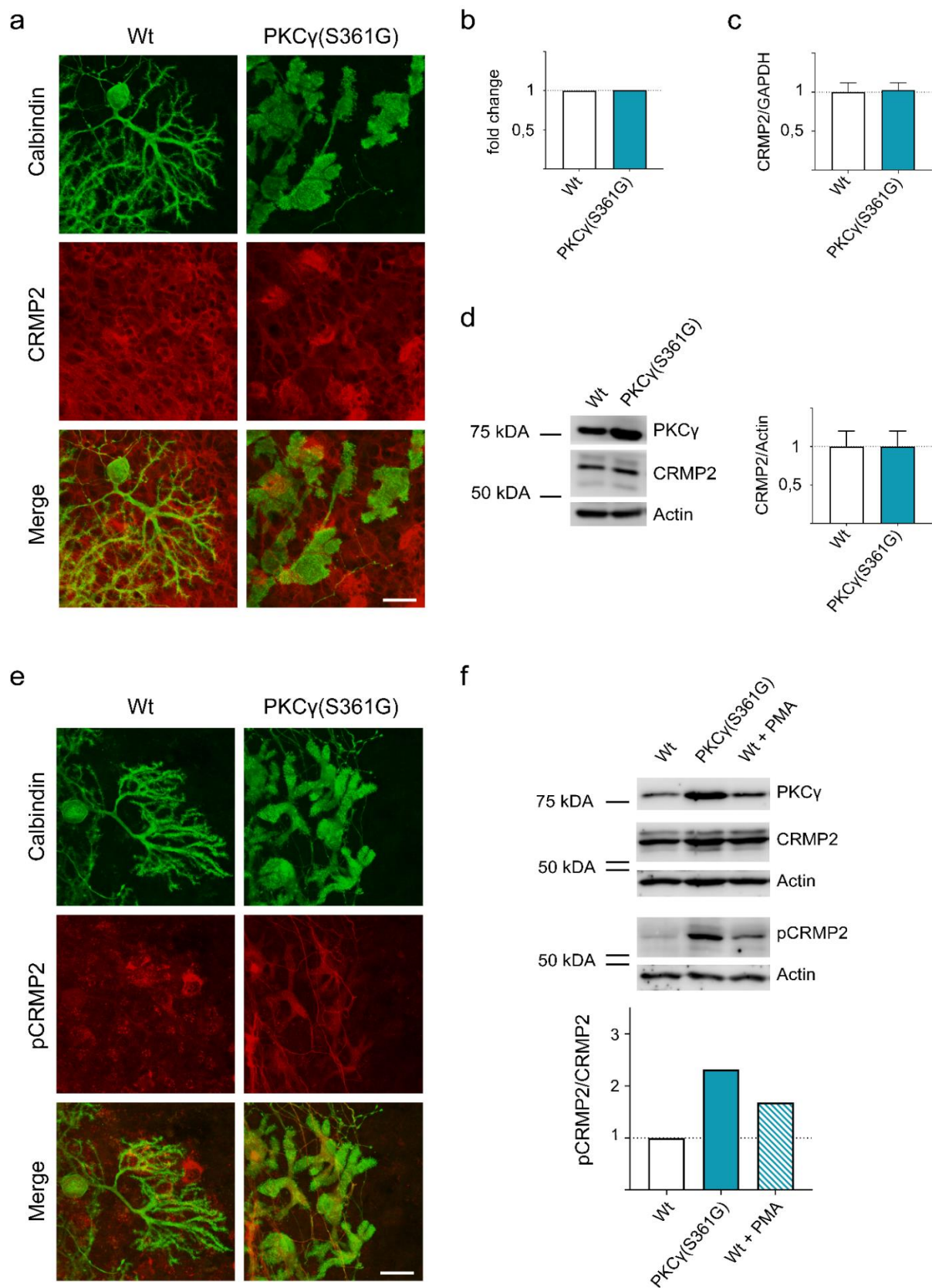


### Figure 2 Phosphorylation of CRMP2 is increased in PKC $\gamma$ (S361G)-mice

a) Immunostainings of CRMP2 in cerebellar OTSCs from Wt- and PKC $\gamma$ (S361G)-mice show no visible differences in localization or expression of CRMP2. b) No changes in gene expression were detected in a gene chip assay and c) quantitative RT-PCR. d) Immunoblot of CRMP2 expression in cerebellar lysates prepared from Wt- and PKC $\gamma$ (S361G)-mice. Summary of the Western blot analysis of five independent experiments showing that the expression of CRMP2 normalized to actin is unchanged. e) Immunostainings of pCRMP2 in cerebellar OTSCs from Wt- and PKC $\gamma$ (S361G)-mice show an upregulation of phosphorylated CRMP2 in Purkinje cells. f) Immunoblot of cerebellar lysates prepared from OTSCs. There is an increase of pCRMP2 in PKC $\gamma$ (S361G)-OTSCs or Wt-cultures treated with 1  $\mu$ M PMA. Summary of the Western blot analysis showing the mean of five independent experiments. The expression of pCRMP2 normalized to total CRMP2 is upregulated approximately 2.3-fold in PKC $\gamma$ (S361G)-mice and 1.7-fold in PMA treated cultures compared to untreated controls. Scale bars = 25  $\mu$ m.

Since CRMP2 functions are primarily regulated by posttranslational modifications, we decided to focus on the Thr555 phosphorylation site, which had been previously shown to be a target of PKC (Marques et al., 2013). In PKC $\gamma$ (S361G)-transgenic mice, while total CRMP2 expression and localization remained unchanged, levels of CRMP2 phosphorylated at Thr555 (pCRMP2) were strongly increased in OTSCs. The upregulation of pCRMP2 in PKC $\gamma$ (S361G)-mice was essentially confined to Purkinje cells confirming the strong cell-specific upregulation (Figure 2e). Analysis of immunoblots comparing samples from organotypic slice cultures also confirmed the increase in CRMP2 phosphorylation in PKC $\gamma$ (S361G)-cultures and in wildtype cultures treated with the PKC activator Phorbol 12-myristate 13-acetate (PMA) (Figure 2f). It therefore seems likely that the increase in CRMP2 phosphorylation is a consequence of increased PKC $\gamma$  kinase activity in PKC $\gamma$ (S361G)-mice while overall expression of CRMP2 remained unaffected.

### *Knockdown of CRMP2 impairs dendritic development of cerebellar Purkinje cells*

Since phosphorylation of CRMP2 was upregulated specifically in cerebellar Purkinje cells in PKC $\gamma$ (S361G)-mice, we aimed to further investigate the role of CRMP2 for dendritic development of Purkinje cells. We first overexpressed wildtype CRMP2 (Wt-CRMP2) with an added GFP-tag in dissociated cerebellar cultures specifically in Purkinje cells using a vector containing the L7 promotor. Purkinje cells transfected with a GFP control vector showed normal dendritic development. Also, the overexpression of CRMP2 did not alter dendritic development as determined by measuring the Purkinje cell dendritic area (Figure 3a-b).

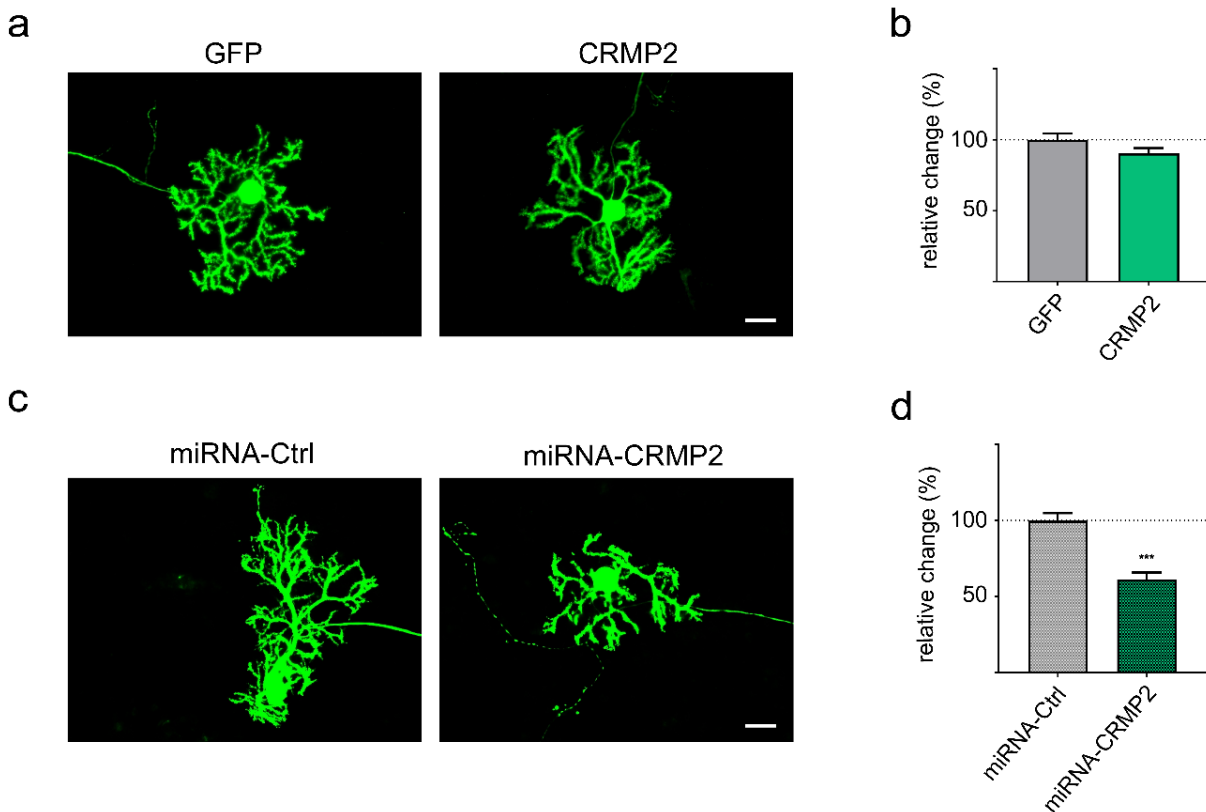


**Figure 3 CRMP2 regulates dendritic development of cerebellar Purkinje cells**

a) Dissociated cerebellar cultures showing Purkinje cells stained with calbindin. Cultures were transfected with GFP or GFP-tagged wildtype CRMP2 under the control of a Purkinje cell specific promotor to overexpress wildtype CRMP2. More examples of Purkinje cells for the different treatments are shown in Supplementary Figure 3b) Quantification of Purkinje cell dendritic area shows no significant changes (GFP only:  $n = 49$ ; CRMP2-GFP:  $n = 109$ ). c) miRNA mediated knockdown of CRMP2. Transfection of dissociated cultures using knockdown constructs containing the L7-promotor, a His-GST reporter and either a control miRNA or CRMP2 specific miRNA. d) Quantification of the gross dendritic area shows a statistically significant decrease of the Purkinje cell dendritic area after CRMP2 knockdown ( $p < 0.001$ ; miRNA-Ctrl:  $n = 130$ ; miRNA-CRMP2:  $n = 73$ ); Data were acquired from 4 independent experiments respectively and are shown as the mean  $\pm$  SEM. Scale bar = 25  $\mu$ m.

We then explored the effect of a reduction of CRMP2 by miRNA mediated knockdown of the protein. The miRNA sequence used for transfection was selected based on its knockdown efficiency in HEK293 cells (Supplementary Figure 1a). The miRNA was then expressed using a L7-plasmid containing a His-GST fusion protein as a reporter. Purkinje cells transfected with the miRNA displayed reduced CRMP2 expression levels (Supplementary Figure 1b) and had a significantly decreased Purkinje cell dendritic area (Figure 3c-d). This finding shows that CRMP2 is required for correct dendritic development in Purkinje cells while an excess of the wildtype protein does not seem to exert a negative effect.

---

*Purkinje cell dendritic development is modulated by CRMP2 phosphorylation*

Since Purkinje cell dendritic development is impaired in PKC $\gamma$ (S361G)-mice, we investigated the relationship between the phosphorylation of CRMP2 and dendritic outgrowth and created constructs for the expression of phospho-defective (T555A) and phospho-mimetic (T555D) mutants of CRMP2. The mutant-CRMP2 variants were expressed with a GFP-tag under the control of the L7-promotor for Purkinje cell specific expression and transfected into dissociated cerebellar cultures. Transfection of the phospho-defective T555A-CRMP2 resulted in a small but significant decrease of Purkinje cell dendritic area (Figure 4a-b). Transfection of the phospho-mimetic T555D mutant resulted in a more pronounced reduction of the Purkinje cell dendritic area (Figure 4a-b). Since transfected Purkinje cells still express native CRMP2 that retains the ability to be phosphorylated, potential effects of transfected T555A-CRMP2 could have been quenched by native CRMP2. The phospho-mimetic mutant resulted in a strong inhibition of dendritic growth reminiscent of the morphology seen in Purkinje cells derived from PKC $\gamma$ (S361G)-mice (Figure 4c). As CRMP2-phosphorylation is greatly increased in PKC $\gamma$ (S361G) transgenic Purkinje cells, the phosphorylation of CRMP2 could be one of the mediators of the reduction of dendritic growth seen in these cells.

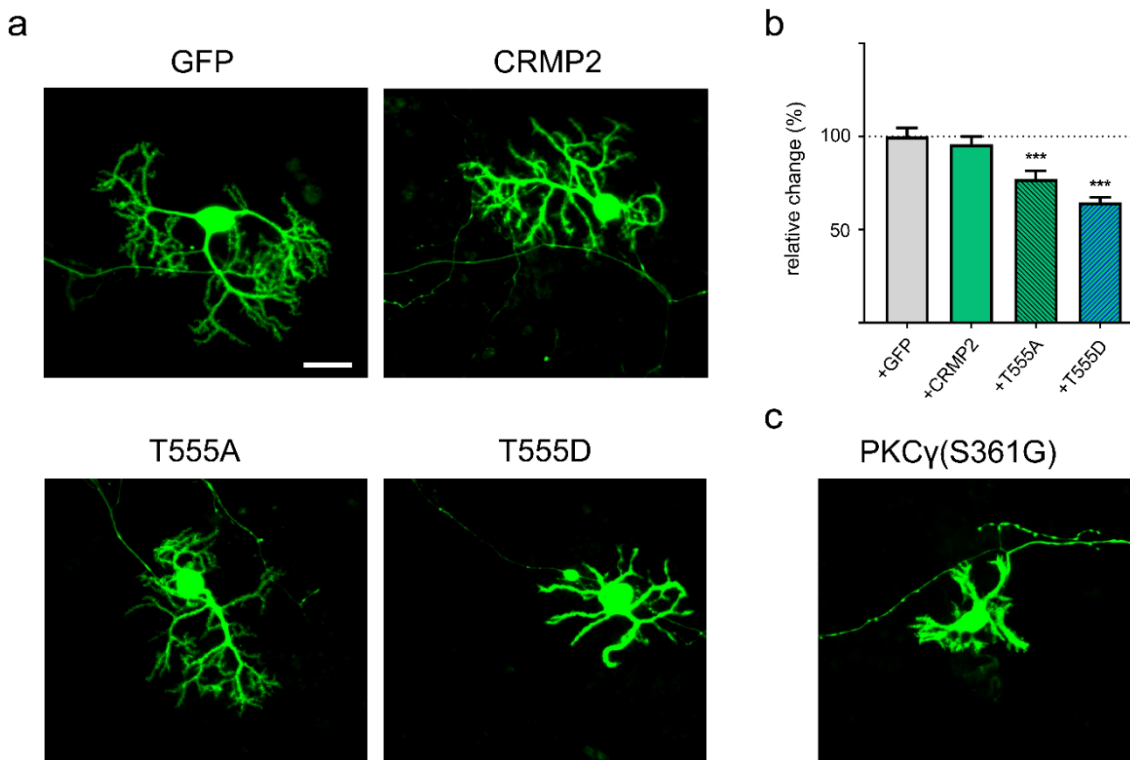


**Figure 4 Dendritic development in Purkinje cells is modulated by CRMP2 phosphorylation**

a) Dissociated cerebellar cultures showing Purkinje cells expressing GFP. Cells were transfected with GFP or GFP-tagged wildtype CRMP2, phospho-defective (T555A) or phospho-mimetic (T555D) CRMP2 under a Purkinje cell specific promoter. More examples of Purkinje cells for the different treatments are shown in Supplementary Figure 4. Scale bar = 25  $\mu$ m. b) Analysis of the Purkinje cell dendritic area shows a statistically significant reduction in cells transfected with T555A- or T555D-CRMP2 ( $p < 0.001$ ; GFP only:  $n = 49$ ; CRMP2-GFP:  $n = 109$ ; T555A-GFP:  $n = 58$ ; T555D:  $n = 126$ ). c) Example of a typical Purkinje cell in dissociated cerebellar cultures prepared from PKC $\gamma$ (S361G)-mice showing the typical stunted dendritic morphology. Data were acquired from 4 independent experiments of GFP-, CRMP2- and T555D-transfections and 3 independent experiments for T555A. Data are shown as the mean  $\pm$  SEM.

### *Generation of CRMP2<sup>ki/ki</sup>-mice*

Because the presence of native CRMP2 could have compensatory effects in transfection experiments, we created a CRMP2 knock-in mouse carrying the T555A mutation using the CRISPR/Cas9/-system in an FVB background (Figure 5a-c).

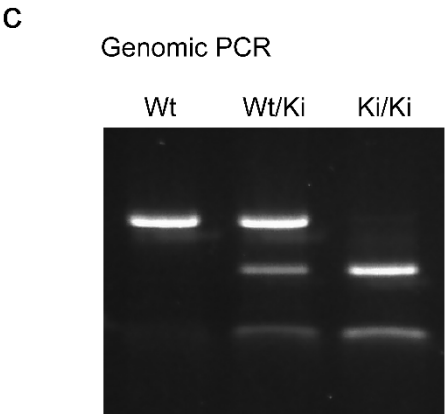
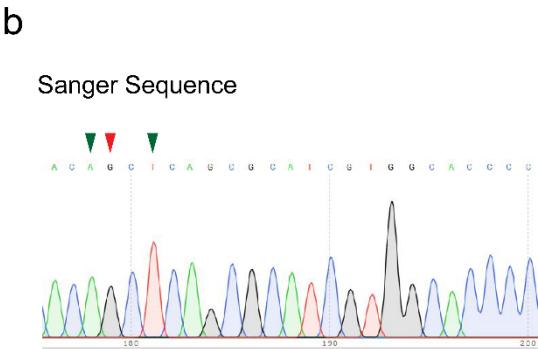
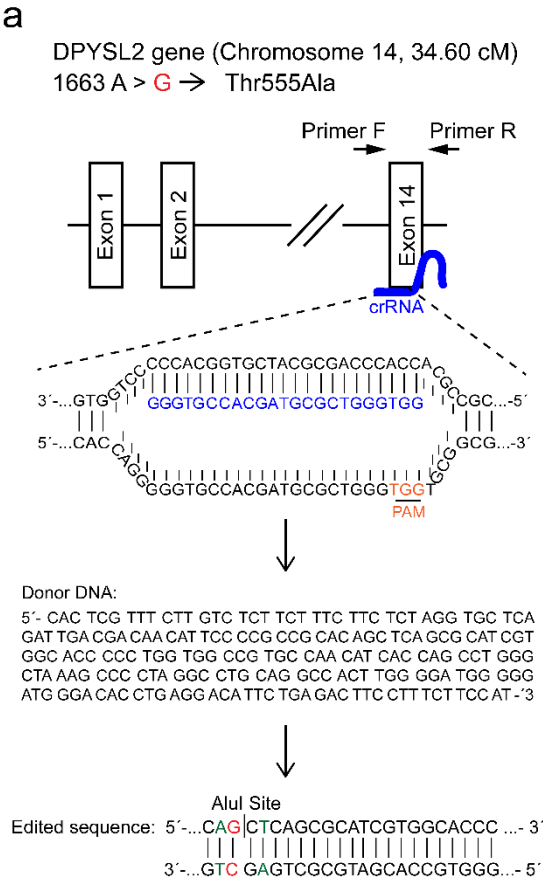


**Figure 5 Generation of CRMP2<sup>ki/ki</sup>-mice**

The single point mutant (c. 1663 A>G; p. Thr555Ala) in knock-in mice was generated in FVB background with the CRISPR/Cas9 engineering system. a) Schematic representation of the *DPYSL2* gene (Chromosome 14, 34.60 cM) and the Crispr RNA target locus. crRNA sequence is outlined in blue. The protospacer adjacent motif (PAM) is outlined in orange. The displayed donor DNA sequence was introduced to generate the edited final sequence including an AluI restriction site. The 1663 A>G mutation is indicated in red and mutations of the restriction site in green. b) The mutations were confirmed by DNA sequencing. Arrowheads successful introduction of the respective mutations. c) Genomic PCR shows multiple bands after AluI digestion, indicating presence of the mutation.

In these knock-in mice, general cerebellar development and Purkinje cell dendritic development in OTSCs from CRMP2<sup>ki/ki</sup>-mice was unchanged (Figure 6a-c). Immunostainings showed that expression levels of CRMP2 remained unchanged in CRMP2<sup>ki/ki</sup>-OTSCs compared to cultures prepared from control animals (Fig. 6b), while phosphorylation of CRMP2 at Thr555 was abolished (Figure 6d). When these cultures were treated with PMA there was no increase in pCRMP2 (Figure 6e), confirming the successful knock-in of the mutation.



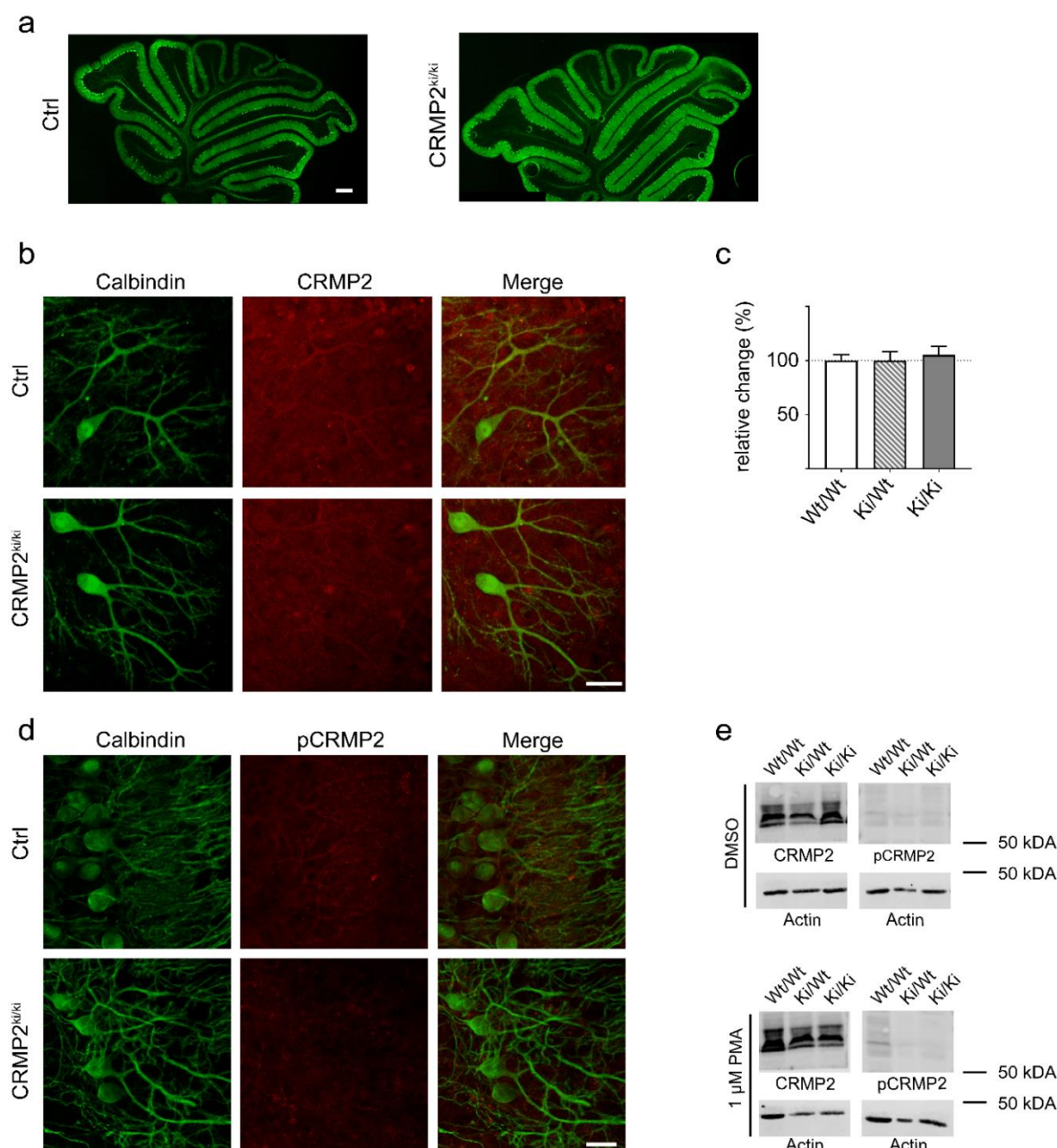


**Figure 6 CRMP2 phosphorylation at Thr555 is abolished in CRMP2<sup>ki/ki</sup>-mice**

a) Frozen cerebellar sections from Ctrl- and CRMP2<sup>ki/ki</sup>-mice (postnatal day 12); Scale bar = 200 μM. Gross cerebellar morphology appears normal in CRMP2<sup>ki/ki</sup>-mice. b) Immunostainings of OTSCs prepared from Ctrl- and CRMP2<sup>ki/ki</sup>-mice show no differences in CRMP2 expression. Scale bar = 25 μm; c) Cerebellar OTSCs from CRMP2<sup>ki/ki</sup>-mice show normal development as shown by the analysis of Purkinje cell dendritic area (CRMP2<sup>Wt/Wt</sup>: n = 93; CRMP2<sup>Ki/Wt</sup>: n = 63; CRMP2<sup>Ki/Ki</sup>: n = 77). Data were acquired from 4 independent experiments of CRMP2<sup>wt/wt</sup>-cultures and 3 independent experiments for CRMP2<sup>Ki/Wt</sup> for CRMP2<sup>Ki/Ki</sup>. Data are shown as the mean ± SEM. d) Immunostainings of pCRMP2 in cerebellar OTSCs from Ctrl- and CRMP2<sup>ki/ki</sup>-mice show that CRMP2 phosphorylation was successfully abolished; Scale bar = 25 μm; e) Immunoblots of CRMP2 and pCRMP2 expression in cerebellar OTSCs from CRMP2<sup>Wt/Wt</sup>-, CRMP2<sup>Ki/Wt</sup>- and CRMP2<sup>Ki/Ki</sup>-mice show that pCRMP2 expression is abolished in knock-in animals and cannot be increased by treatment with PMA.

*Dendritic development in dissociated cerebellar cultures from CRMP2<sup>ki/ki</sup>-mice is impaired and can be rescued by transfection of Wt- or T555D-CRMP2*

In contrast to our findings in OTSCs, we observed that in dissociated cerebellar cultures, dendritic development of Purkinje cells derived from CRMP2<sup>ki/ki</sup>-mice was strongly impaired (Figure 7a, c). The dendritic reduction in this case was more pronounced than when dissociated cultures from control animals were transfected with the T555A-mutant (Figure 7c). We attempted to rescue CRMP2 function by transfecting the wildtype or the T555D-mutant of CRMP2 into dissociated cerebellar cultures from CRMP2<sup>ki/ki</sup>-mice to reconstitute internal levels of pCRMP2. Purkinje cells transfected with wildtype CRMP2 showed an almost complete rescue that was statistically significant (Figure 7c). Transfection of the phospho-mimetic CRMP2 only resulted in a much smaller increase of the Purkinje cell dendritic area, which still reached statistical significance (Figure 7c). These results indicate that dynamic phosphorylation and dephosphorylation of CRMP2 is essential for Purkinje cell dendritic development. This could only be fully restored in the mutant by transfection of Wt-CRMP2, transfection of the phospho-mimetic mutant had a much smaller rescuing effect.

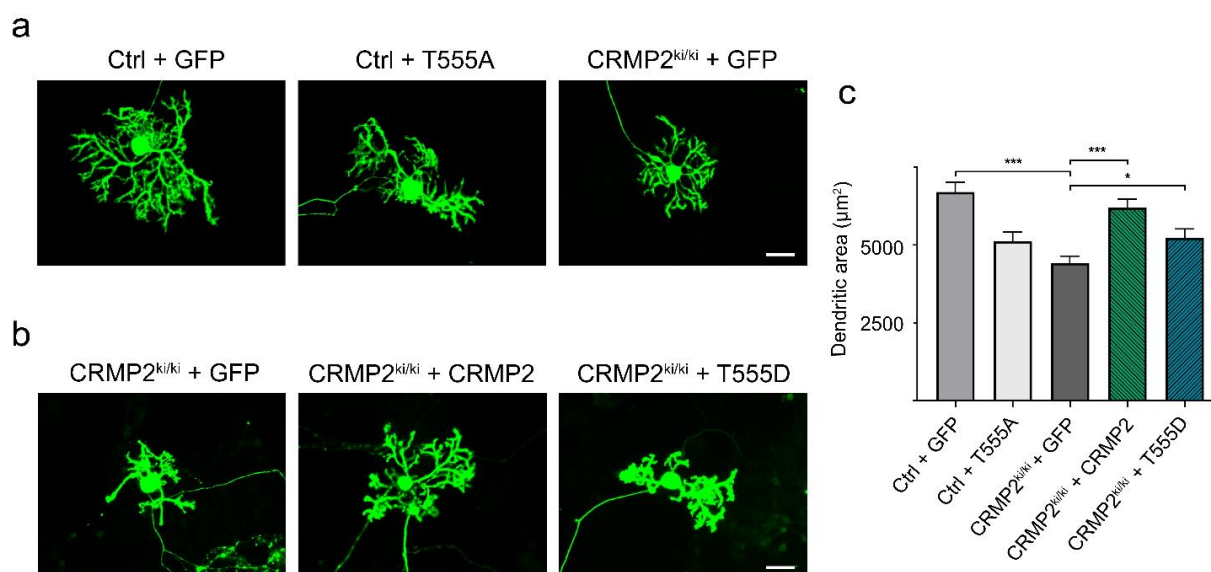


**Figure 7 Dendritic development in CRMP2<sup>ki/ki</sup>-mice is impaired in dissociated cerebellar cultures and can be rescued by transfection of Wt- or T555D-CRMP2**

a) Dissociated cerebellar cultures prepared from Ctrl-mice transfected with GFP only or GFP-T555A compared to cultures prepared from CRMP2<sup>ki/ki</sup>-mice transfected with GFP only. b) Dissociated cultures from from CRMP2<sup>ki/ki</sup>-mice transfected with GFP only, GFP-CRMP2 or GFP-T555D. More examples of Purkinje cells for the different treatments are shown in Supplementary Figure 5c) Analysis of Purkinje cell dendritic area shows a statistically significant reduction of Purkinje cell dendritic area in CRMP2<sup>ki/ki</sup>-cells transfected with GFP when compared to controls transfected with GFP ( $p < 0.001$ ). There is a virtually complete rescue effect of the Purkinje cell dendritic area after transfection of Wt-CRMP2 ( $p < 0.001$ ) and a less pronounced rescue after transfection with T555D-CRMP2 ( $p < 0.05$ ) (Ctrl + GFP:  $n = 49$ ; Ctrl + T555A:  $n = 58$ ; CRMP2<sup>ki/ki</sup> + GFP:  $n = 40$ ; CRMP2<sup>ki/ki</sup> + CRMP2:  $n = 49$ ; CRMP2<sup>ki/ki</sup> + T555D:  $n = 40$ ). Data were acquired from 4 independent experiments for Ctrl + GFP, 3 independent experiments for Ctrl + T555A and CRMP2<sup>ki/ki</sup> + GFP, and 2 independent experiments for CRMP2<sup>ki/ki</sup> + CRMP2 and CRMP2<sup>ki/ki</sup> + T555D. Data are shown as the mean  $\pm$  SEM. Scale bars = 25  $\mu$ m.

## 2.6 Discussion

In this manuscript we have identified CRMP2 as a major target of PKC $\gamma$  phosphorylation in cerebellar Purkinje cells. The interaction of PKC $\gamma$  and CRMP2 could be confirmed by co-immunoprecipitation and the proximity ligation assay. Furthermore, CRMP2 phosphorylation at Thr555 was strongly increased in the PKC $\gamma$ (S361G)-mouse model with a constitutive active PKC $\gamma$  kinase domain. As in this mouse model Purkinje cell development is severely impaired, we have further explored the effects of CRMP2 phosphorylation at Thr555 on dendritic development. Surprisingly, Purkinje cell dendritic development was impaired when CRMP2 expression in Purkinje cells was knocked down or when either a phospho-defective or a phospho-mimetic version of CRMP2, but not when wildtype CRMP2 was overexpressed in Purkinje cells highlighting the crucial role of Thr555 phosphorylation for the regulation of

dendritic development. This finding was confirmed in Purkinje cells from a novel knock-in mouse model with a CRMP2 containing a phospho-defective Thr555 phosphorylation site. Dendritic development of Purkinje cells from this mouse model was also strongly impaired and could be restored by transfection of wildtype, but less so with phospho-mimetic CRMP2 suggesting that dynamic phosphorylation and dephosphorylation at this site are required for proper Purkinje cell dendritic development. Our findings show that CRMP2 phosphorylation at Thr555 is a major mediator of the regulation of Purkinje cell dendritic growth by PKC $\gamma$ .

### *Identification of CRMP2 as a phosphorylation target and an interactor of PKC $\gamma$ in Purkinje cells*

CRMP2 is a well-known member of the CRMP family of proteins controlling axonal outgrowth and dendritic development (for review see Quach et al. 2015, Yamashita and Goshima 2012). The activity and function of CRMP2 is strongly determined by its phosphorylation state (Yamashita and Goshima, 2012) and one of its phosphorylation sites, Thr555, is subject to phosphorylation by protein kinase C (Marques et al., 2013). We have identified CRMP2 as a protein pulled down by immunoprecipitation of PKC $\gamma$  followed by mass spectrometry. The interaction of CRMP2 with PKC $\gamma$  was then confirmed with classical co-immunoprecipitation experiments and a proximity ligation assay. In the PKC $\gamma$ (S361G) mouse model there is a Purkinje cell specific expression of a mutated form of PKC $\gamma$  with a constitutive active kinase domain. Strikingly, in Purkinje cells from these mice phosphorylation of CRMP2 at Thr555 is strongly increased confirming phosphorylation by PKC $\gamma$ . At the same time, the gene and protein expression levels of total CRMP2 remained equal compared to wildtype controls.

CRMP2 is known to regulate neurite outgrowth (Arimura et al., 2000; Fukata et al., 2002) and regulates dendritic development of CA1 pyramidal neurons (Zhang et al., 2016) and cortical pyramidal cells (Yamashita et al., 2012). We therefore focused on CRMP2 as a potential mediator of the effects of PKC $\gamma$  for Purkinje cell dendritic development.

### *CRMP2 phosphorylation regulates dendritic outgrowth of cerebellar Purkinje cells*

We have studied the role of CRMP2 for Purkinje cell dendritic development mostly in dissociated cerebellar cultures allowing the transfection of Purkinje cells with the appropriate expression plasmids. In agreement with our findings that there are only minor changes of CRMP2 protein expression in cells of the PKC $\gamma$ (S361G)-mouse, overexpression of wildtype CRMP2 protein had no detectable effects on dendritic development. In contrast, miRNA-

mediated knockdown of CRMP2 led to a reduction of dendritic tree development. This is consistent with the notion that a lack of CRMP2 cannot be fully compensated for by changes in its phosphorylation state when the expression levels simply get too low. These experiments suggest that CRMP2 plays an important role for Purkinje cell dendritic growth. In order to address how CRMP2 phosphorylation affects dendritic development, we generated DNA constructs to transfect mutants of CRMP2 into dissociated cultures that either lacked the ability to be phosphorylated (T555A) or mimicked the phosphorylated state of CRMP2 (T555D). Transfection of both phospho-mutants reduced dendritic tree development markedly, with the T555D-mutant having the more pronounced effect. These results point to a negative effect exerted by phosphorylated CRMP2, which is also consistent with the situation in the PKC $\gamma$ (S361G) mouse model where CRMP2 phosphorylation is increased and dendritic development is compromised. In fact, phosphorylation of CRMP2 at Thr555 has been associated with decreased neurite outgrowth, growth cone collapse and decreased association to microtubules (Arimura et al., 2000). Furthermore, increased levels of CRMP2 phosphorylated at Thr555 were found in spinal cord neurons from patients with Alzheimer's disease and active multiple sclerosis lesions (Petratos et al., 2012; Mokhtar et al., 2018). Interestingly, also the transfection of the phospho-deficient mutant T555A resulted in a reduction of dendritic development. A simple model assuming that T555A promotes and T555D inhibits dendritic growth thus does not apply, rather transfection of any mutant suppressing dynamic phosphorylation and dephosphorylation appears to have a negative effect.

### *Importance of phosphorylation dynamics for Purkinje cell dendritic growth confirmed by T555A-CRMP2<sup>ki/ki</sup>-mice*

It is important to bear in mind that in cultures transfected with the phosphorylation-mutants of CRMP2, Purkinje cells still express the wildtype protein. Therefore, potential detrimental effects of phospho-deficient CRMP2 could have been quenched by endogenous CRMP2. For a better understanding of the effects of deactivated CRMP2 phosphorylation, we generated a knock-in mouse model using the CRISPR/Cas9 system, inserting the T555A point mutation. In this mouse model, potential background effects of native CRMP2 are eliminated.

Morphologically, cerebella from CRMP2<sup>ki/ki</sup>-mice appeared normal and organotypic slice cultures prepared from these mice did not show any overt changes in dendritic outgrowth of Purkinje cells. However, Purkinje cells in dissociated cerebellar cultures show impaired dendritic development which was more pronounced than after transfection with T555A or

T555D. This phenotype could be rescued almost completely by transfecting wildtype CRMP2. Transfecting the T555D variant gave some improvement but could not completely rescue the phenotype. This indicates that having both CRMP2-T555A and CRMP2-T555D present in the Purkinje cell is better than only having one variant, but in order to achieve full recovery the dynamic switch between the phosphorylation states is required. This is in agreement with the known growth dynamics of Purkinje cell dendrites which go through stages of elongation and retraction (Lordkipanidze and Dunaevsky, 2005), a process which would require a continuous change between phosphorylation and de-phosphorylation of CRMP2.

### *PKC $\gamma$ , CRMP2 phosphorylation and Purkinje cell dendritic development*

Our findings are compatible with a simple model in which increased activity of PKC $\gamma$  will lead to increased phosphorylation of CRMP2 at Thr555 and to a destabilization of the dendrites, probably through a destabilization of the microtubule network (Fukata et al., 2002; Chae et al., 2009). CRMP2 in this model is an important downstream effector of increased PKC activity explaining at least partially the impaired dendritic growth seen with PKC activation in Purkinje cells. Dynamic microtubule stability is important for correct dendritic development and knockdown or overexpression of the microtubule destabilizer stathmin both decrease dendritic development of cultured cerebellar Purkinje cells (Ohkawa et al., 2007). CRMP2 as a microtubule stabilizing protein could similarly influence microtubule dynamics in Purkinje cell dendritic development (see Figure 8).

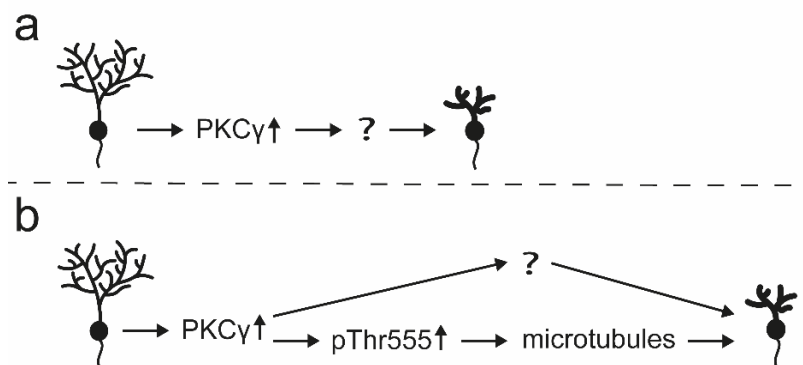


**Figure 8 Model for the regulation of Purkinje cell dendritic development via PKC $\gamma$  activity and CRMP2 phosphorylation**

a) Increased PKC $\gamma$  activity leads to impaired dendritic development in cerebellar Purkinje cells. The mediators of this effect are largely unknown. b) We have found that an increase in PKC $\gamma$  activity results in elevated CRMP2 phosphorylation at threonine 555, which could decrease microtubule stability and impair dendritic development. This can explain some of the effects of increased PKC $\gamma$  activity on dendritic development.

In our experiments, the effects of CRMP2 for dendritic outgrowth were much more evident in dissociated cerebellar cultures compared to the in situ native development of frozen cerebellar sections. This might be explained by the fact that CRMP2 is a member of a family of proteins comprised of CRMP1-5, some of which share similar functions and can interact with one another. It is therefore likely that other family members like CRMP1 and CRMP5 might have compensated for the effects of CRMP2 in these experiments (Brot et al., 2010). In dissociated cerebellar cultures Purkinje cells are more fragile and have less cellular contacts compared to organotypic slice cultures or the in vivo situation, thus effects from inadequate CRMP2 phosphorylation will be more penetrant. Furthermore, CRMP2 itself has additional phosphorylation sites like the GSK3 $\beta$  target site Thr514 or the Cdk5 phosphorylation site Ser522, which are also important for dendritic development (Yamashita and Goshima, 2012; Tan et al., 2013; Yamazaki et al., 2020) and which might be partially overlapping in activity with the Thr555 site. We found that pSer522 levels were unchanged in PKC $\gamma$ (S361G)-mice and after PMA treatment of OTSCs (Supplementary Figure 2c) and that Thr514 was only weakly increased (Supplementary Figure 2d), which is likely to be a downstream effect of Thr555 phosphorylation (Ikezu et al., 2020).

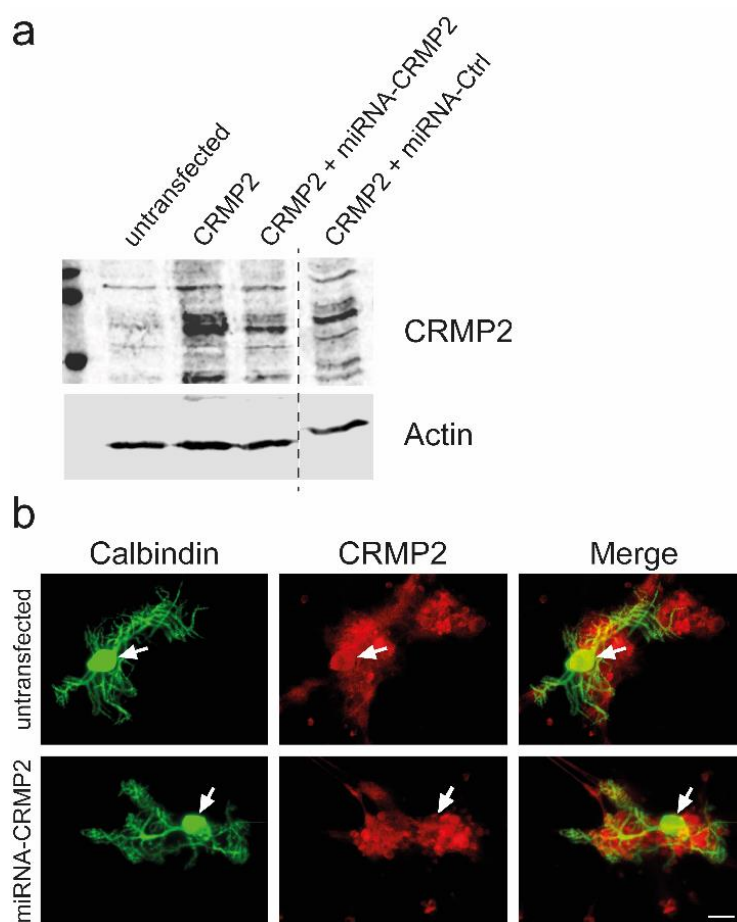
Taken together, our findings show that CRMP2 is a major target of PKC $\gamma$  phosphorylation and an important effector of the reduction of dendritic growth seen after increased PKC $\gamma$  activity.

### *Acknowledgments*

We thank Dr. John A. Hammer III (National Heart, Lung and Blood Institute, NIH, Bethesda, MD, USA) and Wolfgang Wagner (Center for Molecular Neurobiology Hamburg (ZMNH), Falkenried 94, 20251 Hamburg) for providing the pL7-mGFP plasmid and Markus Saxer and Aleksandar Kovacevic for technical assistance. Dr. Alexander Schmidt from the Proteomics Core Facility of the University of Basel assisted with the mass spectrometry experiments.

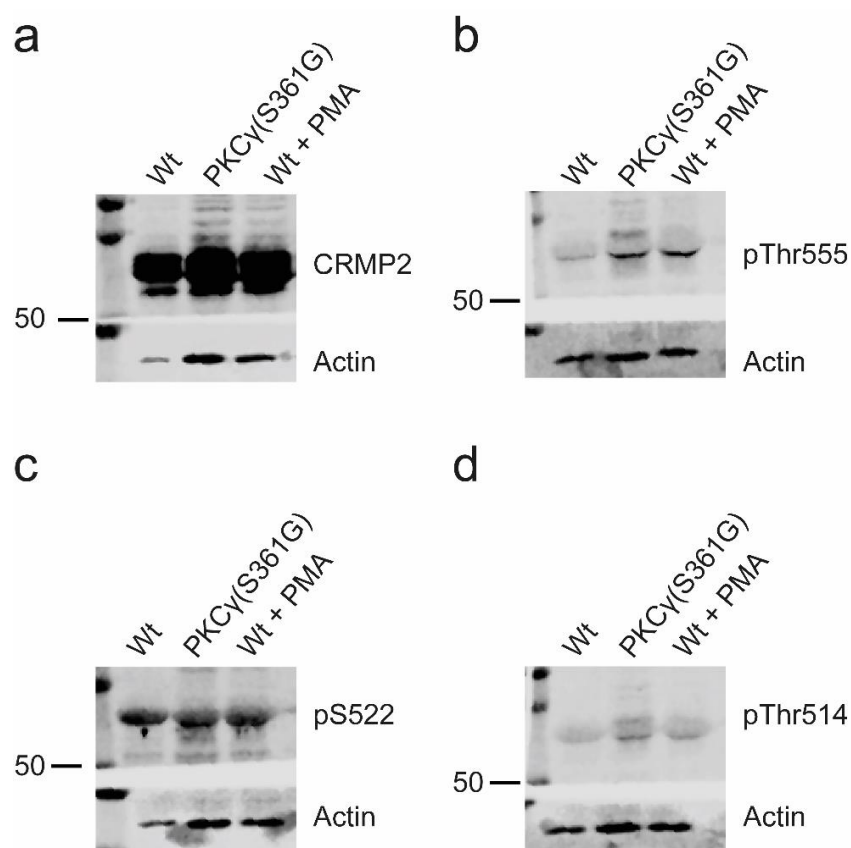
### *Authors' contributions*

Sabine Winkler designed and performed experiments, analyzed experimental data and wrote the manuscript. Etsuko Shimobayashi designed and performed experiments, analyzed experimental data and reviewed the manuscript. Josef P. Kapfhammer designed experiments, acquired funding and wrote and reviewed the manuscript.

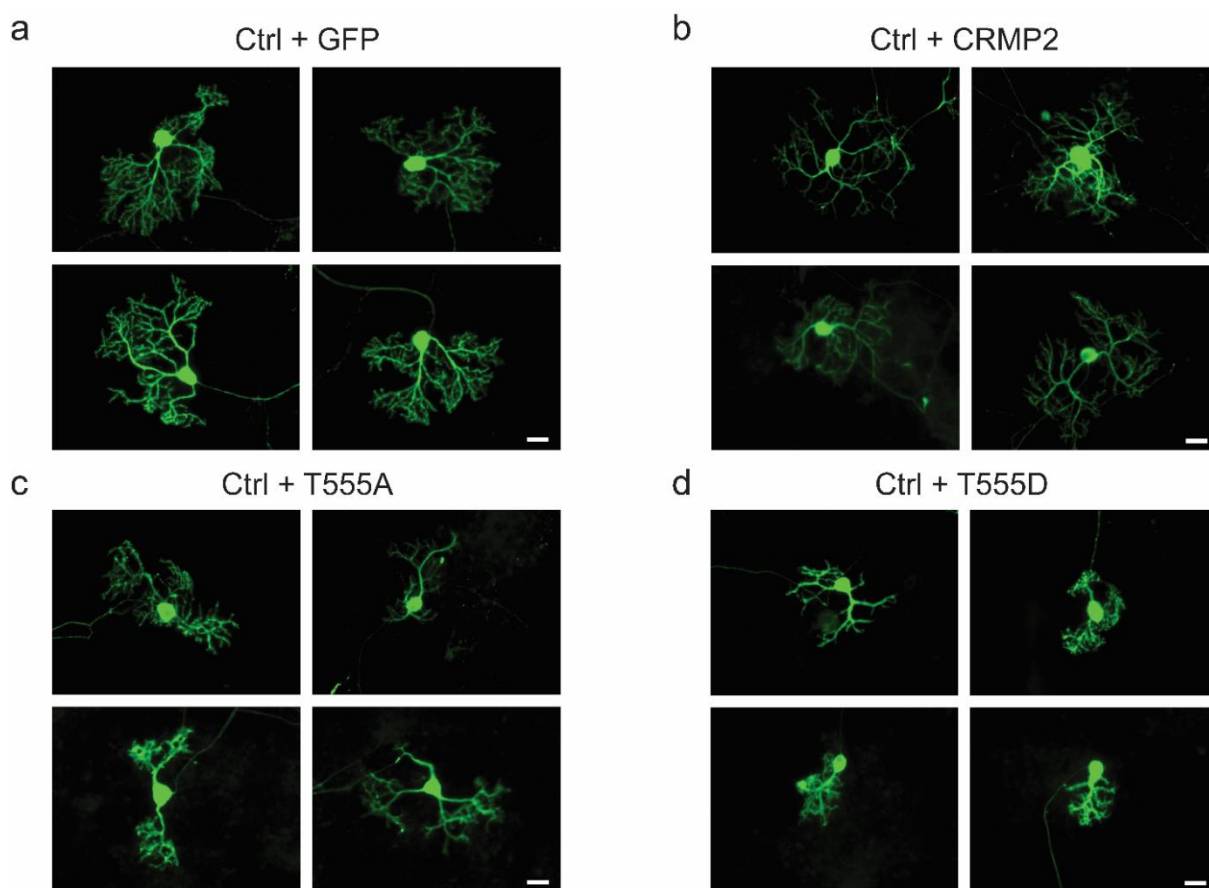
**Supplementary Figure 1 miRNA-mediated knockdown of CRMP2**

a) HEK293 cells were transfected with CRMP2 and either CRMP2-specific miRNA or an unspecific control miRNA. b) CRMP2 expression is reduced in dissociated Purkinje cells either transfected with CRMP2-miRNA. Arrows show the Purkinje cell soma. Scale bar =25μm.



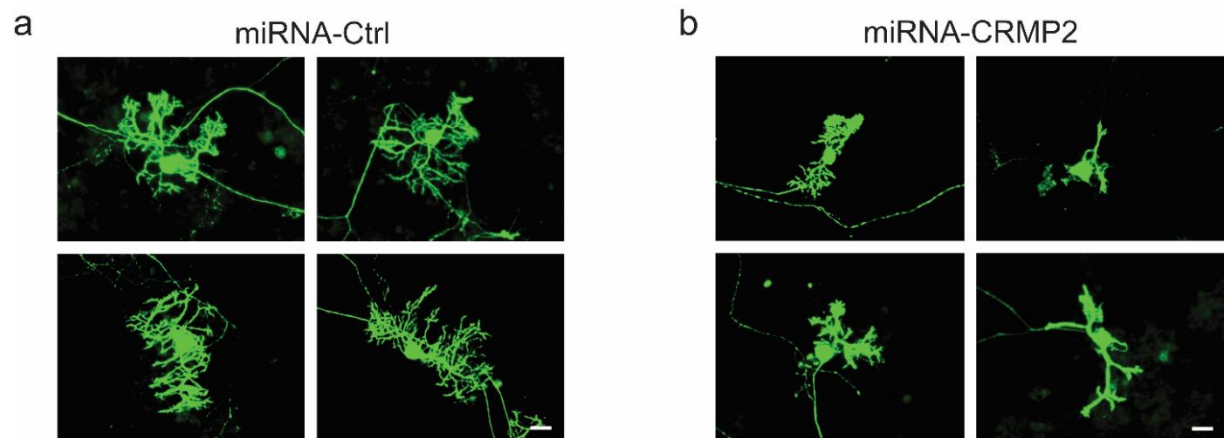
**Supplementary Figure 2 CRMP2 phosphorylation in PKCγ(S361G)-mice**

Immunoblots prepared from OTSCs of Wt- or PKCγ(S361G)-mice or Wt-cultures treated with PMA showing the expression of total CRMP2 (a), pThr555-CRMP2 (b), pS522-CRMP2 (c) or pThr514-CRMP2 (d).



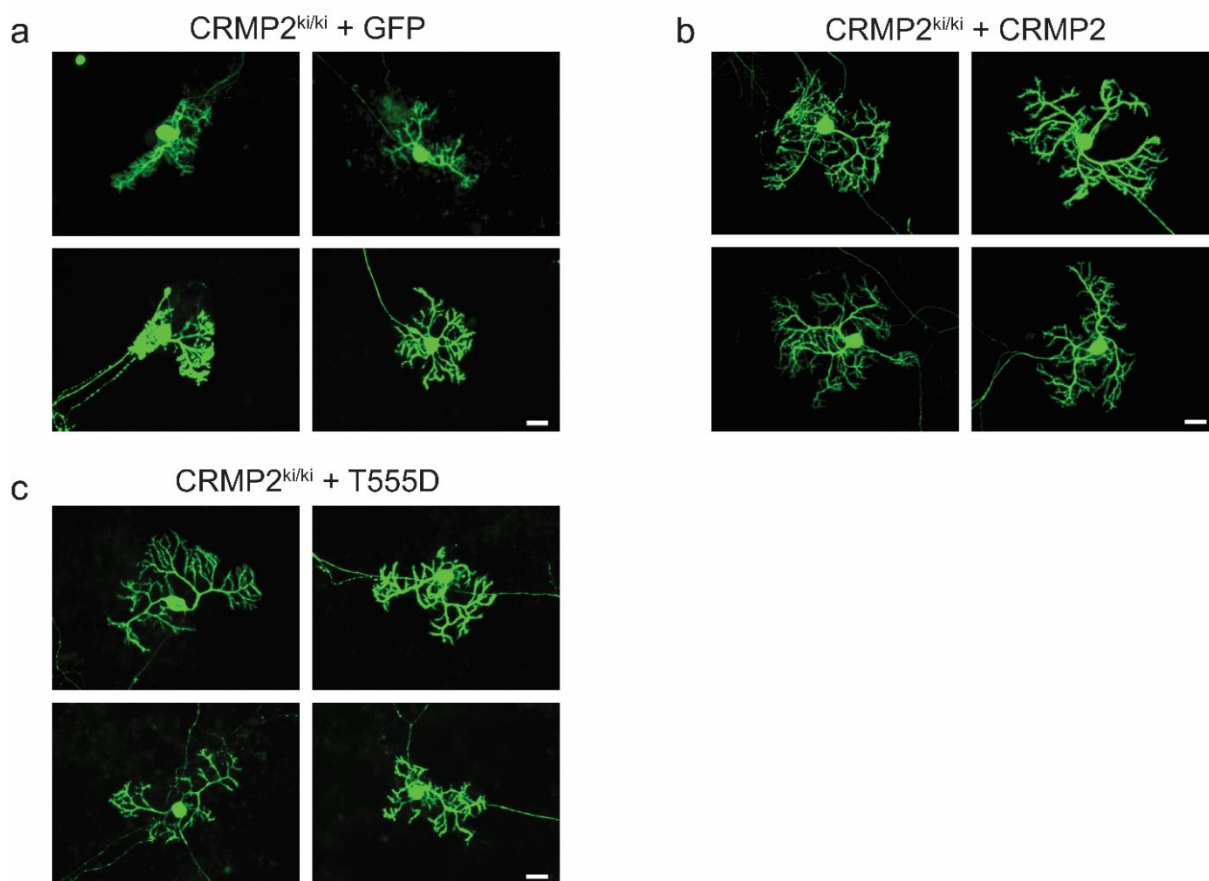
**Supplementary Figure 3 Examples of transfected cells for the overexpression of CRMP2 or its phospho-mimetic and phospho-defective mutants**

Additional images of dissociated cerebellar cultures showing Purkinje cells expressing GFP. Cells were transfected with GFP (a) or GFP-tagged wildtype CRMP2 (b), phospho-defective (T555A) (c) or phospho-mimetic (T555D) (d) CRMP2 under a Purkinje cell specific promotor; Scale bars = 25  $\mu$ m.



**Supplementary Figure 4 Examples of transfected cells for the knockdown of CRMP2**

Additional images of transfected dissociated cultures using knockdown constructs containing the L7-promotor, a His-GST reporter and either a control miRNA (a) or CRMP2 specific miRNA (b). Scale bars = 25  $\mu$ m.



**Supplementary Figure 5 Examples of transfected CRMP2<sup>ki/ki</sup> cultures transfected with wildtype CRMP2 or the T555D-mutant**

Additional images of dissociated cultures from CRMP2<sup>ki/ki</sup>-mice transfected with GFP only (a), GFP-CRMP2 (b) or GFP-T555D (c). Scale bars = 25  $\mu$ m.

**Supplementary Table 1 Report of results LC-MS/MS**

Samples were prepared from either PKC $\gamma$ (S361G)- or PKC $\gamma$ <sup>-/-</sup>-mice. Antibodies against vGlut1, PKC $\gamma$  or CRMP2 were used for the immunoprecipitation of the bait proteins. Total spectra of two sample duplicates are shown for the identified proteins. The table can be found online at: [https://static-content.springer.com/esm/art%3A10.1007%2Fs12035-020-02038-6/MediaObjects/12035\\_2020\\_2038\\_MOESM6\\_ESM.xlsx](https://static-content.springer.com/esm/art%3A10.1007%2Fs12035-020-02038-6/MediaObjects/12035_2020_2038_MOESM6_ESM.xlsx)

---

## 3. Additional Data

---

The following section contains unpublished results.

### 3.1 Phosphorylation of CRMP2 in PKC $\gamma$ (S361G)-mice is unchanged at GSK3 $\beta$ and Cdk5 target sites

CRMP protein functions are closely regulated by phosphorylation through several kinases. Phosphorylation of Ser522 via Cdk5 seems to act as a priming step enabling subsequent phosphorylation at GSK3 $\beta$  (Yoshimura et al., 2005; Cole et al., 2006). Recently, CRMP2 was shown to be a new downstream target of Tau-tubulin kinase 1 (TTBK1) (Ikezu et al., 2020). In vitro, TTBK1 induced phosphorylation of CRMP2 at T514, which was completely prevented by the mutation of serine 522 to alanine. Interestingly, mutation of threonine 555 to alanine was also partially able to abolish TTBK1-dependent phosphorylation, suggesting that also Thr555 could have some priming function.

To investigate whether phosphorylation of CRMP2 was also altered at other sites in our PKC $\gamma$ (S361G) mouse model, we performed antibody stainings on OTSCs. As observed before, CRMP2 expression was comparable between wildtype and PKC $\gamma$ (S361G)-mice (Figure IX a) while the levels of pThr555-CRMP2 were upregulated specifically in Purkinje cells (Figure IX d). Additionally, phosphorylation of Thr514 appeared to be generally upregulated to a small degree as well (Figure IX b). Phosphorylation of Ser522 on the other hand appeared unchanged between wildtype and PKC $\gamma$ (S361G)-mice (Figure IX c).

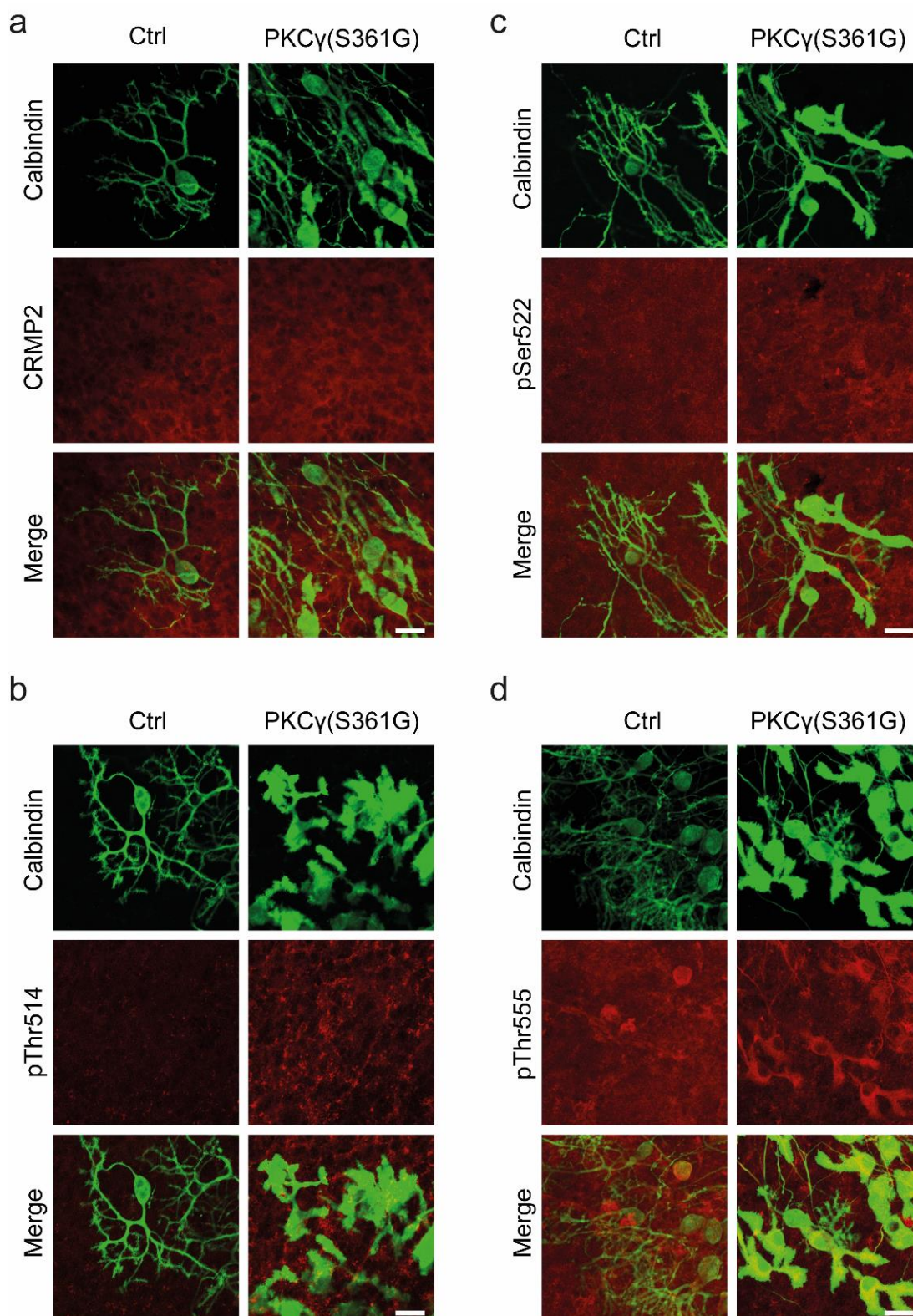


**Figure IX Phosphorylation of different CRMP2 target sites**

Immunostainings of CRMP2 and different pCRMP2 variants in cerebellar OTSCs from Wt- and PKC $\gamma$ (S361G)-mice. a) There is no visible difference in localization or expression of CRMP2. b) CRMP2 phosphorylated at Thr514 appears to be generally upregulated in PKC $\gamma$ (S361G)-mice, while phosphorylation at Ser522 seems unchanged c). As shown before, phosphorylation of CRMP2 at Thr555 is specifically upregulated in Purkinje cells in PKC $\gamma$ (S361G)-mice. Scale bars = 25  $\mu$ m.



CRMP2 phosphorylation at either Thr514, Ser522 or Thr555 was also investigated using Western blots. Phosphorylation of CRMP2 at Thr555 was upregulated in both, cultures prepared from PKC $\gamma$ (S361G)-mice and cultures treated with PMA. This also seemed to be the case, if much less pronounced, for Thr514, while Ser522 phosphorylation was similar across wildtype, PKC $\gamma$ (S361G)- and wildtype cultures treated with PMA (see Supplementary Figure 2).

To further explore the contribution of other phosphorylation sites on Purkinje cell dendritic development, we performed preliminary tests of CRMP2 phosphorylation inhibitors. Cerebellar organotypic slice cultures were treated with either (S)-lacosamide or naringenin and its derivative naringenin-7-*O*-glucuronide (N7O). (S)-lacosamide was shown to inhibit CRMP2 phosphorylation at Ser522 likely through the prevention of the Thr514 priming phosphorylation (Wilson et al., 2014). Naringenin and N7O have been associated with the inhibition of CRMP2 phosphorylation only recently and apparently act on the Thr514 phosphorylation site (Khan *et al.*, 2012; Yang, Kuboyama and Tohda, 2017; Lawal, Olotu and Soliman, 2018).

Our first experiments do not show an effect of lacosamide on the dendritic development of neither control- or PKC $\gamma$ (S361G)-cultures (Figure X a). However, more concentrations should be tested to see whether the dose used was sufficient to elicit a biological effect.

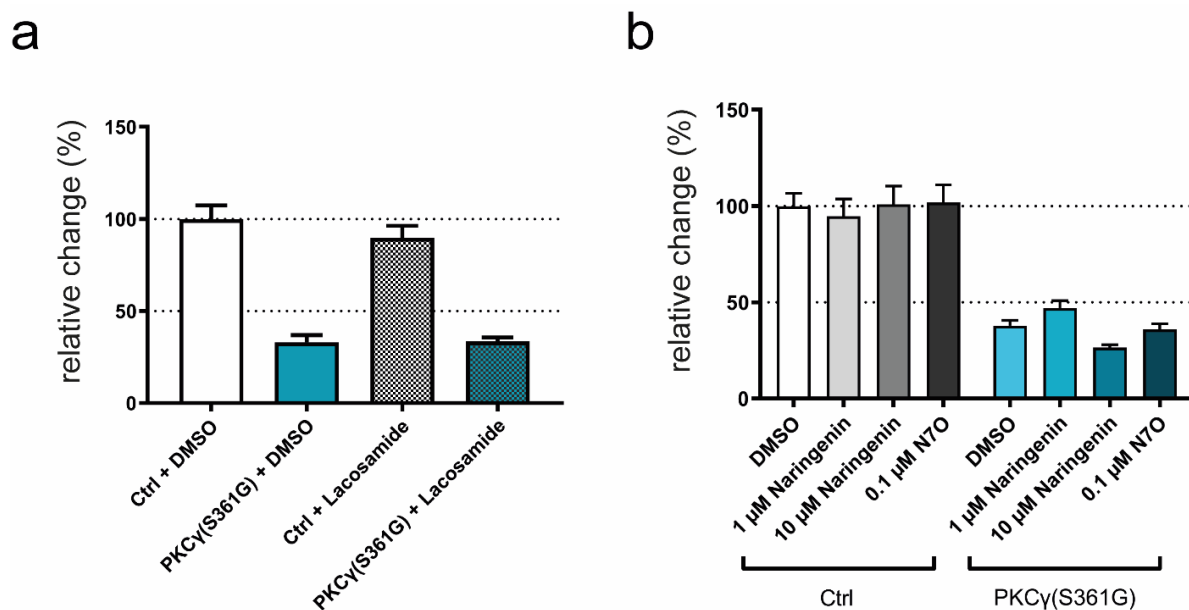


### Figure X Treatment of organotypic slice cultures with inhibitors of CRMP2 phosphorylation

Quantification of Purkinje cell dendritic area in OTSCs from either control- or PKCγ(S361G)-mice. a) Cultures were treated with either with DMSO or with 200 μM (S)-lacosamide. Dendritic outgrowth is impaired similarly in cultures from PKCγ(S361G)-mice treated with DMSO or (S)-lacosamide. At least 20 cells were measured per group. Data were acquired from 1 experiment. b) Cultures were treated with different concentrations of naringenin and its derivative N7O. Decreased dendritic expansion of Purkinje cells was similar between most groups except in cultures treated with 1 μM naringenin, where dendritic development was slightly improved compared to DMSO treated cultures. At least 18 cells were measured per group. Data were acquired from 1 experiment. Data are shown as the mean  $\pm$  SEM.

In case of naringenin and N7O, more concentrations were tested. Generally, there was only a slight effect on the Purkinje cell dendritic area in cultures treated with 1 μM of naringenin which was also the most potent concentration in another study exploring Aβ-induced axonal atrophy (Yang et al., 2017). The effects of naringenin/N7O have so far not been extensively characterized, however, this pilot experiment offers an interesting starting point to examine the cross-effects of different CRMP2 phosphorylations.

## 3.2 Inhibition of CaMKII does not decrease Thr555 phosphorylation in PKCγ(S361G)-mice

Our findings have shown that there is an increase in CRMP2 phosphorylation at threonine 555 in PKCγ(S361G)-mice. PKC is only one kinase targeting of the Thr555 phosphorylation site amongst others such as CaMKII and ROCK2 (Arimura et al., 2000, 2005; Hou et al., 2009). Additionally, PKC has been shown to also modulate CaMKII and RhoA activity (Sugawara et al., 2017; Rosas-Hernández et al., 2019). In order to exclude that the increase



of pCRMP2 is mediated through an indirect effect via CaMKII, we treated OTSCs with the CaMKII inhibitor KN-93. In these experiments, KN-93 did not improve dendritic outgrowth of Purkinje cells in cultures prepared from PKC $\gamma$ (S361G)-mice when compared to DMSO treated cultures (Figure XI a). We also checked whether the inhibition of CaMKII effectively decreased pCRMP2 protein levels in Western blots and could not detect any apparent changes (Figure XI b).

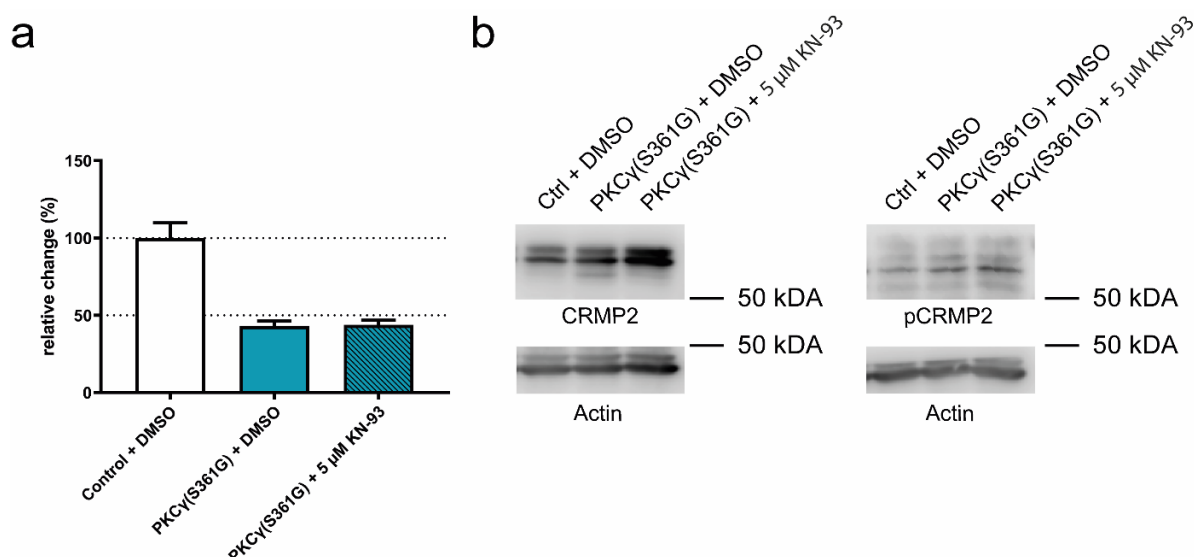


### Figure XI Inhibition of CaMKII does not decrease Thr555 phosphorylation in PKC $\gamma$ (S361G)-mice

Organotypic slice cultures prepared from control or PKC $\gamma$ (S361G)-mice were treated with either DMSO or the CaMKII inhibitor 5  $\mu$ M KN-93. a) Quantification of Purkinje cell dendritic area in OTSCs shows no rescue of dendritic development through the inhibition of CaMKII. (Control + DMSO: n = 13; PKC $\gamma$ (S361G) + DMSO: n = 28; PKC $\gamma$ (S361G) + KN-93: n = 28) Data were acquired from 1 experiment for Ctrl + DMSO and 2 independent experiments for PKC $\gamma$ (S361G) + DMSO or KN-93 respectively. Data are shown as the mean  $\pm$  SEM. b) Western blot analysis of CRMP2 phosphorylation shows similar levels of pThr555-CRMP2 in DMSO and KN-93 treated PKC $\gamma$ (S361G)-cultures.

These early experiments suggest that CaMKII is not involved in the upregulation of pCRMP2 in PKC $\gamma$ (S361G)-mice and suggest that CRMP2 phosphorylation at the Thr555 site was by direct interaction with PKC $\gamma$ . Nevertheless, further experiments with inhibitors of ROCK2 activity will be necessary to further exclude a possible involvement of other kinases in CRMP2 phosphorylation in the context of Purkinje cell dendritic development.

### 3.3 Impaired dendritic development of Purkinje cells from PKC $\gamma$ (S361G)-mice cannot be rescued through the transfection of CRMP2

Transfection of the T555D-mutant into dissociated wildtype cerebellar cultures leads to reduced dendritic expansion of Purkinje cells (Figure 4 a-b). This negative effect of the

phospho-mimetic CRMP2 on dendritic outgrowth could at least partially explain the reduced size of Purkinje cell dendritic trees in PKC $\gamma$ (S361G)-mice. We therefore aimed to explore whether a reconstitution of non-phosphorylated CRMP2 could rescue dendritic growth in dissociated cultures.

Purkinje cells in dissociated cerebellar cultures prepared from PKC $\gamma$ (S361G)-mice show a strongly diminished dendritic tree with thickened, short dendrites (Figure 4c). Transfection of neither wildtype, nor phospho-defective CRMP2 was able to rescue the dendritic reduction of Purkinje cells, while transfection of phospho-mimetic T555D-CRMP2 further reduced dendritic outgrowth significantly (Fig. VIII, a-b;  $p < 0.05$ ).

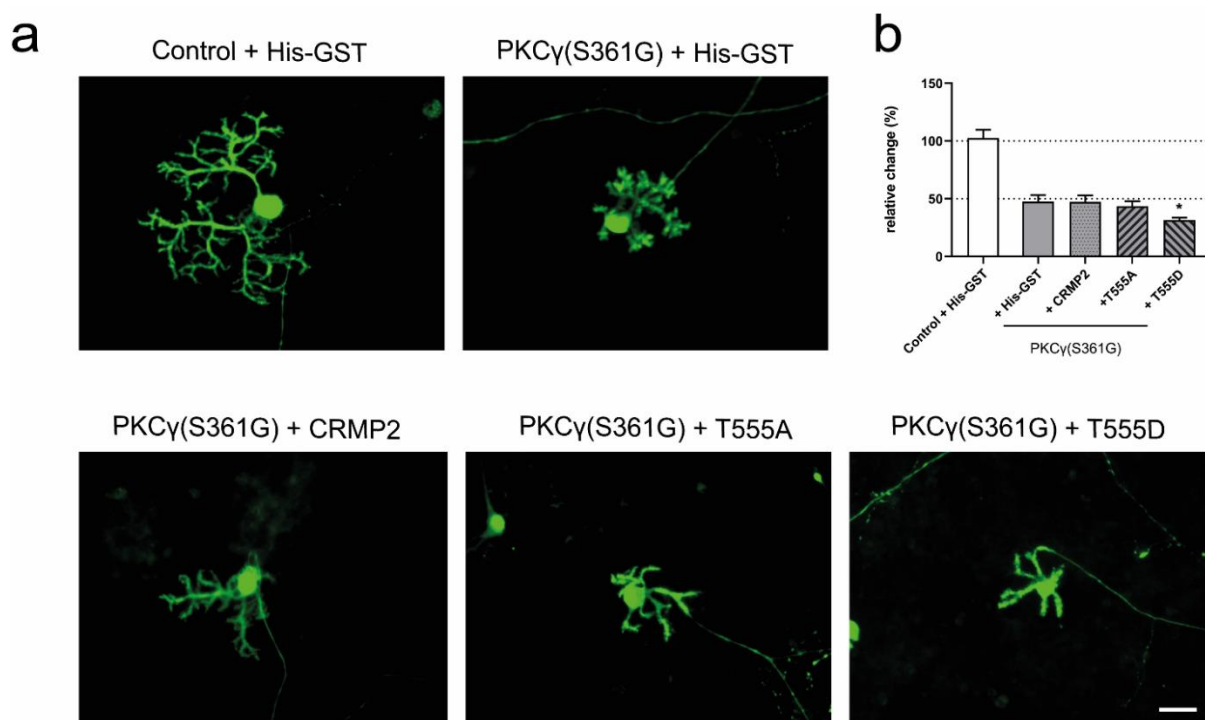


**Figure VIII Reconstitution of CRMP2 phosphorylation does not rescue dendritic development in PKC $\gamma$ (S361G)-dissociated cultures**

a) Transfected Purkinje cells in dissociated cerebellar cultures prepared from control- or PKC $\gamma$ (S361G)-mice. Purkinje cells from PKC $\gamma$ (S361G)-mice show a strong reduction of Purkinje cell dendritic area. b) Analysis of the dendritic Purkinje cell area. Transfection of His-CRMP2 or His-T555A did not change Purkinje cell dendritic outgrowth. When PKC $\gamma$ (S361G)-cultures are transfected with His-T555D, dendritic expansion is even further decreased ( $p < 0.05$ ). (Wildtype + His-GST:  $n = 32$ ; PKC $\gamma$ (S361G) + His-GST:  $n = 10$ ; PKC $\gamma$ (S361G) + His-CRMP2:  $n = 27$ ; PKC $\gamma$ (S361G) + His-T555A:  $n = 24$ ; PKC $\gamma$ (S361G) + His-T555D:  $n = 42$ ). Data were acquired from 1 experiment for Ctrl + His-GST, PKC $\gamma$ (S361G) + His-GST and PKC $\gamma$ (S361G) + His-CRMP2, 3 independent experiments for Ctrl + T555A and CRMP2<sup>ki/ki</sup>+ GFP, and 2 independent experiments for PKC $\gamma$ (S361G) + His-T555A and PKC $\gamma$ (S361G) + T555D. Data are shown as the mean  $\pm$  SEM. Scale bar = 25  $\mu$ m.

These results confirm a negative effect of T555D-CRMP2. Our findings also suggest that overexpression of CRMP2 with different phosphorylation levels cannot revert the effects PKC activation in PKC $\gamma$ (S361G)-mice.

### **3.4 Tubulin stabilization is impaired in PKC $\gamma$ (S361G)-mice**

As we have shown in this study, a dysregulation of CRMP2 phosphorylation at threonine 555 impairs dendritic development in cerebellar Purkinje cells in dissociated cultures. CRMP2 is a protein involved in a plethora of different interactions and the pathways affected in Purkinje cell dendritic development still remain unclear. Phosphorylation of CRMP2 at most of its known phosphorylation sites leads to impaired neurite outgrowth (see Moutal, White, et al., 2019 for a detailed review). This effect is thought to be mediated by disrupting the binding of CRMP2 to components of the cytoskeleton, especially tubulin.

Acetylation of tubulin occurs on lysine 40 after it has been polymerized into microtubules and is therefore an indication of stabilized microtubules. In cerebellar Purkinje cells, tubulin acetylation has been shown to promote dendritogenesis (Ohkawa et al., 2008).

We therefore stained cerebellar sections of control-, PKC $\gamma$ (S361G)- and CRMP2<sup>ki/ki</sup>-mice at postnatal day 12 for acetylated- $\alpha$ -tubulin. In control and CRMP2<sup>ki/ki</sup>-mice, acetylated tubulin is found in the soma and dendrites of Purkinje cells in the cerebellum (Figure IX a, c). In PKC $\gamma$ (S361G)-mice, this is also the case in most areas of the cerebellum. However, morphologically aberrant cells, mostly found in lobule VII, seem largely devoid of acetylated- $\alpha$ -tubulin (Figure IX b).

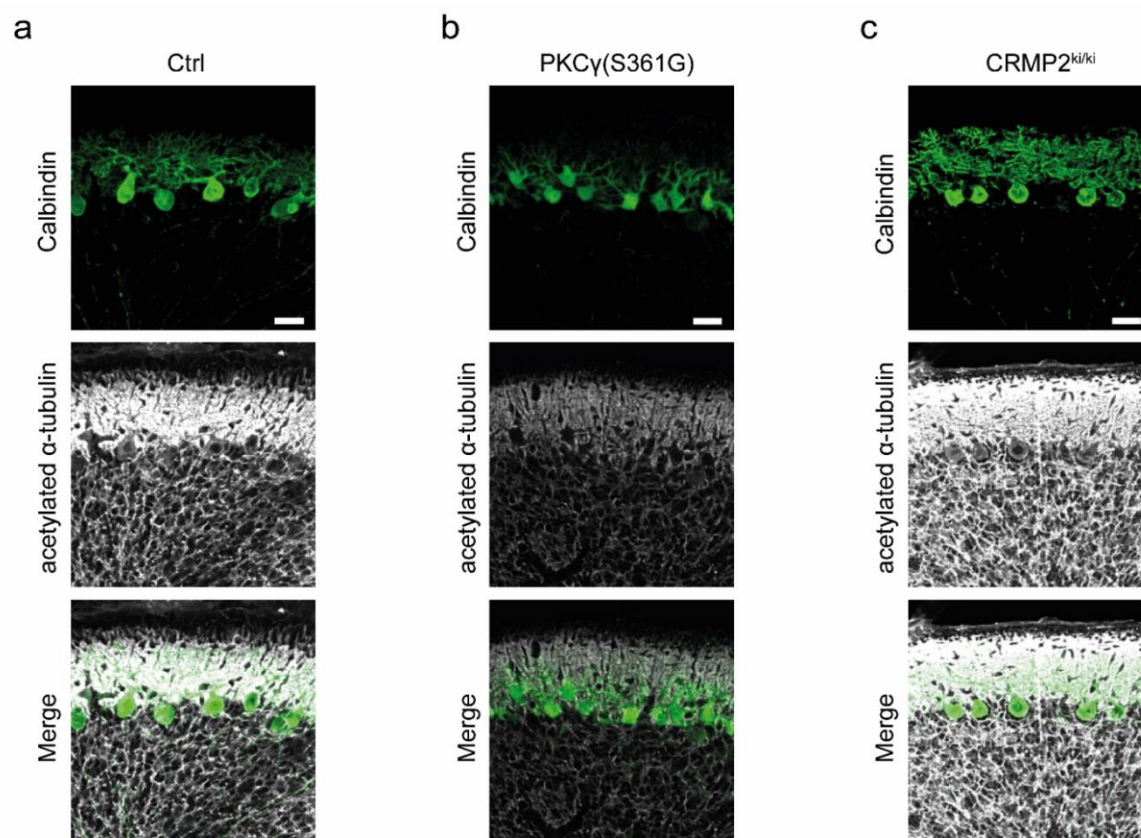


### Figure IX Tubulin acetylation is decreased in PKCγ(S361G)-mice

Frozen sagittal sections of the cerebellum from control-, PKCγ(S361g)- and CRMP2<sup>ki/ki</sup>-mice at postnatal day 12. While acetylated α-tubulin is detected in soma and dendrites of Purkinje cells in control (a) and CRMP2<sup>ki/ki</sup>-animals (c), especially morphologically aberrant cells in lobule VII are largely devoid of acetylated tubulin (b). Scale bars = 25 μm.

We additionally attempted to detect changes in tubulin acetylation levels by Western blot, which did not show any changes between control, PKCγ(S361G)- and CRMP2<sup>ki/ki</sup>-mice (Figure X).

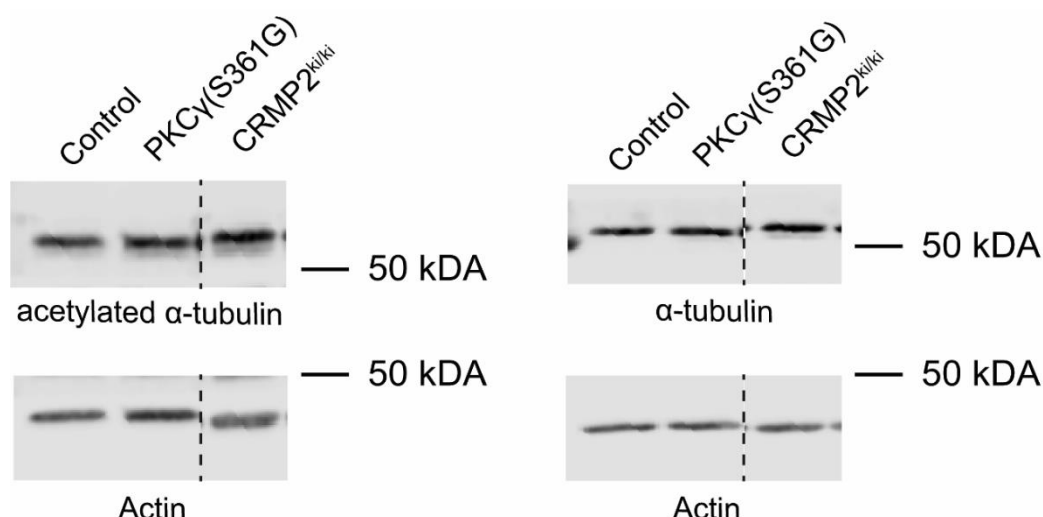


**Figure X Tubulin acetylation in cerebellar lysates**

Western blot of analysis of tubulin acetylation compared between control, PKC $\gamma$ (S361G)- and CRMP2<sup>ki/ki</sup>-mice. Both, the expression of  $\alpha$ -tubulin and the levels of tubulin acetylation appear unchanged between groups.

As the changes in total acetylated tubulin are most likely only minimally altered due to the relatively small number of cells affected, this assay is probably not sensitive enough for our purposes. Our findings could point to a disruption in tubulin stabilization during Purkinje cell development in PKC $\gamma$ (S361G)-mice. However, another methodology should be chosen to confirm the findings and also to explore, whether tubulin acetylation is also affected in our CRMP2<sup>ki/ki</sup>-mouse.

### 3.5 Climbing- and parallel fiber inputs appear normal in CRMP2<sup>ki/ki</sup>-mice

Purkinje cells receive excitatory input from parallel fibers of the granule cells and climbing fibers originating from cells in the inferior olive. During development, especially climbing fiber synapses undergo excessive pruning until a one climbing fiber to one Purkinje cell relationship is established. Recently, it has been shown that synaptic pruning is defective in CRMP2<sup>-/-</sup>-mice (Ziak et al., 2020). To check whether climbing- and parallel fiber inputs might also be affected in our CRMP2<sup>ki/ki</sup>-mouse model we stained frozen cerebellar sections for the synaptic markers vGlut1 and vGlut2. In comparison to control mice, CRMP2<sup>ki/ki</sup>-mice do not show overt signs of a change in synaptic innervation (Figure

XI).

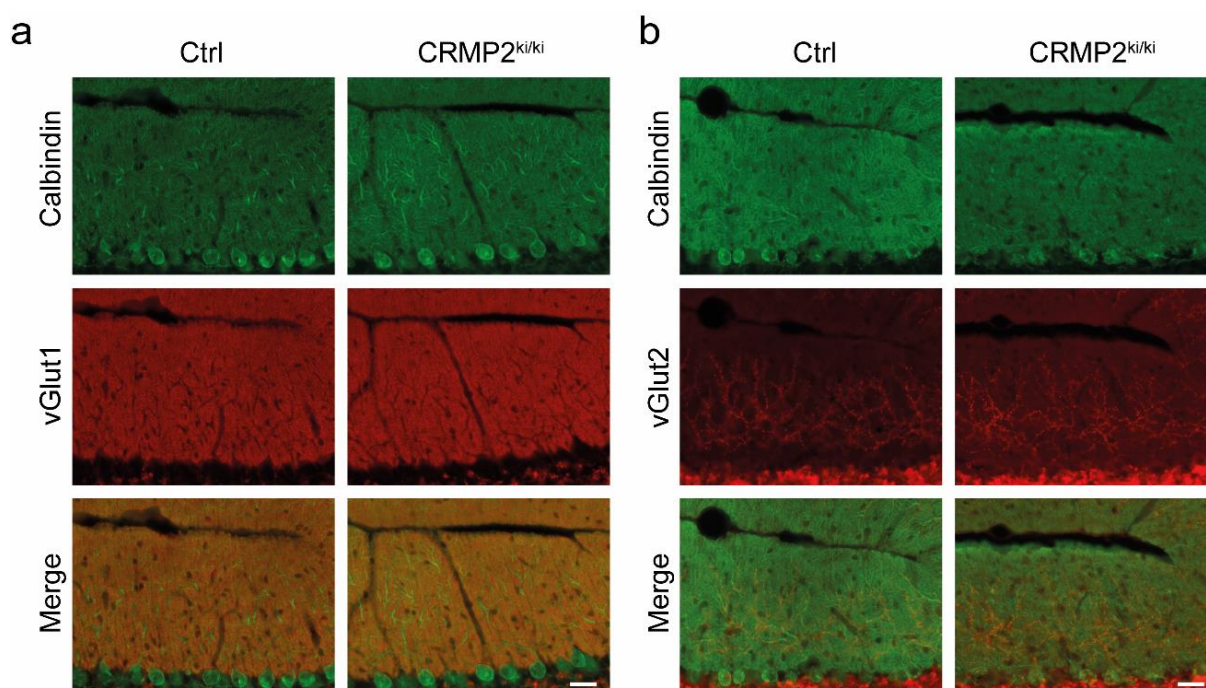


**Figure XI Parallel and climbing fiber innervation is normal in CRMP2<sup>ki/ki</sup>-mice**

Frozen sagittal sections of the cerebellum from control- and CRMP2<sup>ki/ki</sup>-mice. Parallel fiber (a) and climbing fiber inputs (b) seem normal in CRMP2 knock-in mice. Scale bars = 25  $\mu$ m.

These findings are consistent with our previous observations that the general cerebellar morphology appears to be unchanged in these animals (Figure 6 a) and shows that cerebellar development is also unaltered on a cellular level.

### 3.6 CRMP2<sup>ki/ki</sup>-mice are not protected from the effects of PMA-mediated reduction of dendritic growth

As we have shown, phosphorylation of CRMP2 at threonine 555 was successfully abolished in our CRMP2<sup>ki/ki</sup>-model (Figure 6 d-e). We now wanted to assess, whether a disruption of CRMP2 phosphorylation could protect Purkinje cells from a PMA-induced reduction of dendritic outgrowth. Organotypic slice cultures prepared from homozygous wildtype, heterozygous knock-in or homozygous knock-in mice were all equally susceptible to a PMA-induced dendritic reduction (Figure XII).



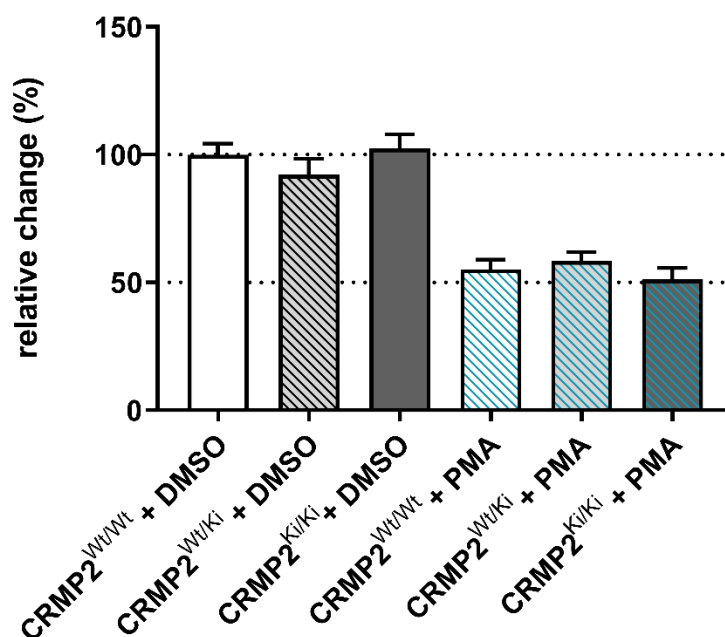


**Figure XII Purkinje cells from CRMP2<sup>Ki/Ki</sup>-mice are not protected from the effects of PMA-stimulation**

Quantification of Purkinje cell dendritic area in OTSCs treated either with DMSO or with 100 nm PMA. Dendritic outgrowth is similarly impaired in slice cultures from wildtype, hetero- and homozygous animals. (CRMP2<sup>Wt/Wt</sup> + DMSO: n = 57; CRMP2<sup>Wt/Ki</sup> + DMSO: n = 58; CRMP2<sup>Ki/Ki</sup> + DMSO: n = 69; CRMP2<sup>Wt/Wt</sup> + PMA: n = 58; CRMP2<sup>Wt/Ki</sup> + PMA: n = 56; CRMP2<sup>Ki/Ki</sup> + PMA: n = 52. Data were acquired from 3 independent experiments and shown as the mean ± SEM.

This observation supports the notion that CRMP2 participates in, but is not the sole modulator of PKC activity-induced changes of dendritic development in cerebellar Purkinje cells. The use of a lower PMA concentration might reveal more subtle effects.

---

## 4. General Discussion

---

### 4.1 The role of CRMPs in Purkinje cells

All CRMP family members have been found to be expressed in the cerebellum. CRMP1-4 are expressed at higher levels during embryonic development and soon after birth. In adulthood, their expression is generally downregulated with CRMP2 being the only family member showing persistent expression. Interestingly, the temporal expression of CRMP5 appears to develop in the opposite manner. In immunostainings, CRMP5 was detected at low levels after p12 and at high levels in cerebella of adult mice (Bretin et al., 2005; Yamashita et al., 2011). This is in line with the results from our mass spectrometry analyses prepared from p12 cerebella, in which all CRMP family members were detected except for CRMP5.

In Purkinje cells, CRMP1, 2 and 4 have been detected in the soma, axons and dendrites of mouse and rat cerebellum (Wang and Strittmatter, 1996; Bretin et al., 2005; Yamazaki et al., 2020). All CRMPs were furthermore found in the granule cell layer, where CRMP3 expression persists until adulthood in rat (Wang and Strittmatter, 1996).

It was shown, that overexpression of CRMP5 had a negative effect on the development of primary dendrites in cultured hippocampal neurons, while knockdown increased the length and number of dendritic neurites (Brot et al., 2010). Overexpression of CRMP2 was able to induce dendritic outgrowth which was suppressed by the overexpression of CRMP5. The authors detected a constant expression of CRMP2 in these neurons, while the onset of CRMP5 expression started later and then increased over time. CRMP5 and CRMP2 therefore both seem to orchestrate dendritic outgrowth at different stages of development, likely by competitive binding to tubulin (Brot et al., 2010).

In CRMP5 knockout mice, Purkinje cells show abnormal dendritic development with thickened primary dendrites and enlarged somata (Yamashita et al., 2011). These morphological abnormalities develop after postnatal day 21 which is when CRMP5 expression became detectable in Purkinje cells. CRMP5 therefore seems to regulate Purkinje cell dendritic outgrowth only at later stages of cerebellar development. As BDNF failed to induce the formation in primary dendrites of cultured hippocampal neurons of CRMP5<sup>-/-</sup> mice, CRMP5 could take part in BDNF-mediated dendritic development.

Recently it was shown that CRMP2 phosphorylation is an important regulator of Purkinje cell migration (Yamazaki et al., 2020). In this study, the effect of several CRMP family members was explored by using CRMP1 and CRMP4 knockout mice either alone or in combination with the knock-in of an alanine at the S522 phosphorylation site in CRMP2. On



their own, CRMP4 knockout and CRMP2 knock-in induced subtle alterations to Purkinje cell migration in the cerebellum, while CRMP1 knockout alone was sufficient to significantly increase the number of misaligned Purkinje cells. Crossing the different mouse lines to obtain double mutants increased the number of misaligned cells in comparison to the single mutants. Combination of CRMP1 and 4 knockouts with the CRMP2 knock-in severely disturbed Purkinje cell migration and led to overt mislocalization, especially in lobule X. CRMP-triple mutant mice furthermore show signs of impaired motor coordination in the balance beam test. In another study, the authors showed that a combined knockout of CRMP4 and S522A knock-in in CRMP2 led to increased dendritic branching and disrupted *Sema3A* dendritic outgrowth promotion in hippocampal neurons (Niisato et al., 2013). The authors also combined the knockout of CRMP1 with the S522A-knock-in in CRMP2 and observed severe alterations in the dendritic patterning of cortical pyramidal neurons (Yamashita et al., 2012).

Taken together these studies have provided some insight into the regulation of different CRMP family members in dendritic development and introduced the potential role of CRMP2 phosphorylation in such processes. Understanding the interplay of different CRMP family members will be crucial to elucidate their roles also in Purkinje cell dendritic development specifically.

## **4.2 Mechanisms of disrupted CRMP2 signaling in cerebellar Purkinje cells**

In our study, we observed reduced dendritic outgrowth of cerebellar Purkinje cells after mRNA mediated knockdown of CRMP2 in dissociated cultures. In cerebellar granule cells, knockdown of CRMP2 also leads to reduced dendritic outgrowth (Jiang et al., 2020), which appears to be the result of a disruption of the *Sema3A* pathway. Generally, other CRMP family members seem to be upregulated in CRMP2<sup>ko/ko</sup>-mice (Hirano et al., 2016) and could conserve *Sema3A* signaling (Ziak et al., 2020). In Purkinje cells, *Sema3A* mRNA has been detected as early as embryonic day 11 and persistently until adulthood (Catalano et al., 1998). However, *Sema3A* knockout mice do not show any developmental abnormalities of the cerebellum (Catalano et al., 1998). Knockdown of *Sema3A* in cerebellar Purkinje cells accelerates climbing fiber elimination (Uesaka et al., 2014; Uesaka and Kano, 2018). In our CRMP2-T555A knock-in mice, climbing fiber innervation appears normal as judged by vGlut2-immunostaining. However, as phosphorylated CRMP2 is generally considered to be the “inactive” form of CRMP2, the T555A-mouse model most likely does not recapitulate the same consequences as were observed after CRMP2 knockdown. In PKC $\gamma$ (S361G)-mice, we

have shown that climbing fiber innervation appears normal in most parts, however, climbing fiber innervation is impaired in lobule VII, where also Purkinje cell morphology is markedly altered (Trzesniewski et al., 2019). As we have now shown in this study, phosphorylation of CRMP2 is increased strongly at threonine 555 in these mice. In the future, it would therefore be interesting to also develop a mouse model expressing the phospho-mimetic T555D-CRMP2 mutant form and investigate whether these mice would show similar morphological abnormalities.

Many mutations causing SCA14 in humans have been shown to lead to an increase of intracellular calcium in vitro (Adachi et al., 2008). CRMP2 can interact with and regulate the surface expression of NCX3, Cav2.2 and NMDAR (Al-Hallaq et al., 2007; Brittain et al., 2012; Brustovetsky et al., 2014). A 15-amino acid fragment of CRMP2 fused to the TAT cell-penetrating motif of the HIV-1 protein (TAT-CBD3) is able to disrupt CRMP2 binding to Cav2.2 and NMDAR, likely by occupying the respective binding sites, which leads to the internalization of Cav2.2. Disassociation from NMDAR was shown to inhibit its activity, however, its membrane localization was unchanged. Application of the CBD3 protein furthermore led to increased CRMP2 binding to NCX3 and likewise, to its internalization. CRMP2 binding therefore can modulate the activity of these calcium regulating proteins in different ways, which in turn could potentially lead to altered internal calcium levels. Exploring the intracellular calcium levels and channel functions in PKC $\gamma$ (S361G)- and CRMP2<sup>ki/ki</sup>-mice therefore poses a promising field of study in future experiments.

### **4.3 Differential phosphorylation of CRMP2**

The best studied targets of CRMP2 phosphorylation are threonine 514 (GSK3 $\beta$ ), serine 522 (Cdk5), and threonine 555 (ROCK2/CaMKII/PKC). While Thr514 and Ser522 are conserved in CRMP1 and 4, the Thr555 phosphorylation site is not conserved amongst other CRMP family members (Cole et al., 2006).

We have found that apart from Thr555 phosphorylation, also the phosphorylation of CRMP2 at Thr514 was upregulated slightly. As mentioned above, phosphorylation of Thr555 and subsequently Ser522 have been proposed to act as priming steps for the GSK3 $\beta$ -mediated phosphorylation at Thr514. However, our Western blot results do not show an upregulation of Ser522, which makes the possibility that Thr555 priming is required for Thr514 phosphorylation questionable.

GSK3 $\beta$  itself is a target of phosphorylation via PKC (Goode et al., 1992). This phosphorylation, however, has generally been shown to inhibit GSK3 $\beta$  activity and does

therefore not explain our findings either. It is therefore likely that a possible upregulation of Thr514 phosphorylation in CRMP2 is mediated by another intermediate factor.

In recent years, several compounds were discovered that influence CRMP2 phosphorylation. First, the antiepileptic drug (R)-lacosamide (Vimpat®), was identified as a binding partner of CRMP2 and shown to enhance slow inactivation of voltage-gated sodium channels in a CRMP2 dependent manner (Beyreuther et al., 2007; Errington et al., 2008; Ki et al., 2009; Wang et al., 2010). (R)-lacosamide furthermore impairs CRMP2-driven tubulin polymerization (Wilson et al., 2012) and (S)-lacosamide was shown to have the same effect by preventing the priming phosphorylation of CRMP2 via Cdk5, leading to a decrease of pThr514-CRMP2 (Wilson et al., 2014). However, the binding affinity of lacosamide to CRMP2 is low and the interaction has been questioned (Wolff et al., 2012). Another group of molecules, naringenin and its metabolites, were shown to be effective in the treatment of Alzheimer pathology in mice and to be able to cross the blood-brain-barrier where they target CRMP2 and downregulate its phosphorylation (Khan et al., 2012; Yang et al., 2017; Lawal et al., 2018). Also in the case of naringenin, however, the binding affinity for CRMP2 is low and its direct effect on CRMP2 is not confirmed (Zhou et al., 2019).

We have performed preliminary experiments with (S)-lacosamide, naringenin and N7O to explore their effect on dendritic development of Purkinje cells in OTSCs. Treating OTSCs prepared from PKC $\gamma$ (S361G)-mice with (S)-lacosamide did not improve dendritic development. However, the concentrations used for treating the cultures could be optimized. In case of naringenin and N7O we tested a broader range of concentrations and observed a small improvement of dendritic development in cultures treated with 1  $\mu$ M naringenin. Further experiments will have to be performed to corroborate these findings and additional analyses of the effect of naringenin on the different phosphorylation sites will need to be examined.

Apart from the compounds tested so far, more molecules have been proposed to influence CRMP2 phosphorylation. LKE, a synthetic, cell-permeable lanthionine ketimine ester, was shown to decrease phosphorylation of CRMP2 at Thr514 and to exert protective effects in a mouse model of Alzheimer's disease (Hensley et al., 2010, 2013). The most recently discovered CRMP2 binding agent, the small molecule edonerpipic maleate was postulated to act on CRMP2 phosphorylation through direct binding and improve recovery after cryoinjury to the motor cortex, which it failed to do in CRMP2-deficient mice (Abe et al., 2018). Also in the case of edonerpipic maleate, however, the findings remain controversial as others could not recapitulate the binding to CRMP2 or its effect on CRMP2 phosphorylation (Moutal et al., 2019b).

To find compounds acting on and especially reducing CRMP2 phosphorylation has been a goal in the search for treatments of several neurological diseases. The exact mechanisms of action of many of the identified drugs nonetheless are so far only poorly understood and the specificity of some of the compounds remains questionable. Nevertheless, some of these drugs are commercially available and could be helpful for studying the role of phosphorylation sites of CRMP2 for its function on Purkinje cell dendritic development, as they can be applied to cell culture systems.

#### **4.4 CRMP2 and microtubule dynamics**

In our studies, acetylated  $\alpha$ -tubulin was present in soma and dendrites of Purkinje cells in frozen cerebellar sections prepared from wildtype mice at postnatal day 12. In sections from PKC $\gamma$ (S361G)-mice, acetylated tubulin was also present and distributed normally in most Purkinje cells, however, it was absent in morphologically abnormal Purkinje cells in lobule VII. Western blots comparing the amount of acetylated tubulin in wildtype and PKC $\gamma$ (S361G)-mice did not show a detectable difference. This is most likely attributable to the fact that Purkinje cells make up only a small percentage of cells in the cerebellum and that only a few Purkinje cells showed reduced tubulin acetylation, a change too small to be detected by this method.

Dynamic microtubule stability is important for correct dendritic development and knockdown or overexpression of the microtubule destabilizer stathmin both decrease dendritic development of cultured cerebellar Purkinje cells (Ohkawa et al., 2007). CRMP2 as a microtubule stabilizing protein could similarly influence microtubule dynamics in Purkinje cell dendritic development (see Figure 8). Additional experiments will be necessary to see if the decrease in dendritic outgrowth as seen after transfection of phospho-mimetic CRMP2 is caused by its interaction with microtubules.

---

## 5. Conclusion and Outlook

---

Our results establish CRMP2 as a mediator of PKC $\gamma$ -driven modulation of Purkinje cell dendritic development. In mice expressing the overactive S361G-mutant of PKC $\gamma$ , phosphorylation of CRMP2 was upregulated in Purkinje cells, while overall expression remained unchanged. This finding suggests role of CRMP2 in the regulation of dendritic development dependent of its phosphorylation status.

Introducing phospho-mimetic or phospho-defective CRMP2 mutants showed that disbalancing internal pCRMP2 levels negatively impacts dendritic development of Purkinje cells in dissociated cerebellar cultures. Interestingly, overexpression of the T555D-mutant more strongly impaired dendritic outgrowth and could recapitulate the negative impact of pCRMP2 in Purkinje cell of PKC $\gamma$ (S361G)-mice.

### I. Generation of a T555D-knock-in mouse

CRMP2 has been shown to be involved in many different processes that can impact axonal or dendritic outgrowth such as the regulation of ion-channel localization and function, protein trafficking and microtubule stabilization. Phosphorylation of most CRMP2 phosphorylation sites is generally considered to decrease tubulin binding and negatively affect microtubule polymerization. Immunostainings of cerebellar sections from PKC $\gamma$ (S361G)-mice revealed that tubulin acetylation, a hallmark of microtubule stabilization, is strongly decreased in Purkinje cells with morphological abnormalities in lobule VII, while it was normal in control mice and in CRMP2<sup>ki/ki</sup>-mice in agreement with the normal dendritic morphology of Purkinje cells in these mice. We have already shown that overexpression of the T555D-mutant in wildtype Purkinje cells leads to decreased dendritic development in transfected dissociated cultures. It would be interesting to generate a T555D-knock-in mouse to see whether Purkinje cells developed similar morphological abnormalities as we observe in the PKC $\gamma$ (S361G)-mouse model. These mice could furthermore provide an interesting tool to understand tubulin acetylation in correlation with CRMP2 phosphorylation.

## **II. Investigate the effect of other CRMP2 phosphorylation sites and other kinases on Purkinje cell dendritic development**

Apart from PKC, also other kinases have been implicated in the phosphorylation of the CRMP2 Thr555 site. We have performed preliminary experiments on a potential protective effect of the inhibition of CaMKII activity on Purkinje cell dendritic development in OTSCs prepared from PKC $\gamma$ (S361G)-mice. Inhibiting CaMKII activity did not show a positive effect on diminished dendritic outgrowth in these cultures, proposing that this kinase is not involved in the upregulation of pCRMP2 in these mice. Nevertheless, also ROCK2 has been shown to phosphorylate CRMP2 at Thr555. We therefore plan to perform additional experiments using ROCK2 inhibitors and investigate its effect on CRMP2 phosphorylation and dendritic development in PKC $\gamma$ (S361G)-cultures.

As well as the T555D-mutant, also transfection of phospho-defective T555A-CRMP2 decreased dendritic development of Purkinje cells in dissociated cerebellar cultures albeit to a smaller extent. In DRG neurons, ROCK2-mediated phosphorylation of Thr555 is increased after lysophosphatidic acid (LPA) or ephrin-A5-induced growth cone collapse (Arimura et al., 2000, 2005). Interestingly, also in these studies introduction of T555A-CRMP2 was only partially able to prevent growth cone collapse, which suggests the involvement of other phosphorylation sites. As phosphorylation of threonine 514 and serine 522 have also been shown to impair CRMP2-mediated microtubule polymerization, it is worth considering additional cross-effects of these sites. Apart from the upregulation of Thr555 CRMP2 in PKC $\gamma$ (S361G)-mice, we also observed a small upregulation of Thr514, which was however not restricted to Purkinje cells. Inhibiting this phosphorylation site either pharmacologically or also through a genomic approach should thereby be considered for future experiments.

## **III. Explore the effect of other CRMP family members on dendritic development**

Another possible explanation for the moderate effects of T555A-transfection on dendritic development of Purkinje cells in dissociated cultures could be the interference of other CRMP family members. The transfection of T555A-CRMP2 into dissociated cerebellar cultures could therefore be combined with the additional knockdown of other CRMP family members to elucidate their respective participation in dendritic development.

#### **IV. Further analyses in CRMP2<sup>ki/ki</sup>-mice**

We have generated the T555A knock-in mouse to eliminate compensatory background effects of other CRMP family members. Cerebella of the mice appear largely normal. However, several studies have now shown that CRMP2 phosphorylation can impact the development and morphology of dendritic spines (Jin et al., 2016; Makihara et al., 2016; Zhang et al., 2018; Ziak et al., 2020). Investigating the more detailed dendritic morphology by examining dendritic spine morphology in our CRMP2<sup>ki/ki</sup>-mice should therefore be considered in the future.

Unlike to dissociated cerebellar cultures, Purkinje cell morphology in organotypic slice cultures and on cerebellar cryosections from CRMP2<sup>ki/ki</sup>-mice appeared normal. It is possible that, as mentioned above in the case of T555A-transfections, other CRMP family members could compensate for disrupted CRMP2 function in CRMP2<sup>ki/ki</sup>-mice. Using a mass spectrometry approach, we could examine cerebellar lysates from CRMP2<sup>ki/ki</sup>-mice in order to explore whether the levels of other CRMP family members are altered compared to wildtype mice. Furthermore, by immunoprecipitating CRMP2, we could investigate the changes in interactions with CRMP2 binding partners caused by the introduction of our mutation. This approach could improve our understanding of the mechanisms affected by hyper- or hypo-phosphorylation of CRMP2 in the cerebellum.

#### **V. Investigate the effect of CRMP2 phosphorylation on microtubule stabilization**

Preliminary experiments have shown that tubulin acetylation appears to be decreased in morphologically aberrant Purkinje cells in PKCγ(S361G)-mice at postnatal day 12. The changes we observe in immunostainings, however, are only present in a small region preventing its detection by Western blot. Fluorescence-activated cell sorting (FACS) has been used to purify cerebellar Purkinje cells and could offer the opportunity to compare levels of acetylated tubulin in Purkinje cells of wildtype and PKCγ(S361G)-mice (Tomomura et al., 2001).

An estimation of the levels of several tubulin modifications could also be achieved through quantitative mass spectrometry analysis. Apart from comparing wildtype to PKCγ(S361G)-mice, CRMP2<sup>ki/ki</sup>-samples could also be included in the study and, as mentioned above, yield valuable data also on other CRMP2 interactions.

---

## 6. Materials & Methods

---

Only methods which are not included in the publication of Chapter 2 are described here.

### *Immunostainings of organotypic cerebellar slice cultures*

Organotypic cerebellar slice cultures were prepared as previously described [10]. A more detailed description of the procedure and the immunostaining protocol can be found in chapter 2.4.

Primary antibodies mouse anti-Calbindin (1:500, Swant; No. 300), rabbit anti-pSer522-CRMP2 (1:250; Abcam; ab193226) or rabbit anti-pThr514-CRMP2 (1:250; Cell Signaling; #9397) were diluted in PB with 0.03% Triton-X and 3% normal goat serum. Slices were then incubated overnight at 4°C under gentle agitation. Plates were washed three times with PB and secondary antibodies Alexa Fluor-568 goat anti-rabbit (Molecular Probes, Eugene, USA; A11011) and Alexa Fluor-488 goat anti-mouse (Molecular Probes, Eugene, USA; A11001) were added at a concentration of 1:500 in PB with 0.01% Triton-X. Plates were washed again three times for 5 minutes, detached from the membranes and then mounted in Mowiol.

### *Treatments of organotypic cerebellar slice cultures*

For treatments with PMA, 1.5 µL of a 50 µM stock solution were added to 750 µL (final concentration = 100 nM) of medium and added to the cultures with the first medium exchange at day 3 or 4 in vitro and at every following medium exchange. 1.5 µL DMSO in 750 µL medium was used in control wells.

The procedure was similar for (S)-lacosamide, where 1.5 µL of a stock solution of 100 mM were used to achieve a final concentration of 200 µM in 750 µL medium.

For treatments with naringenin or N7O, different stock solutions were prepared and either 1.5 µL or 0.75 µL were added to 750 µL of medium to achieve final concentrations of 10 or 1 µM for naringenin and 0.1 µM for N7O.

**Table III Stock solutions of naringenin and N7O**

	Stock I	Stock II	Stock III
Naringenin	100 mM	5 mM	500 µM
N7O	50 mM	50 µM	-



### *Perfusion & cryosections*

Mice were euthanized by an overdose of Pentobarbital (Eskonarkon ad us. vet., Streuli, Swissmedic no. 55'815). The thorax was opened and the right ventricle perforated. The animal was perfused through the left ventricle with PBS + 50 IU/ml Heparin followed by 4% PFA in PBS + 5% sucrose. Brains were retrieved from the skull and postfixed in 4% PFA in PBS + 5% sucrose overnight. The next day, brains were moved to 30% sucrose solution overnight for cryoprotection. On the third day, brains were mounted in Tissue-Tek (Tissue-Tek® O.C.T.™ Compound, Sakura, Ca. no. SA62550-01) and frozen by immersion in -40°C isopentane. Frozen brains were mounted onto a specimen holder and 25 µm sections were cut in the sagittal plane.

### *Immunohistochemistry of cryosections*

Cerebellar sections were stained free-floating in 6-well plates. Primary antibodies rabbit anti- $\alpha$ -tubulin (1:1000; Proteintech; 11224-1-AP), mouse anti-acetylated- $\alpha$ -tubulin (6-11B-1; 1:1000; Invitrogen; 32-2700), rabbit anti-vGlut1 (1:500; Synaptic Systems; 135 303), guinea pig anti-vGlut2 (1:500; Merck Millipore; AB2251-I), rabbit anti-Calbindin (1:1000; Swant; CB38) and mouse anti-Calbindin (1:500, Swant; No. 300) were diluted in PB with 0.03% Triton-X and 3% normal goat serum. Tissues were incubated overnight at 4°C under gentle agitation. Plates were washed 3x with PB and secondary antibodies were added at a concentration of 1:500 in PB + 0.01% Triton-X. Plates were washed again 3x for 5 minutes and the sections were then mounted in Mowiol. Sections were prepared at postnatal day 12 for stainings with tubulin and p28/30 for vGlut1 and vGlut2 respectively.

### *Generation of the pL7-His-CRMP2/T555A/T555D plasmids*

The pL7-GFP-CRMP2, pL7-GFP-T555A or pL7-GFP-T555D vector was used as a template and amplified with the following primers to add a 6x His-tag to the N-terminus: His-CRMP2-F: 5'-AGC GGC CGC GCC ACC ATG GCC CAT CAT CAT CAT CAT TCT TAT CAG GGG AAG AAA AAT-3'; CRMP2-ORF-pL7-R: 5'- AGC AGG ATC CGT CGA CTT AGC CCA GGC TGG TGA TGT-3'. Vector and inserts were digested using NotI (New England BioLabs, Ipswich, USA) and Sall-HF (New England BioLabs, Ipswich, USA) restriction enzymes and the vector was dephosphorylated using calf intestinal alkaline phosphatase (New England BioLabs, Ipswich, USA). After digestion, vector and inserts were run on a 1% agarose gel for 30 mins at 120 V. Bands of correct size were cut from the gel and the DNA was extracted

using the QIAquick Gel Extraction Kit (Qiagen, Hilden, Germany). Vector and inserts were ligated using the LigaFast™ Rapid DNA Ligation System (Promega, Madison, USA) for 15 mins at room temperature and the ligation reaction was transformed into DH5α-E. Coli. Expression vectors were confirmed by sequencing.

### *Generation of the pL7-His-GST plasmid*

We first generated a pL7-His-Myc plasmid using the following oligomers, generated and supplied by Microsynth (Microsynth, Balgach, Switzerland): His-Myc-F: 5'-TCC AGC GGC CGC GCC ACC ATG GCC CAT CAT CAC CAT CAC CAT ACA GAT CTC GAG CAG AAA CTC ATC TCA GAA GAG GAT CTG TAA GTC GAC GGA-3'; His-Myc-R: 5'-TCC GTC GAC TTA CAG ATC CTC TTC TGA GAT GAG TTT CTG CTC GAG ATC TGT ATG GTG ATG GTG ATG ATG GGC CAT GGT GGC GCG GCC GCT GGA-3'. 25 mM of each oligomer were annealed in annealing buffer (10 mM Tris, pH 7.5 - 8.0; 50 mM NaCl; 1 mM EDTA) for 5 mins at 95°C and then cooled down to 4°C in 60 minutes.

pL7-His-T555A vector and annealed oligomers were digested with Sall-HF and NotI. Digested products were purified using the QIAquick PCR Purification Kit (Qiagen, Hilden, Germany) and ligated as mentioned above before transformation into DH5α-E.Coli. Successfully amplified constructs were sequenced for validation.

The pGEX-6P-1 plasmid (GE28-9546-48; Sigma-Aldrich, Buchs, Switzerland) was used as a template to amplify the GST insert using the following primers: GST-F: 5'-ACC ATC ACC ATA CAG ATC TAA TGT CCC CTA TAC TAG GTT ATT GGA AAA TTA AG-3'; GST-R: 5'-GCA GGA TCC GTC GAC ATT TTG GAG GAT GGT CGC CAC C-3'. Digested pL7-His-Myc vector and insert digested with Sall-HF and BglII and ligated as mentioned above before transformation into DH5α-E.Coli. Successfully amplified constructs were sequenced for validation.

### *Western blot analysis*

Western blots were performed as described in chapter 2.4. Furthermore, the following antibodies were used: rabbit anti-pSer522-CRMP2 (1:500; Abcam; ab193226), rabbit anti-pThr514-CRMP2 (1:500; Cell Signaling; #9397), rabbit anti-α-tubulin (1:500; Proteintech; 11224-1-AP) or mouse anti-acetylated-α-tubulin (6-11B-1; 1:1000; Invitrogen; 32-2700) overnight at 4°C. Secondary antibodies IRDye® 800CW Donkey anti-mouse (Li-Cor, Bad-Homburg, Germany; 926-32212) and IRDye® 680LT Donkey anti-rabbit (Li-Cor; 926-68023) were added at a concentration of 1:5000 diluted in TBS-T. After washing, signal was

detected using a LI-COR Odyssey and software (LI-COR Biosciences, Bad Homburg, Germany).

---

## 7. References

---

- Abe H, Jitsuki S, Nakajima W, Murata Y, Jitsuki-Takahashi A, Katsuno Y, Tada H, Sano A, Suyama K, Mochizuki N, Komori T, Masuyama H, et al. 2018. CRMP2-binding compound, edonerpipic maleate, accelerates motor function recovery from brain damage. *Science* (80- ) 360:50–57.
- Abeliovich A, Chen C, Goda Y, Silva AJ, Stevens CF, Tonegawa S. 1993. Modified hippocampal long-term potentiation in PKC $\gamma$ -mutant mice. *Cell* 75:1253–1262.
- Adachi N, Kobayashi T, Takahashi H, Kawasaki T, Shirai Y, Ueyama T, Matsuda T, Seki T, Sakai N, Saito N. 2008. Enzymological analysis of mutant protein kinase C $\gamma$  causing spinocerebellar ataxia type 14 and dysfunction in Ca<sup>2+</sup> homeostasis. *J Biol Chem* 283:19854–19863.
- Adcock KH, Metzger F, Kapfhammer JP. 2004. Purkinje cell dendritic tree development in the absence of excitatory neurotransmission and of brain-derived neurotrophic factor in organotypic slice cultures. *Neuroscience* 127:137–145.
- Al-Hallaq RA, Conrads TP, Veenstra TD, Wenthold RJ. 2007. NMDA di-heteromeric receptor populations and associated proteins in rat hippocampus. *J Neurosci* 27:8334–8343.
- Albus S. 1971. A theory of cerebellar function. *Math Biosci* 10:25–61.
- Alder J, Cho NK, Hatten ME. 1996. Embryonic precursor cells from the rhombic lip are specified to a cerebellar granule neuron identity. *Neuron* 17:389–399.
- Antal CE, Violin JD, Kunkel MT, Skovsø S, Newton AC. 2014. Intramolecular conformational changes optimize protein kinase C signaling. *Chem Biol* 21:459–469.
- Aoki S, Coulon P, Ruigrok TJH. 2019. Multizonal cerebellar influence over sensorimotor areas of the rat cerebral cortex. *Cereb Cortex* 29:598–614.
- Ardeshiri A, Kelley MH, Korner IP, Hurn PD, Herson PS. 2006. Mechanism of progesterone neuroprotection of rat cerebellar Purkinje cells following oxygen-glucose deprivation. *Eur J Neurosci* 24:2567–2574.
- Arimura N, Hattori A, Kimura T, Nakamura S, Funahashi Y, Hirotsune S, Furuta K, Urano T, Toyoshima YY, Kaibuchi K. 2009. CRMP-2 directly binds to cytoplasmic dynein and interferes with its activity. *J Neurochem* 111:380–390.
- Arimura N, Inagaki N, Chihara K, Ménager C, Nakamura N, Amano M, Iwamatsu A, Goshima Y, Kaibuchi K. 2000. Phosphorylation of collapsin response mediator protein-2 by Rho-kinase: Evidence for two separate signaling pathways for growth cone collapse. *J Biol Chem* 275:23973–23980.

- Arimura N, Ménager C, Kawano Y, Yoshimura T, Kawabata S, Hattori A, Fukata Y, Amano M, Goshima Y, Inagaki M, Morone N, Usukura J, et al. 2005. Phosphorylation by Rho kinase regulates CRMP-2 activity in growth cones. *Mol Cell Biol* 25:9973–9984.
- Armstrong CL, Krueger-Naug AM, Currie RW, Hawkes R. 2000. Constitutive expression of the 25-kDa heat shock protein Hsp25 reveals novel parasagittal bands of Purkinje cells in the adult mouse cerebellar cortex. *J Comp Neurol* 416:383–397.
- Beyreuther BK, Freitag J, Heers C, Krebsfänger N, Scharfenecker U, Stöhr T. 2007. Lacosamide: A review of preclinical properties. *CNS Drug Rev* 13:21–42.
- Bird TD. 2019. Hereditary ataxia overview. GeneReviews®, 2019 Jul 2e. © 1993-2020 University of Washington,.
- Bretin S, Reibel S, Charrier E, Maus-Moatti M, Auvergnon N, Thevenoux A, Glowinski J, Rogemond V, Prémont J, Honnorat J, Gauchy C. 2005. Differential expression of CRMP1, CRMP2A, CRMP2B, and CRMP5 in axons or dendrites of distinct neurons in the mouse brain. *J Comp Neurol* 486:1–17.
- Brittain JM, Pan R, You H, Brustovetsky T, Brustovetsky N, Zamponi GW, Lee W-H, Khanna R. 2012. Disruption of NMDAR–CRMP-2 signaling protects against focal cerebral ischemic damage in the rat middle cerebral artery occlusion model. *Channels* 6:52–59.
- Brkanac Z, Bylenok L, Fernandez M, Matsushita M, Lipe H, Wolff J, Nochlin D, Raskind WH, Bird TD. 2002. A new dominant spinocerebellar ataxia linked to chromosome 19q13.4-qter. *Arch Neurol* 59:1291–1295.
- Brochu G, Maler L, Hawkes R. 1990. Zebrin II: A polypeptide antigen expressed selectively by purkinje cells reveals compartments in rat and fish cerebellum. *J Comp Neurol* 291:538–552.
- Brot S, Rogemond V, Perrot V, Chounlamountri N, Auger C, Honnorat J, Moradi-Améli M. 2010. CRMP5 interacts with tubulin to inhibit neurite outgrowth, thereby modulating the function of CRMP2. *J Neurosci* 30:10639–10654.
- Brown M, Jacobs T, Eickholt B, Ferrari G, Teo M, Monfries C, Qi RZ, Leung T, Lim L, Hall C. 2004.  $\alpha$ 2-chimaerin, cyclin-dependent kinase 5/p35, and its target collapsin response mediator protein-2 are essential components in semaphorin 3A-induced growth-cone collapse. *J Neurosci* 24:8994–9004.
- Brown WJ, Verity MA, Smith RL. 1976. Inhibition of cerebellar dendrite development in neonatal thyroid deficiency. *Neuropathol Appl Neurobiol* 2:191–207.
- Brustovetsky T, Pellman JJ, Yang XF, Khanna R, Brustovetsky N. 2014. Collapsin response mediator protein 2 (CRMP2) interacts with N-methyl-D-aspartate (NMDA) receptor and  $\text{Na}^+/\text{Ca}^{2+}$  exchanger and regulates their functional activity. *J Biol Chem* 289:7470–7482.

- Byk T, Dobransky T, Cifuentes-Diaz C, Sobel A. 1996. Identification and molecular characterization of Unc-33-like phosphoprotein (Ulip), a putative mammalian homolog of the axonal guidance-associated unc-33 gene product. *J Neurosci* 16:688–701.
- Byk T, Ozon S, Sobel A. 1998. The Ulip family phosphoproteins common and specific properties. *Eur J Biochem* 254:14–24.
- Catalano SM, Messersmith EK, Goodman CS, Shatz CJ, Chédotal A. 1998. Many major CNS axon projections develop normally in the absence of semaphorin III. *Mol Cell Neurosci* 11:173–182.
- Cayco-Gajic NA, Silver RA. 2019. Re-evaluating circuit mechanisms underlying pattern separation. *Neuron* 101:584–602.
- Chae YC, Lee S, Heo K, Ha SH, Jung Y, Kim JH, Ihara Y, Suh PG, Ryu SH. 2009. Collapsin response mediator protein-2 regulates neurite formation by modulating tubulin GTPase activity. *Cell Signal* 21:1818–1826.
- Chelban V, Wiethoff S, Fabian-Jessing BK, Haridy NA, Khan A, Efthymiou S, Becker EBE, O'Connor E, Hersheson J, Newland K, Hojland AT, Gregersen PA, et al. 2018. Genotype-phenotype correlations, dystonia and disease progression in spinocerebellar ataxia type 14. *Mov Disord* 33:1119–1129.
- Chen C, Kano M, Abeliovich A, Chen L, Bao S, Kim JJ, Hashimoto K, Thompson RF, Tonegawa S. 1995. Impaired motor coordination correlates with persistent multiple climbing fiber innervation in PKC $\gamma$  mutant mice. *Cell* 83:1233–1242.
- Chi CL, Martinez S, Wurst W, Martin GR. 2003. The isthmus organizer signal FGF8 is required for cell survival in the prospective midbrain and cerebellum. *Development* 130:2633–2644.
- Chung S-H, Kim C-T, Hawkes R. 2008. Compartmentation of gaba b receptor2 expression in the mouse cerebellar cortex. *The Cerebellum* 7:295–303.
- Cole AR, Causeret F, Yadirgi G, Hastie CJ, McLauchlan H, McManus EJ, Hernández F, Eickholt BJ, Nikolic M, Sutherland C. 2006. Distinct priming kinases contribute to differential regulation of collapsin response mediator proteins by glycogen synthase kinase-3 in vivo. *J Biol Chem* 281:16591–16598.
- Cole AR, Noble W, Aalten L Van, Plattner F, Meimaridou R, Hogan D, Taylor M, LaFrancois J, Gunn-Moore F, Verkhatsky A, Oddo S, Laferla F, et al. 2007. Collapsin response mediator protein-2 hyperphosphorylation is an early event in Alzheimer's disease progression. *J Neurochem* 103:1132–1144.
- Cole RN, Hart GW. 2001. Cytosolic O-glycosylation is abundant in nerve terminals. *J Neurochem* 79:1080–1089.

- Colgan LA, Hu M, Misler JA, Parra-Bueno P, Moran CM, Leitges M, Yasuda R. 2018. PKC $\alpha$  integrates spatiotemporally distinct Ca<sup>2+</sup> and autocrine BDNF signaling to facilitate synaptic plasticity. *Nat Neurosci* 21:1027–1037.
- Crews L, Ruf R, Patrick C, Dumaop W, Trejo-Morales M, Achim CL, Rockenstein E, Masliah E. 2011. Phosphorylation of collapsin response mediator protein-2 disrupts neuronal maturation in a model of adult neurogenesis: Implications for neurodegenerative disorders. *Mol Neurodegener* 6:67.
- D'Angelo E, Casali S. 2013. Seeking a unified framework for cerebellar function and dysfunction: from circuit operations to cognition. *Front Neural Circuits* 6:1–23.
- Dahmane N, Ruiz A. 1999. Sonic hedgehog and cerebellum development. *Development* 130:3089–3100.
- Deo RC, Schmidt EF, Elhabazi A, Togashi H, Burley SK, Strittmatter SM. 2004. Structural bases for CRMP function in plexin-dependent semaphorin3A signaling. *EMBO J* 23:9–22.
- Doran G, Davies KE, Talbot K. 2008. Activation of mutant protein kinase C $\gamma$  leads to aberrant sequestration and impairment of its cellular function. *Biochem Biophys Res Commun* 372:447–453.
- Dries DR, Gallegos LL, Newton AC. 2007. A single residue in the C1 domain sensitizes novel protein kinase C isoforms to cellular diacylglycerol production. *J Biol Chem* 282:826–830.
- Dustrude ET, Wilson SM, Ju W, Xiao Y, Khanna R. 2013. CRMP2 protein SUMOylation modulates NaV1.7 channel trafficking. *J Biol Chem* 288:24316–24331.
- Dutil EM, Newton AC. 2000. Dual role of pseudosubstrate in the coordinated regulation of protein kinase C by phosphorylation and diacylglycerol. *J Biol Chem* 275:10697–10701.
- Ebner TJ, Wang X, Gao W, Cramer SW, Chen G. 2012. Parasagittal zones in the cerebellar cortex differ in excitability, information processing, and synaptic plasticity. *Cerebellum* 11:418–419.
- Elder DA, Karayal AF, Ercole AJD, Calikoglu AS. 2000. Effects of hypothyroidism on insulin-like growth factor-I expression during brain development in mice. 293:99–102.
- Erö C, Gewaltig MO, Keller D, Markram H. 2018. A cell atlas for the mouse brain. *Front Neuroinform* 12:1–16.
- Errington AC, Stöhr T, Heers C, Lees G. 2008. The investigational anticonvulsant lacosamide selectively enhances slow inactivation of voltage-gated sodium channels. *Mol Pharmacol* 73:157–169.

- Fleming JT, He W, Hao C, Ketova T, Pan FC, Wright CCV, Litingtung Y, Chiang C. 2013. The Purkinje neuron acts as a central regulator of spatially and functionally distinct cerebellar precursors. *Dev Cell* 27:278–292.
- Fukada M, Watakabe I, Yuasa-Kawada J, Kawachi H, Kuroiwa A, Matsuda Y, Noda M. 2000. Molecular characterization of CRMP5, a novel member of the collapsin response mediator protein family. *J Biol Chem* 275:37957–37965.
- Fukata Y, Itoh TJ, Kimura T, Ménager C, Nishimura T, Shiromizu T, Watanabe H, Inagaki N, Iwamatsu A, Hotani H, Kaibuchi K. 2002. CRMP-2 binds to tubulin heterodimers to promote microtubule assembly. *Nat Cell Biol* 4:583–591.
- Gallegos LL, Kunkel MT, Newton AC. 2006. Targeting protein kinase C activity reporter to discrete intracellular regions reveals spatiotemporal differences in agonist-dependent signaling. *J Biol Chem* 281:30947–30956.
- Gao T, Brognard J, Newton AC. 2008. The phosphatase PHLPP controls the cellular levels of protein kinase C. *J Biol Chem* 283:6300–6311.
- Gao X, Pang J, Li LY, Liu WP, Di JM, Sun QP, Fang YQ, Liu XP, Pu XY, He D, Li MT, Su ZL, et al. 2010. Expression profiling identifies new function of collapsin response mediator protein 4 as a metastasis-suppressor in prostate cancer. *Oncogene* 29:4555–4566.
- Garza JC, Qi X, Gjeluci K, Leussis MP, Basu H, Reis SA, Zhao WN, Piguel NH, Penzes P, Haggarty SJ, Martens GJ, Poelmans G, et al. 2018. Disruption of the psychiatric risk gene Ankyrin 3 enhances microtubule dynamics through GSK3/CRMP2 signaling. *Transl Psychiatry* 8:.
- Gellert M, Venz S, Mitlöhner J, Cott C, Hanschmann EM, Lillig CH. 2013. Identification of a dithiol-disulfide switch in collapsin response mediator protein 2 (CRMP2) that is toggled in a model of neuronal differentiation. *J Biol Chem* 288:35117–35125.
- Glatter T, Ludwig C, Ahrné E, Aebersold R, Heck AJR, Schmidt A. 2012. Large-scale quantitative assessment of different in-solution protein digestion protocols reveals superior cleavage efficiency of tandem Lys-C/trypsin proteolysis over trypsin digestion. *J Proteome Res* 11:5145–5156.
- Gögel S, Lange S, Leung KY, Greene NDE, Ferretti P. 2010. Post-translational regulation of Crmp in developing and regenerating chick spinal cord. *Dev Neurobiol* 70:456–471.
- Goldowitz D, Hamre K. 1998. The cells and molecules that make a cerebellum. *Trends Neurosci* 21:375–382.
- Goode N, Hughes K, Woodgettq JR, Parkersli PJ. 1992. Differential regulation of glycogen synthase kinase-3P by protein kinase C isotypes. 267:16878–16882.



- Goshima Y, Nakamura F, Strittmatter P, Strittmatter SM. 1995. Collapsin-induced growth cone collapse mediated by an intracellular protein related to UNC-33. *Nature* 376:509–514.
- Gugger OS, Hartmann J, Birnbaumer L, Kapfhammer JP. 2012. P/Q-type and T-type calcium channels, but not type 3 transient receptor potential cation channels, are involved in inhibition of dendritic growth after chronic metabotropic glutamate receptor type 1 and protein kinase C activation in cerebellar Purkinje c. *Eur J Neurosci* 35:20–33.
- Hallem JS, Thompson JH, Gundappa-Sulur G, Hawkes R, Bjaalie JG, Bower JM. 1999. Spatial correspondence between tactile projection patterns and the distribution of the antigenic Purkinje cell markers anti-zebrin I and anti-zebrin II in the cerebellar folium crus IIa of the rat. *Neuroscience* 93:1083–1094.
- Hamajima N, Matsuda K, Sakata S, Tamaki N, Sasaki M, Nonaka M. 1996. A novel gene family defined by human dihydropyrimidinase and three related proteins with differential tissue distribution. *Gene* 180:157–163.
- Hedges VL, Chen G, Yu L, Krentzel AA, Starrett JR, Zhu J, Suntharalingam P, Remage-healey L, Wang J, Ebner TJ, Mermelstein PG. 2018. Local estrogen synthesis regulates parallel fiber – Purkinje cell neurotransmission within the cerebellar cortex. 159:1328–1338.
- Heijden ME van der, Lackey EP, İşleyen FS, Brown AM, Perez R, Lin T, Zoghbi HY, Sillitoe R V. 2020. Maturation of Purkinje cell firing properties relies on granule cell neurogenesis. *bioRxiv* 2020.05.20.106732.
- Hensley K, Gabbita SP, Venkova K, Hristov A, Johnson MF, Eslami P, Harris-White ME. 2013. A derivative of the brain metabolite lanthionine ketimine improves cognition and diminishes pathology in the 3×Tg-AD mouse model of alzheimer disease. *J Neuropathol Exp Neurol* 72:955–969.
- Hensley K, Venkova K, Christov A. 2010. Emerging biological importance of central nervous system lanthionines. *Molecules* 15:5581–5594.
- Hirano H, Makihara H, Kawamoto Y, Jitsuki-Takahashi A. 2016. Comprehensive behavioral study and proteomic analyses of CRMP2-deficient mice. *Genes to Cells* 21:1059–1079.
- Honnorat J, Antoine JC, Derrington E, Aguera M, Belin MF. 1996. Antibodies to a subpopulation of glial cells and a 66 kDa developmental protein in patients with paraneoplastic neurological syndromes. *J Neurol Neurosurg Psychiatry* 61:270–278.
- Hoshino M, Nakamura S, Mori K, Kawauchi T, Terao M, Nishimura Y V., Fukuda A, Fuse T, Matsuo N, Sone M, Watanabe M, Bito H, et al. 2005. Ptf1a, a bHLH transcriptional gene, defines GABAergic neuronal fates in cerebellum. *Neuron* 47:201–213.
- Hou ST, Jiang SX, Aylsworth A, Ferguson G, Slinn J, Hu H, Leung T, Kappler J, Kaibuchi K. 2009. CaMKII phosphorylates collapsin response mediator protein 2 and modulates axonal damage during glutamate excitotoxicity. *J Neurochem* 111:870–881.

Humphries MJ, Ohm AM, Schaack J, Adwan TS, Reyland ME. 2008. Tyrosine phosphorylation regulates nuclear translocation of PKC $\delta$ . *Oncogene* 27:3045–3053.

Ikezu S, Ingraham Dixie KL, Koro L, Watanabe T, Kaibuchi K, Ikezu T. 2020. Tau-tubulin kinase 1 and amyloid- $\beta$  peptide induce phosphorylation of collapsin response mediator protein-2 and enhance neurite degeneration in Alzheimer disease mouse models. *Acta Neuropathol Commun* 8:12.

Inagaki N, Chihara K, Arimura N, Ménager C, Kawano Y, Matsuo N, Nishimura T, Amano M, Kaibuchi K. 2001. CRMP-2 induces axons in cultured hippocampal neurons. *Nat Neurosci* 4:781–782.

Inatome R, Tsujimura T, Hitomi T, Mitsui N, Hermann P, Kuroda S, Yamamura H, Yanagi S. 2000. Identification of CRAM, a novel unc-33 gene family protein that associates with CRMP3 and protein-tyrosine kinase(s) in the developing rat brain. *J Biol Chem* 275:27291–27302.

Ishida Y, Kawakami H, Kitajima H, Nishiyama A, Sasai Y, Inoue H, Muguruma K. 2016. Vulnerability of Purkinje cells generated from spinocerebellar ataxia type 6 patient-derived iPSCs. *Cell Rep* 17:1482–1490.

Ito M. 2006. Cerebellar circuitry as a neuronal machine. *Prog Neurobiol* 78:272–303.

Jezierska J, Goedhart J, Kampinga HH, Reits E a., Verbeek DS. 2014. SCA14 mutation V138E leads to partly unfolded PKC $\gamma$  associated with an exposed C-terminus, altered kinetics, phosphorylation and enhanced insolubilization. *J Neurochem* 128:741–751.

Ji J, Hassler ML, Shimobayashi E, Paka N, Streit R, Kapfhammer JP. 2014. Increased protein kinase C gamma activity induces Purkinje cell pathology in a mouse model of spinocerebellar ataxia 14. *Neurobiol Dis* 70:1–11.

Jiang T, Zhang G, Liang Y, Cai Z, Liang Z, Lin H, Tan M. 2020. PlexinA3 interacts with CRMP2 to mediate Sema3A signalling during dendritic growth in cultured cerebellar granule neurons. *Neuroscience* 434:83–92.

Jin X, Sasamoto K, Nagai J, Yamazaki Y, Saito K, Goshima Y, Inoue T, Ohshima T. 2016. Phosphorylation of CRMP2 by Cdk5 regulates dendritic spine development of cortical neuron in the mouse hippocampus. *Neural Plast* 2016:.

Joyner AL, Liu A, Millet S. 2000. Otx2, Gbx2 and Fgf8 interact to position and maintain a mid-hindbrain organizer. *Curr Opin Cell Biol* 12:736–741.

Ju W, Li Q, Wilson SM, Brittain JM, Meroueh L, Khanna R. 2013. SUMOylation alters CRMP2 regulation of calcium influx in sensory neurons. *Channels* 7:153–159.

Kaneko M, Yamaguchi K, Eiraku M, Sato M, Takata N, Mishina M, Hirase H, Hashikawa T, Kengaku M. 2011. Remodeling of monopolar Purkinje cell dendrites during cerebellar circuit formation. *6*:.

- Kano M, Hashimoto K, Chen C, Abeliovich A, Aiba A, Kurihara H, Watanabe M, Inoue Y, Tonegawa S. 1995. Impaired synapse elimination during cerebellar development in PKC $\gamma$  mutant mice. *Cell* 83:1223–1231.
- Kano M, Hashimoto K, Kurihara H, Watanabe M, Inoue Y, Aiba A, Tonegawa S. 1997. Persistent multiple climbing fiber Innervation of cerebellar Purkinje cells in mice lacking mGluR1. *Neuron* 18:71–79.
- Kano M, Hashimoto K, Watanabe M, Kurihara H, Offermanns S, Jiang H, Wu Y, Jun K, Shin H-S, Inoue Y, Simon MI, Wu D. 1998. Phospholipase C $\beta$ 4 synapse elimination in the developing cerebellum. *Proc Natl Acad Sci U S A* 95:15724–15729.
- Kapfhammer JP. 2004. Cellular and molecular control of dendritic growth and development of cerebellar Purkinje cells. *Prog Histochem Cytochem* 39:131–182.
- Kato Y, Hamajima N, Inagaki H, Okamura N, Koji T, Sasaki M, Nonaka M. 1998. Post-meiotic expression of the mouse dihydropyrimidinase-related protein 3 (DRP-3) gene during spermiogenesis. *Mol Reprod Dev* 51:105–111.
- Kawano Y, Yoshimura T, Tsuboi D, Kawabata S, Kaneko-Kawano T, Shirataki H, Takenawa T, Kaibuchi K. 2005. CRMP-2 is involved in kinesin-1-dependent transport of the Sra-1/WAVE1 complex and axon formation. *Mol Cell Biol* 25:9920–9935.
- Kelly RM, Strick PL. 2003. Cerebellar loops with motor cortex and prefrontal cortex of a nonhuman primate. *J Neurosci* 23:8432–8444.
- Khan MB, Khan MM, Khan A, Ahmed ME, Ishrat T, Tabassum R, Vaibhav K, Ahmad A, Islam F. 2012. Naringenin ameliorates Alzheimer's disease (AD)-type neurodegeneration with cognitive impairment (AD-TNDCI) caused by the intracerebroventricular-streptozotocin in rat model. *Neurochem Int* 61:1081–1093.
- Khidekel N, Ficarro SB, Clark PM, Bryan MC, Swaney DL, Rexach JE, Sun YE, Coon JJ, Peters EC, Hsieh-Wilson LC. 2007. Probing the dynamics of O-GlcNAc glycosylation in the brain using quantitative proteomics. *Nat Chem Biol* 3:339–348.
- Ki DP, Morieux P, Salomé C, Cotten SW, Reamtong O, Eysers C, Gaskell SJ, Stables JP, Liu R, Kohn H. 2009. Lacosamide isothiocyanate-based agents: Novel agents to target and identify lacosamide receptors. *J Med Chem* 52:6897–6911.
- Kikkawa U, Saito N, Kikkawa U, Nishizuka Y, Tanaka C. 1988. Distribution of protein kinase C-like immunoreactive neurons in rat. *J Neurosci* 8:369–382.
- Kimura T, Arimura N, Fukata Y, Watanabe H, Iwamatsu A, Kaibuchi K. 2005. Tubulin and CRMP-2 complex is transported via Kinesin-1. *J Neurochem* 93:1371–1382.
- Kita Y, Tanaka K, Murakami F. 2015. Specific labeling of climbing fibers shows early synaptic interactions with immature Purkinje cells in the prenatal cerebellum. *Dev Neurobiol* 75:927–934.

- Klebe S, Faivre L, Forlani S, Dussert C, Tourbah A, Brice A, Stevanin G, Durr A. 2007. Another mutation in cysteine 131 in protein kinase  $\text{C}\gamma$  as a cause of spinocerebellar ataxia type 14. *Arch Neurol* 64:913–914.
- Konishi H, Tanaka M, Takemura Y, Matsuzaki H, Ono Y, Kikkawa U, Nishizuka Y. 1997. Activation of protein kinase C by tyrosine phosphorylation in response to  $\text{H}_2\text{O}_2$ . *Proc Natl Acad Sci U S A* 94:11233–11237.
- Konishi H, Yamauchi E, Taniguchi H, Yamamoto T, Matsuzaki H, Takemura Y, Ohmae K, Kikkawa U, Nishizuka Y. 2001. Phosphorylation sites of protein kinase C  $\delta$  in  $\text{H}_2\text{O}_2$ -treated cells and its activation by tyrosine kinase in vitro. *Proc Natl Acad Sci U S A* 98:6587–6592.
- Lawal M, Olotu FA, Soliman MES. 2018. Across the blood-brain barrier: Neurotherapeutic screening and characterization of naringenin as a novel CRMP-2 inhibitor in the treatment of Alzheimer's disease using bioinformatics and computational tools. *Comput Biol Med* 98:168–177.
- Lee HW, Smith L, Pettit GR, Vinitsky A, Smith JB. 1996. Ubiquitination of protein kinase C- $\alpha$  and degradation by the proteasome. *J Biol Chem* 271:20973–20976.
- Leitges M, Kovac J, Plomann M, Linden DJ. 2004. A unique PDZ ligand in PKC $\alpha$  confers induction of cerebellar long-term synaptic depression. *Neuron* 44:585–594.
- Leney AC, Atmioui D El, Wu W, Ovaa H, Heck AJR. 2017. Elucidating crosstalk mechanisms between phosphorylation and O-GlcNAcylation. *Proc Natl Acad Sci U S A* 114:E7255–E7261.
- Lim NKH, Hung LW, Pang TY, Mclean CA, Liddell JR, Hilton JB, Li QX, White AR, Hannan AJ, Crouch PJ. 2014. Localized changes to glycogen synthase kinase-3 and collapsin response mediator protein-2 in the Huntington's disease affected brain. *Hum Mol Genet* 23:4051–4063.
- Lin D, Edwards AS, Fawcett JP, Mbamalu G, Scott JD, Pawson T. 2000. A mammalian PAR-3-PAR-6 complex implicated in Cdc42/Rac1 and aPKC signalling and cell polarity. *Nat Cell Biol* 2:540–547.
- Lin D, Takemoto DJ. 2005. Oxidative activation of protein kinase  $\text{C}\gamma$  through the C1 domain: Effects on gap junctions. *J Biol Chem* 280:13682–13693.
- Lin PC, Chan PM, Hall C, Manser E. 2011. Collapsin response mediator proteins (CRMPs) are a new class of microtubule-associated protein (MAP) that selectively interacts with assembled microtubules via a taxol-sensitive binding interaction. *J Biol Chem* 286:41466–41478.
- Linden DJ, Connor JA. 1991. Participation of postsynaptic PKC in cerebellar long-term depression in culture. *Science* (80- ) 254:1656–1659.

- Lindholm D, Castr E, Tsoulfas P, Kolbeck R, Berzaghi P, Leing A, Heisenberg C, Tesarollo L, Parada LF, Thoenen H. 1993. Neurotrophin-3 induced by tri-iodothyronine in cerebellar granule cells promotes Purkinje cell differentiation. 122:443–450.
- Lordkipanidze T, Dunaevsky A. 2005. Purkinje cell dendrites grow in alignment with Bergmann glia. *Glia* 51:229–234.
- Luca A De, Parmigiani E, Tosatto G, Martire S, Hoshino M, Buffo A, Leto K, Rossi F. 2015. Exogenous Sonic Hedgehog modulates the pool of GABAergic interneurons during cerebellar development. *Cerebellum* 14:72–85.
- Makihara H, Nakai S, Ohkubo W, Yamashita N, Nakamura F, Kiyonari H, Shioi G, Jitsuki-Takahashi A, Nakamura H, Tanaka F, Akase T, Kolattukudy P, et al. 2016. CRMP1 and CRMP2 have synergistic but distinct roles in dendritic development. *Genes to Cells* 21:994–1005.
- Marques JM, Rodrigues RJ, Valbuena S, Rozas JL, Selak S, Marin P, Aller MI, Lerma J. 2013. CRMP2 tethers kainate receptor activity to cytoskeleton dynamics during neuronal maturation. *J Neurosci* 33:18298–18310.
- Marr BYD. 1969. A theory of cerebellar cortex. 202:437–470.
- Matsuda S, Mikawa S, Hirai H. 1999. Phosphorylation of serine-880 in GluR2 by protein kinase C prevents its C terminus from binding with glutamate receptor-interacting protein. *J Neurochem* 73:1765–1768.
- Mckay BE, Turner RW. 2005. Physiological and morphological development of the rat cerebellar Purkinje cell. 3:829–850.
- McMahon AP, Bradley A. 1990. The Wnt-1 (int-1) proto-oncogene is required for development of a large region of the mouse brain. *Cell* 62:1073–1085.
- Metzger F, Kapfhammer JP. 2000. Protein kinase C activity modulates dendritic differentiation of rat Purkinje cells in cerebellar slice cultures. *Eur J Neurosci* 12:1993–2005.
- Mileusnic R, Rose SPR. 2011. The memory enhancing effect of the APP-derived tripeptide Ac-rER is mediated through CRMP2. *J Neurochem* 118:616–625.
- Minturn JE, Fryer HJL, Geschwind DH, Hockfield S. 1995. TOAD-64, a gene expressed early in neuronal differentiation in the rat, is related to unc-33, a *C. elegans* gene involved in axon outgrowth. *J Neurosci* 15:6757–6766.
- Mokhtar SH, Kim MJ, Magee KA, Aui PM, Thomas S, Bakhuraysah MM, Alrehaili AA, Lee JY, Steer DL, Kenny R, McLean C, Azari MF, et al. 2018. Amyloid-beta-dependent phosphorylation of collapsin response mediator protein-2 dissociates kinesin in Alzheimer's disease. *Neural Regen Res* 13:1066–1080.

Morinaka A, Yamada M, Itofusa R, Funato Y, Yoshimura Y, Nakamura F, Yoshimura T, Kaibuchi K, Goshima Y, Hoshino M, Kamiguchi H, Miki H. 2011. Thioredoxin mediates oxidation-dependent phosphorylation of CRMP2 and growth cone collapse. *Sci Signal* 4:1–13.

Moutal A, Dustrude ET, Largent-Milnes TM, Vanderah TW, Khanna M, Khanna R. 2018. Blocking CRMP2 SUMOylation reverses neuropathic pain. *Mol Psychiatry* 23:2119–2121.

Moutal A, Kalinin S, Kowal K, Marangoni N, Dupree J, Lin SX, Lis K, Lisi L, Hensley K, Khanna R, Feinstein DL. 2019a. Neuronal conditional knockout of collapsin response mediator protein 2 Ameliorates Disease severity in a mouse model of Multiple Sclerosis. *ASN Neuro* 11:.

Moutal A, Shan Z, Miranda VG, François-Moutal L, Madura CL, Khanna M, Khanna R. 2019b. Evaluation of edonergic maleate as a CRMP2 inhibitor for pain relief. *Channels* 13:498–504.

Moutal A, White KA, Chefdeville A, Laufmann RN, Vitiello PF, Feinstein D, Weimer JM, Khanna R. 2019c. Dysregulation of CRMP2 post-translational modifications drive its pathological functions. *Mol Neurobiol* 56:6736–6755.

Muha V, Williamson R, Hills R, McNeilly AD, McWilliams TG, Alonso J, Schimpl M, Leney AC, Heck AJR, Sutherland C, Read KD, McCrimmon RJ, et al. 2019. Loss of CRMP2 O-GlcNAcylation leads to reduced novel object recognition performance in mice. *Open Biol* 9:.

Nagai J, Owada K, Kitamura Y, Goshima Y, Ohshima T. 2016. Inhibition of CRMP2 phosphorylation repairs CNS by regulating neurotrophic and inhibitory responses. *Exp Neurol* 277:283–295.

Neveu I, Arenas E. 1996. Neurotrophins promote the survival and development of neurons in the cerebellum of hypothyroid rats in vivo. 133:631–646.

Newton AC. 2018. Protein kinase C as a tumor suppressor. *Semin Cancer Biol* 48:18–26.

Nicholson JL, Altman J. 1972. Synaptogenesis in the rat cerebellum: effects of early hypo- and hyperthyroidism. 176:530–531.

Niisato E, Nagai J, Yamashita N, Nakamura F, Goshima Y, Ohshima T. 2013. Phosphorylation of CRMP2 is involved in proper bifurcation of the apical dendrite of hippocampal CA1 pyramidal neurons. *Dev Neurobiol* 73:142–151.

Nishimura T, Fukata Y, Kato K, Yamaguchi T, Matsuura Y, Kamiguchi H, Kaibuchi K. 2003. CRMP-2 regulates polarized Numb-mediated endocytosis for axon growth. *Nat Cell Biol* 5:819–826.

Nishizuka Y. 1992. Intracellular signaling by hydrolysis of phospholipids and activation of protein kinase C. *Science (80- )* 258:607–614.

- Niwa S, Nakamura F, Tomabechi Y, Aoki M, Shigematsu H, Matsumoto T, Yamagata A, Fukai S, Hirokawa N, Goshima Y, Shirouzu M, Nitta R. 2017. Structural basis for CRMP2-induced axonal microtubule formation. *Sci Rep* 7:1–17.
- Ohkawa N, Fujitani K, Tokunaga E, Furuya S, Inokuchi K. 2007. The microtubule destabilizer stathmin mediates the development of dendritic arbors in neuronal cells. *J Cell Sci* 120:1447–1456.
- Ohkawa N, Sugisaki S, Tokunaga E, Fujitani K, Hayasaka T, Setou M, Inokuchi K. 2008. N-acetyltransferase ARD1-NAT1 regulates neuronal dendritic development. *Genes to Cells* 13:1171–1183.
- Pan S-H, Chao Y-C, Hung P-F, Chen H-Y, Yang S-C, Chang Y-L, Wu C-T, Chang C-C, Wang W-L, Chan W-K, Wu Y-Y, Che T-F, et al. 2011. The ability of LCRMP-1 to promote cancer invasion by enhancing filopodia formation is antagonized by CRMP-1. 121:3189–3205.
- Parker P, Bosca L, Dekker L, Goode N, Hajibagheri N, Hansra G. 1995. Protein kinase C (PKC)-induced PKC degradation: a model for down-regulation. *Biochem Soc Trans* 23:153–155.
- Petratos S, Ozturk E, Azari MF, Kenny R, Young Lee J, Magee KA, Harvey AR, McDonald C, Taghian K, Moussa L, Mun Aui P, Siatskas C, et al. 2012. Limiting multiple sclerosis related axonopathy by blocking Nogo receptor and CRMP-2 phosphorylation. *Brain* 135:1794–1818.
- Ponnusamy R, Lohkamp B. 2013. Insights into the oligomerization of CRMPs: Crystal structure of human collapsin response mediator protein 5. *J Neurochem* 125:855–868.
- Qiao C, Wang C, Jin F, Zheng D, Liu C. 2015. Expression of collapsin response mediator protein 1 in placenta of normal gestation and link to early-onset preeclampsia. *Reprod Sci* 22:495–501.
- Qu Q, Smith FI. 2005. Neuronal migration defects in cerebellum of the *Largemyd* mouse are associated with disruptions in Bergmann glia organization and delayed migration of granule neurons. *Cerebellum* 4:261–270.
- Quach TT, Duchemin AM, Rogemond V, Aguera M, Honnorat J, Belin MF, Kolattukudy PE. 2004. Involvement of collapsin response mediator proteins in the neurite extension induced by neurotrophins in dorsal root ganglion neurons. *Mol Cell Neurosci* 25:433–443.
- Quinn CC, Chen E, Kinjo TG, Kelly G, Bell AW, Elliott RC, McPherson PS, Hockfield S. 2003. TUC-4b, a novel TUC family variant, regulates neurite outgrowth and associates with vesicles in the growth cone. *J Neurosci* 23:2815–2823.
- Quinn CC, Gray GE, Hockfield S. 1999. A family of proteins implicated in axon guidance and outgrowth. *J Neurobiol* 41:158–164.

- Rahajeng J, Giridharan SSP, Naslavsky N, Caplan S. 2010. Collapsin response mediator protein-2 (Crmp2) regulates trafficking by linking endocytic regulatory proteins to dynein motors. *J Biol Chem* 285:31918–31922.
- Rakic P, Sidman RL. 1973. Organization of cerebellar cortex secondary to deficit of granule cells in weaver mutant mice. *J Comp Neurol* 152:133–161.
- Ricard D, Rogemond V, Charrier E, Aguera M, Bagnard D, Belin MF, Thomasset N, Honnorat J. 2001. Isolation and expression pattern of human Unc-33-like phosphoprotein 6/collapsin response mediator protein 5 (Ulip6/CRMP5): Coexistence with Ulip2/CRMP2 in Sema3A-sensitive oligodendrocytes. *J Neurosci* 21:7203–7214.
- Riso V, Rossi S, Perna A, Nicoletti T, Bosco L, Zanni G, Silvestri G. 2020. NGS-based detection of a novel mutation in PRKCG (SCA14) in sporadic adult-onset ataxia plus dystonic tremor. *Neurol Sci* 2:10–12.
- Rosas-Hernández R, Bastián Y, Juárez Tello A, Ramírez-Saíto Á, Escobar García DM, Pozos-Guillén A, Mendez JA. 2019. AMPA receptors modulate the reorganization of F-actin in Bergmann glia cells through the activation of RhoA. *J Neurochem* 149:242–254.
- Rossi F, Strata P. 1995. Reciprocal trophic interactions in the adult climbing fibre-Purkinje cell system. *Prog Neurobiol* 47:341–369.
- Rosslénbroich V, Dai L, Franken S, Gehrke M, Junghans U, Gieselmann V, Kappler J. 2003. Subcellular localization of collapsin response mediator proteins to lipid rafts. *Biochem Biophys Res Commun* 305:392–399.
- Rouzaut A, López-Moratalla N, Miguel C De. 2000. Differential gene expression in the activation and maturation of human monocytes. *Arch Biochem Biophys* 374:153–160.
- Ruano L, Melo C, Silva MC, Coutinho P. 2014. The global epidemiology of hereditary ataxia and spastic paraplegia: A systematic review of prevalence studies. *Neuroepidemiology* 42:174–183.
- Sacktor TC, Osten P, Valsamis H, Jiang X, Naik MU, Sublette E. 1993. Persistent activation of the  $\zeta$  isoform of protein kinase C in the maintenance of long-term potentiation. *Proc Natl Acad Sci U S A* 90:8342–8346.
- Sakamoto H, Mezaki Y, Shikimi H, Ukena K. 2003. Dendritic growth and spine formation in response to estrogen in the developing Purkinje cell. *144:4466–4477*.
- Sanger TD, Yamashita O, Kawato M. 2020. Expansion coding and computation in the cerebellum: 50 years after the Marr–Albus codon theory. *J Physiol* 598:913–928.
- Sarna JR, Hawkes R. 2003. Patterned Purkinje Cell Death in the Cerebellum. 473–507 p.



- Sarna JR, Marzban H, Watanabe M, Hawkes R. 2006. Complementary stripes of phospholipase C $\beta$ 3 and C $\beta$ 4 expression by Purkinje cell subsets in the mouse cerebellum. *J Comp Neurol* 496:303–313.
- Schilling K, Dickinson MH, Connor JA, Morgan JL. 1991. Electrical activity in cerebellar cultures determines Purkinje cell dendritic growth patterns. 7:.
- Schmidt R. 1964. Die postnatale Genese der Kleinhirndefekte der röntgenbestrahlten Hausmaus (*Mus musculus domesticus* Ruttj 1772). *Naturwissenschaften* 51:162.
- Schrenk K, Kapfhammer JP, Metzger F. 2002. Altered dendritic development of cerebellar Purkinje cells in slice cultures from protein kinase C $\gamma$ -deficient mice. *Neuroscience* 110:675–689.
- Seki T, Adachi N, Ono Y, Mochizuki H, Hiramoto K, Amano T, Matsubayashi H, Matsumoto M, Kawakami H, Saito N, Sakai N. 2005. Mutant protein kinase C $\gamma$  found in spinocerebellar ataxia type 14 is susceptible to aggregation and causes cell death. *J Biol Chem* 280:29096–29106.
- Seki T, Shimahara T, Yamamoto K, Abe N, Amano T, Adachi N, Takahashi H, Kashiwagi K, Saito N, Sakai N. 2009. Mutant  $\gamma$ PKC found in spinocerebellar ataxia type 14 induces aggregate-independent maldevelopment of dendrites in primary cultured Purkinje cells. *Neurobiol Dis* 33:260–273.
- Shih JY, Yang SC, Hong TM, Yuan A, Chen JJW, Yu CJ, Chang YL, Lee YC, Peck K, Wu CW, Yang PC. 2001. Collapsin response mediator protein-1 and the invasion and metastasis of cancer cells. *J Natl Cancer Inst* 93:1392–1400.
- Shimobayashi E, Kapfhammer JP. 2017. Increased biological activity of protein kinase C gamma is not required in spinocerebellar ataxia 14. *Mol Brain* 10:1–11.
- Shimobayashi E, Wagner W, Kapfhammer JP. 2016. Carbonic anhydrase 8 expression in Purkinje cells is controlled by PKC $\gamma$  activity and regulates Purkinje cell dendritic growth. *Mol Neurobiol* 53:5149–5160.
- Shirafuji T, Shimazaki H, Miyagi T, Ueyama T, Adachi N, Tanaka S, Hide I, Saito N, Sakai N. 2019. Spinocerebellar ataxia type 14 caused by a nonsense mutation in the PRKCG gene. *Mol Cell Neurosci* 98:46–53.
- Shuvaev AN, Horiuchi H, Seki T, Goenawan H, Irie T, Iizuka A, Sakai N, Hirai H. 2011. Mutant PKC in spinocerebellar ataxia type 14 disrupts synapse elimination and long-term depression in Purkinje cells in vivo. *J Neurosci* 31:14324–14334.
- Smith L, Chen L, Reyland ME, DeVries TA, Talanian R V., Omura S, Smith JB. 2000. Activation of atypical protein kinase C  $\zeta$  by caspase processing and degradation by the ubiquitin-proteasome system. *J Biol Chem* 275:40620–40627.

Sotelo C. 2004. Cellular and genetic regulation of the development of the cerebellar system. *Prog Neurobiol* 72:295–339.

Sotelo C, Dusart I. 2009. Intrinsic versus extrinsic determinants during the development of Purkinje cell dendrites. *Neuroscience* 162:589–600.

Strømme P, Dobrenis K, Sillitoe R V., Gulinello M, Ali NF, Davidson C, Micsenyi MC, Stephney G, Ellevog L, Klungland A, Walkley SU. 2011. X-linked Angelman-like syndrome caused by *Slc9a6* knockout in mice exhibits evidence of endosomal-lysosomal dysfunction. *Brain* 134:3369–3383.

Sudarov A, Joyner AL. 2007. Cerebellum morphogenesis: The foliation pattern is orchestrated by multi-cellular anchoring centers. *Neural Dev* 2:.

Sugawara T, Hisatsune C, Miyamoto H, Ogawa N, Mikoshiba K. 2017. Regulation of spinogenesis in mature Purkinje cells via mGluR/PKC-mediated phosphorylation of CaMKII. *Proc Natl Acad Sci U S A* 114:E5256–E5265.

Sumi T, Imasaki T, Aoki M, Sakai N, Nitta E, Shirouzu M, Nitta R. 2018. Structural insights into the altering function of CRMP2 by phosphorylation. *Cell Struct Funct* 43:15–23.

Suzuki L, Coulon P, Sabel-Goedknecht EH, Ruigrok TJH. 2012. Organization of cerebral projections to identified cerebellar zones in the posterior cerebellum of the rat. *J Neurosci* 32:10854–10869.

Takahashi H, Adachi N, Shirafuji T, Danno S, Ueyama T, Vendruscolo M, Shuvaev a. N, Sugimoto T, Seki T, Hamada D, Irie K, Hirai H, et al. 2015. Identification and characterization of PKC $\gamma$ , a kinase associated with SCA14, as an amyloidogenic protein. *Hum Mol Genet* 24:525–539.

Takahashi N, Shuvaev AN, Konno A, Matsuzaki Y, Watanabe M, Hirai H. 2017. Regulatory connection between the expression level of classical protein kinase C and pruning of climbing fibers from cerebellar Purkinje cells. *J Neurochem* 143:660–670.

Taketo MM, Araki Y, Matsunaga A, Yokoi A, Tsuchida J, Nishina Y, Nozaki M, Tanaka H, Koga M, Uchida K, Matsumiya K, Okuyama A, et al. 1997. Mapping of eight testis-specific genes to mouse chromosomes. *Genomics* 46:138–142.

Tan F, Thiele CJ, Li Z. 2014. Collapsin response mediator proteins: Potential diagnostic and prognostic biomarkers in cancers (review). *Oncol Lett* 7:1333–1340.

Tan M, Cha C, Ye Y, Zhang J, Li S, Wu F, Gong S, Guo G. 2015. CRMP4 and CRMP2 interact to coordinate cytoskeleton dynamics, regulating growth cone development and axon elongation. *Neural Plast* 2015:.

Tan M, Ma S, Huang Q, Hu K, Song B, Li M. 2013. GSK-3 $\alpha/\beta$ -mediated phosphorylation of CRMP-2 regulates activity-dependent dendritic growth. *J Neurochem* 125:685–697.

- Tanaka M, Yanagawa Y, Obata K, Marunouchi T. 2006. Dendritic morphogenesis of cerebellar Purkinje cells through extension and retraction revealed by long-term tracking of living cells in vitro. *Neuroscience* 141:663–674.
- Thomas KR, Capecchi MR. 1990. Targeted disruption of the murine int-1 proto-oncogene resulting in severe abnormalities in midbrain and cerebellar development. *Nature* 346:847–850.
- Tobe BT, Crain AM, Winkler AM, Calabrese B, Makihara H, Zhao WN, Lalonde J, Nakamura H, Konopaske G, Sidor M, Pernia CD, Yamashita N, et al. 2017. Probing the lithium-response pathway in hiPSCs implicates the phosphoregulatory set-point for a cytoskeletal modulator in bipolar pathogenesis. *Proc Natl Acad Sci U S A* 114:E4462–E4471.
- Tomomura M, Rice DS, Morgan JI, Yuzaki M. 2001. Purification of Purkinje cells by fluorescence-activated cell sorting from transgenic mice that express green fluorescent protein. *Eur J Neurosci* 14:57–63.
- Toyoshima M, Jiang X, Ogawa T, Ohnishi T, Yoshihara S, Balan S, Yoshikawa T, Hirokawa N. 2019. Enhanced carbonyl stress induces irreversible multimerization of CRMP2 in schizophrenia pathogenesis. *Life Sci Alliance* 2:1–18.
- Trzesniewski J, Altmann S, Jäger L, Kapfhammer JP. 2019. Reduced Purkinje cell size is compatible with near normal morphology and function of the cerebellar cortex in a mouse model of spinocerebellar ataxia. *Exp Neurol* 311:205–212.
- Tsumagari R, Kakizawa S, Kikunaga S, Fujihara Y, Ueda S, Yamanoue M, Saito N, Ikawa M, Shirai Y. 2020. DGK $\gamma$  knock-out mice show impairments in cerebellar motor coordination, LTD, and the dendritic development of Purkinje cells through the activation of PKC $\gamma$ . *eNeuro* 7:.
- Tsutsui K, Ukena K, Usui M, Sakamoto H. 2000. Novel brain function: biosynthesis and actions of neurosteroids in neurons. *Neurosci Biobehav Rev* 24:261–273.
- Uchida Y, Ohshima T, Sasaki Y, Suzuki H, Yanai S, Yamashita N, Nakamura F, Takei K, Ihara Y, Mikoshiba K, Kolattukudy P, Honnorat J, et al. 2005. Semaphorin3A signalling is mediated via sequential Cdk5 and GSK3 $\beta$  phosphorylation of CRMP2: Implication of common phosphorylating mechanism underlying axon guidance and Alzheimer's disease. *Genes to Cells* 10:165–179.
- Uchida Y, Ohshima T, Yamashita N, Ogawara M, Sasaki Y, Nakamura F, Goshima Y. 2009. Semaphorin3A signaling mediated by fyn-dependent tyrosine phosphorylation of collapsin response mediator protein 2 at tyrosine 32. *J Biol Chem* 284:27393–27401.
- Uesaka N, Kano M. 2018. Presynaptic mechanisms mediating retrograde semaphorin signals for climbing fiber synapse elimination during postnatal cerebellar development. *Cerebellum* 17:17–22.

Uesaka N, Uchigashima M, Mikuni T, Nakazawa T, Nakao H, Hirai H, Aiba A, Watanabe M, Kano M. 2014. Retrograde semaphorin signaling regulates synapse elimination in the developing mouse brain. *Science* (80- ) 344:1020–1023.

Varrin-Doyer M, Vincent P, Cavagna S, Auvergnon N, Noraz N, Rogemond V, Honnorat J, Moradi-Améli M, Giraudon P. 2009. Phosphorylation of collapsin response mediator protein 2 on Tyr-479 regulates CXCL12-induced T lymphocyte migration. *J Biol Chem* 284:13265–13276.

Verbeek DS, Goedhart J, Bruinsma L, Sinke RJ, Reits EA. 2008. PKC $\gamma$  mutations in spinocerebellar ataxia type 14 affect C1 domain accessibility and kinase activity leading to aberrant MAPK signaling. *J Cell Sci* 121:2339–2349.

Verbeek DS, Knight MA, Harmison GG, Fischbeck KH, Howell BW. 2005. Protein kinase C gamma mutations in spinocerebellar ataxia 14 increase kinase activity and alter membrane targeting. *Brain* 128:436–442.

Vincent P, Collette Y, Marignier R, Vauillat C, Rogemond V, Davoust N, Malcus C, Cavagna S, Gessain A, Machuca-Gayet I, Belin M-F, Quach T, et al. 2005. A role for the neuronal protein collapsin response mediator protein 2 in T lymphocyte polarization and migration. *J Immunol* 175:7650–7660.

Wagner W, McCroskery S, Hammer JA. 2011. An efficient method for the long-term and specific expression of exogenous cDNAs in cultured Purkinje neurons. *J Neurosci Methods* 200:95–105.

Wang G, Krishnamurthy K, Umapathy NS, Verin AD, Bieberich E. 2009. The carboxyl-terminal domain of Atypical protein kinase C $\zeta$  binds to ceramide and regulates junction formation in Epithelial cells. *J Biol Chem* 284:14469–14475.

Wang L-H, Strittmatter SM. 1997. Brain CRMP forms heterotetramers similar to liver dihydropyrimidinase. *J Neurochem* 69:2261–2269.

Wang LH, Strittmatter SM. 1996. A family of rat CRMP genes is differentially expressed in the nervous system. *J Neurosci* 16:6197–6207.

Wang VY, Rose MF, Zoghbi HY. 2005. Math1 expression redefines the rhombic lip derivatives and reveals novel lineages within the brainstem and cerebellum. *Neuron* 48:31–43.

Wang Y, Brittain JM, Jarecki BW, Park KD, Wilson SM, Wang B, Hale R, Meroueh SO, Cummins TR, Khanna R. 2010. In Silico docking and electrophysiological characterization of lacosamide binding sites on collapsin response mediator protein-2 identifies a pocket important in modulating sodium channel slow inactivation. *J Biol Chem* 285:25296–25307.

Wang Y, Wang Y, Zhang H, Gao Y, Huang C, Zhou A, Zhou Y, Li Y. 2016. Sequential posttranslational modifications regulate PKC degradation. *Mol Biol Cell* 27:410–420.

- Wang YY, Wang YY, Dong J, Wei W, Song B, Min H, Teng W, Chen J. 2014. Developmental hypothyroxinaemia and hypothyroidism limit dendritic growth of cerebellar Purkinje cells in rat offspring: Involvement of microtubule-associated protein 2 (MAP2) and stathmin. *Neuropathol Appl Neurobiol* 40:398–415.
- Weaver AH. 2005. Reciprocal evolution of the cerebellum and neocortex in fossil humans. *Proc Natl Acad Sci U S A* 102:3576–3580.
- White JJ, Arancillo M, Stay TL, George-Jones NA, Levy SL, Heck DH, Sillitoe R V. 2014. Cerebellar zonal patterning relies on Purkinje cell neurotransmission. *J Neurosci* 34:8231–8245.
- Wilson SM, Moutal A, Melemedjian OK, Wang Y, Ju W, François-Moutal L, Khanna M, Khanna R. 2014. The functionalized amino acid (S)-lacosamide subverts CRMP2-mediated tubulin polymerization to prevent constitutive and activity-dependent increase in neurite outgrowth. *Front Cell Neurosci* 8:1–15.
- Wilson SM, Xiong W, Wang Y, Ping X, Head JD, Brittain JM, Gagare PD, Ramachandran P V., Jin X, Khanna R. 2012. Prevention of posttraumatic axon sprouting by blocking collapsin response mediator protein 2-mediated neurite outgrowth and tubulin polymerization. *Neuroscience* 210:451–466.
- Wolff C, Carrington B, Varrin-Doyer M, Vandendriessche A, Perren C Van der, Famelart M, Gillard M, Foerch P, Rogemond V, Honnorat J, Lawson A, Miller K. 2012. Drug binding assays do not reveal specific binding of lacosamide to collapsin response mediator protein 2 (CRMP-2). *CNS Neurosci Ther* 18:493–500.
- Wong MMK, Hoekstra SD, Vowles J, Watson LM, Fuller G, Németh AH, Cowley SA, Ansorge O, Talbot K, Becker EBE. 2018. Neurodegeneration in SCA14 is associated with increased PKC  $\gamma$  kinase activity , mislocalization and aggregation. 1–14.
- Wu CC, Chen HC, Chen SJ, Liu HP, Hsieh YY, Yu CJ, Tang R, Hsieh LL, Yu JS, Chang YS. 2008. Identification of collapsin response mediator protein-2 as a potential marker of colorectal carcinoma by comparative analysis of cancer cell secretomes. *Proteomics* 8:316–332.
- Xiong LL, Qiu DL, Xiu GH, Al-Hawwas M, Jiang Y, Wang YC, Hu Y, Chen L, Xia QJ, Wang TH. 2020. DPYSL2 is a novel regulator for neural stem cell differentiation in rats: Revealed by *Panax notoginseng* saponin administration. *Stem Cell Res Ther* 11:1–16.
- Yamamoto K, Seki T, Adachi N, Takahashi T, Tanaka S, Hide I, Saito N, Sakai N. 2010. Mutant protein kinase C gamma that causes spinocerebellar ataxia type 14 (SCA14) is selectively degraded by autophagy. *Genes to Cells* 15:425–438.
- Yamashita N, Goshima Y. 2012. Collapsin response mediator proteins regulate neuronal development and plasticity by switching their phosphorylation status. *Mol Neurobiol* 45:234–246.

- Yamashita N, Mosinger B, Roy A, Miyazaki M, Ugajin K, Nakamura F, Sasaki Y, Yamaguchi K, Kolattukudy P, Goshima Y. 2011. CRMP5 (Collapsin Response Mediator Protein 5) regulates dendritic development and synaptic plasticity in the cerebellar Purkinje cells. *J Neurosci* 31:1773–1779.
- Yamashita N, Ohshima T, Nakamura F, Kolattukudy P, Honnorat J, Mikoshiba K, Goshima Y, Lyon CB, Lyon D, Neurologique H. 2012. Phosphorylation of CRMP2 (collapsin response mediator protein 2) is involved in proper dendritic field organization. 32:1360–1365.
- Yamazaki Y, Nagai J, Akinaga S, Koga Y, Hasegawa M, Takahashi M, Yamashita N, Kolattukudy P, Goshima Y, Ohshima T. 2020. Phosphorylation of CRMP2 is required for migration and positioning of Purkinje cells: Redundant roles of CRMP1 and CRMP4. *Brain Res* 1736:146762.
- Yang Z, Kuboyama T, Tohda C. 2017. A systematic strategy for discovering a therapeutic drug for Alzheimer's disease and its target molecule. *Front Pharmacol* 8:1–13.
- Yoshimura T, Kawano Y, Arimura N, Kawabata S, Kikuchi A, Kaibuchi K. 2005. GSK-3 $\beta$  regulates phosphorylation of CRMP-2 and neuronal polarity. *Cell* 120:137–149.
- Yu Z, Kryzer TJ, Griesmann GE, Kim KK, Benarroch EE, Lennon VA. 2001. CRMP-5 neuronal autoantibody: Marker of lung cancer and thymoma-related autoimmunity. *Ann Neurol* 49:146–154.
- Zeeuw CI De, Hansel C, Bian F, Koekkoek SKE, Alphen AM Van, Linden DJ, Oberdick J. 1998. Expression of a protein kinase C inhibitor in Purkinje cells blocks cerebellar LTD and adaptation of the vestibulo-ocular reflex. *Neuron* 20:495–508.
- Zhang H, Kang E, Wang Y, Yang C, Yu H, Wang Q, Chen Z, Zhang C, Christian KM, Song H, Ming GL, Xu Z. 2016. Brain-specific Crmp2 deletion leads to neuronal development deficits and behavioural impairments in mice. *Nat Commun* 7:.
- Zhang J, Zhao B, Zhu X, Li J, Wu F, Li S. 2018. Phosphorylation and SUMOylation of CRMP2 regulate the formation and maturation of dendritic spines. *Brain Res Bull* 139:21–30.
- Zhang Y, Chen K, Sloan SA, Bennett ML, Scholze AR, O'Keeffe S, Phatnani HP, Guarnieri P, Caneda C, Ruderisch N, Deng S, Liddelow SA, et al. 2014. An RNA-sequencing transcriptome and splicing database of glia, neurons, and vascular cells of the cerebral cortex. *J Neurosci* 34:11929–11947.
- Zhang Y, Snider A, Willard L, Takemoto DJ, Lin D. 2009. Loss of Purkinje cells in the PKC $\gamma$  H101Y transgenic mouse. *Biochem Biophys Res Commun* 378:524–528.
- Zhang Z, Majava V, Greffier A, Hayes R, Kursula P, Wang K. 2008. Collapsin response mediator protein-2 is a calmodulin-binding protein. *Cell Mol Life Scii* 66:526–536.

Zhong W, Jiang MM, Schonemann MD, Meneses JJ, Pedersen RA, Jan LY, Jan YN. 2000. Mouse numb is an essential gene involved in cortical neurogenesis. *Proc Natl Acad Sci U S A* 97:6844–6849.

Zhou Y, Cai S, Moutal A, Yu J, Gómez K, Madura CL, Shan Z, Pham NYN, Serafini MJ, Dorame A, Scott DD, François-Moutal L, et al. 2019. The natural flavonoid naringenin elicits analgesia through inhibition of NaV1.8 voltage-gated sodium channels. *ACS Chem Neurosci* 10:4834–4846.

Ziak J, Weissova R, Jeřábková K, Janikova M, Maimon R, Petrsek T, Pukajova B, Kleisnerova M, Wang M, Brill MS, Kasperek P, Zhou X, et al. 2020. CRMP 2 mediates Sema3F-dependent axon pruning and dendritic spine remodeling . *EMBO Rep* 21:1–22.

## 8. Curriculum Vitae

---



# Sabine Celine Winkler

**Address:** Voltastrasse 79, 4056 Basel, Switzerland

**Phone:** + 49 160 896 93 65 | **E-Mail:** sabinecwinkler@yahoo.de

**LinkedIn:** [www.linkedin.com/in/sabine-winkler-0192b3124/](http://www.linkedin.com/in/sabine-winkler-0192b3124/)

**Other:** residential B-permit (valid until 2023) | Swiss driving license category B

## EXPERIENCE

---

**Since 09/2015**

### PhD candidate

FG Kapfhammer – Developmental Neurobiology and Regeneration,  
Department of Biomedicine, University of Basel

**Thesis:** “PKCγ-mediated phosphorylation of CRMP2 regulates dendritic outgrowth in cerebellar Purkinje cells”

**Skills:** Dissociated- and organotypic cerebellar slice cultures, nucleofection, cryosectioning, co-immunoprecipitation, molecular cloning, PCR, immunohistochemistry, Golgi-staining

**02/2015-07/2015**

### Internship in project management

Springer Spektrum (part of Springer Nature), Heidelberg

**Tasks:** Communicating with authors and freelancers. Assisting in managing book projects and performing general formatting and correction tasks.

**10/2013-06/2014**

### Master's thesis project

AG Pollerberg – Developmental Neurobiology  
Centre for Organismal Studies (COS), Heidelberg

**Thesis:** “The role of cell adhesion molecules in the regeneration of adult spinal neurons”

**Skills:** Primary culture of dorsal root ganglion neurons, bimolecular fluorescence complementation, confocal microscopy

**10/2012-06/2014**

### Master of Science in human biology - major subject: neurobiology

Philipps-University, Marburg, Germany

**Skills:** Preparation of mouse retinal whole mounts, Western Blotting, ELISA

**01/2012-04/2012**

### Studies abroad

Brock University, St. Catharines, Canada

**Coursework:** developmental neurobiology, investigative neurobiology, molecular genetics

**10/2009-10/2012**

### Bachelor of Science in biological sciences

Goethe-University, Frankfurt am Main, Germany

**Thesis:** “The effect of neonicotinoid insecticides on non-associative learning of the honeybee (*Apis mellifera* L.)”



## PUBLICATIONS

Winkler, S.C., Shimobayashi, E. & Kapfhammer, J.P. (2020). "PKC $\gamma$ -Mediated Phosphorylation of CRMP2 Regulates Dendritic Outgrowth in Cerebellar Purkinje Cells." *Molecular Neurobiology*, 57, 5150–5166.

## POSTER PRESENTATIONS

Winkler, S.C. & Kapfhammer, J.P. (2018, February) Searching for molecules contributing to the PKC $\gamma$ -mediated reduction of dendritic growth in cerebellar Purkinje cells. 20<sup>th</sup> Swiss Society for Neuroscience Meeting, Zurich, Switzerland.

Winkler, S.C. & Kapfhammer, J.P. (2018, July) Identification of molecules contributing to the PKC $\gamma$ -mediated reduction of dendritic growth in cerebellar Purkinje cells. 11th FENS Forum of Neuroscience, Berlin, Germany.

Winkler, S.C. & Kapfhammer, J.P. (2019, February) Identification of molecules contributing to the PKC $\gamma$ -mediated reduction of dendritic growth in cerebellar Purkinje cells. 21<sup>st</sup> Swiss Society for Neuroscience Meeting, Bern, Switzerland.

Winkler, S.C., Shimobayashi, E. & Kapfhammer, J.P. (2020, February) PKC $\gamma$ -mediated phosphorylation of CRMP2 regulates dendritic growth in cerebellar Purkinje cells. 22<sup>nd</sup> Swiss Society for Neuroscience Meeting, Bern, Switzerland.

## EXTRACURRICULAR ACTIVITIES

### Since 2016

#### Active member of the DBM PhD-Club

**Tasks:** Organization of social and career events as well as the annual retreat

### 2019

#### Member of the Pint of Science team, Basel

**Tasks:** Organization and implementation of the first Pint of Science event in Switzerland with more than 600 attendants in Basel.

### 2007-2016

#### Volunteer for the "Ministranten St. Leon"

**Tasks:** Organizing and supervising an annual 2-week summer camp

## ADDITIONAL SKILLS

### LTK Module 1

Introductory Course in  
Laboratory Animal  
Science, FELASA B  
(2016)

## SOFTWARE

- Microsoft Office
- ImageJ
- GraphPad PRISM
- OMERO
- R (basics)

## LANGUAGES

**German** – native  
**English** – fluent  
**French** – basic  
**Spanish** – basic

## REFERENCES

### Prof. Dr. Josef Kapfhammer

Anatomisches Institut  
Developmental Neurobiology  
& Regeneration  
Pestalozzistrasse 20,  
4056 Basel, Switzerland  
Phone: + 41 61 207 27 23  
josef.kapfhammer@unibas.ch

### Prof. Dr. Nicole Schaeren-Wiemers

University Hospital Basel  
Neurobiology  
Hebelstrasse 20,  
4031 Basel, Switzerland  
Phone: +41-61 328 73 94  
nicole.schaeren-wiemers@unibas.ch

### Dr. Alexander Schmidt

Biozentrum, University of Basel  
Proteomics Core Facility  
Klingelbergstrasse 50/70,  
4056 Basel, Switzerland  
Phone: +41 61 207 20 59  
alex.schmidt@unibas.ch